THE UNIVERSITY OF ALBERTA

THE STRENGTH-DEFORMATION PROPERTIES OF ALBERTA OIL SANDS

by

KIN-SUN AU

A REPORT

SUBMITTED TO THE FACULTY OF GRADUATE STUDIES AND RESEARCH

IN PARTIAL FULFILMENT OF THE REQUIREMENTS FOR THE DEGREE

OF MASTER OF ENGINEERING

IN

MINERAL ENGINEERING

DEPARTMENT OF MINERAL ENGINEERING

EDMONTON, ALBERTA

November 29, 1983

Abstract

The present study is an attempt to review the strength-deformation properties of Alberta oil sands by examining the available data in the literature. To furnish additional data, two consolidated drained triaxial compression tests were performed on Saline Creek oil sand at effective confining pressures of 2.1 MPa and 3.4 MPa.

As indicated mostly by the results of triaxial tests and direct shear tests, the Athabasca oil sands are highly dilatant. They have unusually high shear strengths compared to ordinary dense sands, and they fail at small axial strains (probably in the range of 0.8% to 1.5%). This is a result of the locked structure of the oil sand matrix. The oil sands in the Grand Rapids Formations have similar but weaker strength properties. In general, the oil sands in the Cold Lake area are weaker than the Athabasca oil sands. That is perhaps because of the higher feldspar content in the Cold Lake oil sands.

The limited amount of test data available in the literature seem to indicate that triaxial tests generally report higher peak and residual shear strengths in Athabasca oil sands than direct shear tests. That is probably because of the non-uniform stress condition inherent in the direct shear tests. In the case of the residual shear strength, the difference in the mode of shearing action between the two tests is perhaps an additional factor.

Oil sands are generally not cemented, and the pore fluid cannot provide a significant cohesive component to the strength of the oil sands. It follows that oil sands have a negligible tensile strength. Under no confining pressure, oil sands have practically no shear strength.

Triaxial test data show that the modulus of elasticity and the shear modulus of the Athabasca oil sands increase with the confining stress. Because of their cohesionless nature and gas exsolution from the bitumen, oil sands used in most tests are invariably disturbed to a certain extent. Compared with the shear strength the modulus of elasticity is a more sensitive indicator of the degree of disturbance. On the other hand, sample disturbance does not appear to have any significant effect on the Poisson's ratio of the Athabasca oil sands, as measured at an axial strain of 0.25%.

Oedometer test and isotropic compression test results suggest that the coefficient of volume compressibility of the Athabasca oil sands is probably between 0.3 and 0.7 $x10^{-6}kPa^{-1}$. The compressibility of the Grand Rapids Formation is slightly lower, whereas the Clearwater Formation at Cold Lake may have a compressibility slightly larger.

Because of their low compressibility, oil sands may yield pore pressure parameter B values significantly less than unity in an undrained triaxial test. In the case of the Saline Creek oil sand, it is not uncommon to obtain B

values lower than 0.9. In an undrained triaxial test on oil sands, the pore pressure parameter $\bar{A}$ typically becomes more negative with increasing axial strain. The value of $\bar{A}$ seems to depend upon the quality of the sample and the limited amount of data available suggest that highly negative $\bar{A}_f$ values usually correspond to high axial strains at failure.

The shear strengths of the intraformational clays and the basal clay shales associated with the McMurray Formation at Athabasca vary within a wide range. That is related to the complex lithologies of the formation. The peak angle of friction of the clay shales can go as high as 29° whereas the residual angle can be as low as 7°.

Acknowledgements

The writer would like to thank Dr. J. D. Scott for his valuable guidance on the present study. Apart from providing direction, Dr. Scott provided much information to broaden the data base upon which the present research was carried out. The writer is also grateful to Dr. B. Stimpson for supervising the study.

Appreciation is heartily expressed to John Agar for his generosity in sharing his time and research data. His contribution significantly enhanced the quality of the data base of this study.

Technical assistance has been provided by Denis Gagnon, Steve Gamble, Christine Hurley, and Gerry Cyre. In particular, the writer is indebted to Denis Gagnon for his immense help in the laboratory. Denis also prepared the oil sand samples for the triaxial tests.

Throughout this study, valuable suggestions have been contributed by Hal Soderberg. Prompt help has also been furnished in the machine shop by Heinz Friedrich and Ken Ellis.

Many thanks are due to the staff of the Department of Mineral Engineering and of the Department of Civil Engineering for their assistance throughout the writer's period of study.

Table of Contents

List of Figures

List of Tables

Chapter 1

INTRODUCTION

1.1 Objectives and Scope

This report reviews the strength-deformation characteristics of Alberta oil sands through a systematic examination of the data available in the published literature and from unpublished technical reports and tests performed at the University of Alberta. Two triaxial tests were performed for this study to supplement the data set collected from the literature.

The report concentrates on the McMurray Formation of the Athabasca oil sands deposit and includes some data from other deposits and from the McMurray Formation clay shales. Generally, only low fines oil sand test results are given.

The properties examined are the bulk density and porosity of samples, parameters from triaxial and direct shear tests, and compressibility from oedometer tests. The majority of triaxial tests performed are consolidated drained tests and the properties determined from these tests are peak shear strengths, some residual shear strengths, volume changes during shear, moduli of elasticity, and Poisson's ratio. Some consolidated undrained triaxial tests with pore pressure measurements have been performed and these tests provide data on peak shear strengths, moduli of elasticity, and the pore pressure parameter $\bar{A}$. Some information on the pore pressure parameter B is also

available from the triaxial tests. The direct shear tests have provided data on peak and residual shear strengths.

Compressibility data for the oil sand has been obtained from the oedometer tests and from the consolidation of the triaxial samples.

1.2 The Need for Representative Strength-Deformation Properties

The development of the heavy oil and oil sand reserves in Alberta involves various technical processes which require accurate knowledge of the strength-deformation properties of the oil sands. The following are some notable areas:

1.2.1 Hydraulic Fracturing

In order to increase the effective permeability of the formation, the hydraulic fracturing process has been used. Injection of hydraulic fluid during the fracturing operation creates fractures perpendicular to the minimum principal stress when the downhole pressure reaches the fracture propagating pressure. At the same time, the injection increases the pore pressures around the injection point. If the pore pressure increase is large enough, shear failure of the oil sands could take place. In addition, hydraulic fractures tend to climb, which results in significant shear stresses at the fracture tip. Therefore the design, control, and

analysis of hydraulic fractures require knowledge of the shear strength properties of oil sands in situ.

One approach to control and optimize hydraulic fracturing involves surface deformation monitoring (Holzhausen, et al, 1980). The analysis and interpretation of the results of deformation monitoring require input of representative values of elastic parameters such as the modulus of elasticity and Poisson's ratio (Ren Jen Sun, 1969).

A related problem is the phenomenon of casing failure in some pilot projects (Smith and Pattillo, 1980). The casing problem is probably due to shear failure of the oil sands by build-up of thermal stress and/or pore pressures. Full investigation of the problem would need understanding in quantitative terms of the strength-deformation characteristics of the oil sands.

1.2.2 Dynamic Fracturing

The process involves pulse loading by means of explosives. Investigation and employment of this process entails input of dynamic strength-deformation parameters.

1.2.3 Structures in or on Oil Sands

The mine assisted in situ processing (MAISP) technique has been seriously considered for development

of oil sands not accessible to surface mining (Mathews, 1980). Regardless of the detailed design, tunnels and shafts in the oil sands would be necessary. The parameters governing design would include strength of oil sands and lining requirements. Determination of the lining requirements necessitates a good understanding of the tendency of the oil sands to expand and deform on stress relief. That again asks for input of realistic strength-deformation relationships. As well, there are structures not related directly to oil sands development, for example, the Saline Creek Tunnel (Smith, et al, 1978), and they equally require the same type of information.

Oil sands are competent foundation materials. However, when important or unusual structures are involved, detailed settlement analysis is still required. Some notable examples include the Mildred Lake Utility Plant (Kolisnyk and Robinson, 1974) and hot bitumen tanks (Kosar, 1983).

1.2.4 Open Pit Mines

In surface mining of oil sands, the stability of the mine slopes is a primary concern. The analysis and design of open pit mines necessitates understanding of the strength properties of oil sands on rapid stress relief.

Experience from full-scale excavations in Athabasca oil sands has indicated that the strength of oil sands is sufficiently great that failures of the pit slope usually occur along clayey seams or other discontinuities dipping unfavourably towards the pit slope and lying within or under the oil sand strata. However, the present trend suggests that much deeper open pit mines will be utilized in the future. In that case, it is necessary to re-evaluate the possibility of slope failure due to failure of the oil sand itself, and the value of the shear strength that can be obtained must be known.

1.3 The Problem of Sample Disturbance

One major difficulty with derivation of the in situ strength and elastic deformation parameters of oil sands is in obtaining undisturbed samples. Oil sand is a four-phase hydrocarbon system. It has a dense interlocked fabric of sand grains with pore spaces occupied by bitumen, water, probably some gas and minor amounts of silt and clay (Harris and Sobkowicz, 1977). Both the bitumen and water may include hydrocarbon gas in solution. Having previously experienced diagenetic changes under high consolidation pressure the sand has an interpenetrative structure. However, the sand grains are usually not cemented and the oil sand has negligible real cohesive strength.

On release of the confining stresses, the gases dissolved in the liquid phase have a tendency to come out of solution. That disrupts the locked structure of the oil sand. As a result, it dramatically reduces the strength and increases the compressibility of the oil sand.

Attempts to minimize sample disturbance have been made by downhole freezing (Dusseault, 1977). However, considerable disturbance on the samples obtained was still observed. For that reason, results of laboratory testing have generally significantly underestimated the true strength of oil sands in situ.

1.4 Previous Studies

Measurements of the shear strength of oil sands were apparently first made by Tustin(1949). Considerable amount of strength testing on disturbed oil sands was performed in the sixties. The researchers who contributed their efforts include Hardy and Hemstock(1963), Round(1964), and Carrigy(1967).

In the seventies, researchers generally have been more conscious about minimizing sample disturbance. This attitude has been maintained into the eighties. For example, Brooker(1975) reported the results of a series of consolidated undrained triaxial tests on relatively undisturbed oil sand samples. The bulk density of the samples was in the order of 2.03 g/cm^3.

The geotechnical properties of the Athabasca oil sands were examined comprehensively by Dusseault(1977). He derived a set of strength data on the basis of several series of triaxial and direct shear tests on carefully sampled and prepared oil sands. Using conventional triaxial tests, Raisbeck and Currie(1981) investigated the stress-strain characteristics of oil sands while Sterne(1981) studied the strength-deformation properties of oil sands by loading the oil sand along three different stress paths. Slightly earlier, Barnes(1980) approached the sample disturbance problem by sampling and testing oil free sands from the McMurray Formation and the Grand Rapids Formation. More recently, some attention has been directed towards the properties of oil sands at elevated temperatures (Agar, 1983).

1.5 Approach Adopted in the Present Study

As a sample loses its locked structure, its bulk density decreases and its strength deteriorates. Thus, the bulk density of a sample as compared to the in-situ value is a partial indicator of the degree of disturbance the sample has experienced. By arranging the data as a function of the bulk density, an attempt has been made to discern meaningful patterns which would allow extrapolation to be made to the in-situ properties.

Chapter 2

BULK DENSITY AND POROSITY OF OIL SANDS

2.1 Athabasca Oil Sands

To serve as the baseline for comparison with the bulk density of test samples, it is necessary to know representative values of in-situ bulk density of oil sands.

Dusseault(1977, 1980) summarized the following list of references on the bulk density of Athabasca oil sands measured geophysically:

(a) 2.18 - 2.05 g/cm³ (porosity 28% - 36%) for very well-sorted, fine-grained, clean sands, and for medium- to coarse-grained sands (that is, the major portion of the Middle and Lower Members of the McMurray Formation).

(b) 2.27 - 2.15 g/cm³ (porosity 23% - 30%) for fine-grained sands (typical of the Middle Member).

(c) 2.40 - 2.24 g/cm³ (porosity 15% - 25%) for sandy and clayey silts and intraformational clays (found predominantly in the Upper Member).

Determination of the bulk density based on core samples is generally unreliable because oil-rich samples have a marked tendency to expand as a result of gas exsolution. For that reason, core analysis usually underestimates the in-situ bulk density of oil sands. The geophysical method has been considered a much more reliable method for measurement of the true bulk density of oil sands. However, porosity measurements made geophysically are perhaps less

accurate.

Three references not included in Dusseault's list reported similar bulk density ranges. The data are summarized in Table 1. Basically, the mean values of bulk density suggested by Dusseault appear to be reasonable in situ representative figures that can be used for core density evaluation.

2.2 Other Locations

There is very little information available regarding the bulk properties of the oil sands in other locations. It has been speculated (Dusseault, 1980) that the saturated in-situ bulk densities of the Clearwater Formation are probably as follows:

(a) 2.08 - 2.16 g/cm^3 with the best sorted (beach) sands having the lowest bulk density.

(b) 2.2 - 2.3 g/cm^3 for clayey silt interbeds.

In general terms, the porosity of the four major oil sand deposits probably falls in the ranges shown in Table 2.

TABLE 1. BULK DENSITY DATA OF ATHABASCA OIL SANDS

BULK DENSITY (g/cm^3)		DIFFERENCE (%)	SOURCE
CORE	GEOPHYSICAL		
1.94 - 2.08	2.06 - 2.37	6.2 (avg.)	Thurber Consultants Ltd., (1977)
1.71 - 2.23	-	as much as 10%	Physical Properties set 74S
2.06	2.10[1]	1.9	Zwicky & Eade (1977)

[1] One of the Geophysical Formation Density Logs is reported in "Application of Shell Canada Limited and Shell Explorer Limited to the Energy Resources Conservation Board". The log indicates that the bulk density ranges from approximately 2.10 to 2.42 g/cm^3.

TABLE 2. POROSITY RANGES OF ALBERTA OIL SAND DEPOSITS (AFTER DUSSEAULT, 1980)

	ATHABASCA	COLD LAKE	WABASCA	PEACE RIVER
POROSITY (%)	30-40	30-35	30-35	25-30

Chapter 3

PEAK STRENGTH PROPERTIES OF OIL SANDS

3.1 General

It should be noted that most of the information available is on Athabasca oil sands. Very little strength data on the oil sands at other locations are available. It appears though that the oil sands at Cold Lake are weaker than the Athabasca oil sands, probably because they contain weaker mineral grains such as feldspar.

3.2 Shear Strength as Measured in Triaxial Tests

The data on Athabasca oil sands are categorized according to the bulk density, and the peak shear strength values are plotted in the form of p'-q diagrams as shown in Figures 3.1 and 3.2. It may be noted that

$$p' = \frac{\sigma_1' + \sigma_3'}{2}$$

$$q = \frac{\sigma_1 - \sigma_3}{2}$$

The diagrams are plotted in terms of p' and q because on a p'-q plot each test is being represented by a stress path instead of a series of semi-circles as in a Mohr-Coulomb diagram. Using the p'-q diagrams, it is easier to evaluate the test results.

It should be noted that most of the tests performed in Triaxial Test Series 75S were consolidated undrained

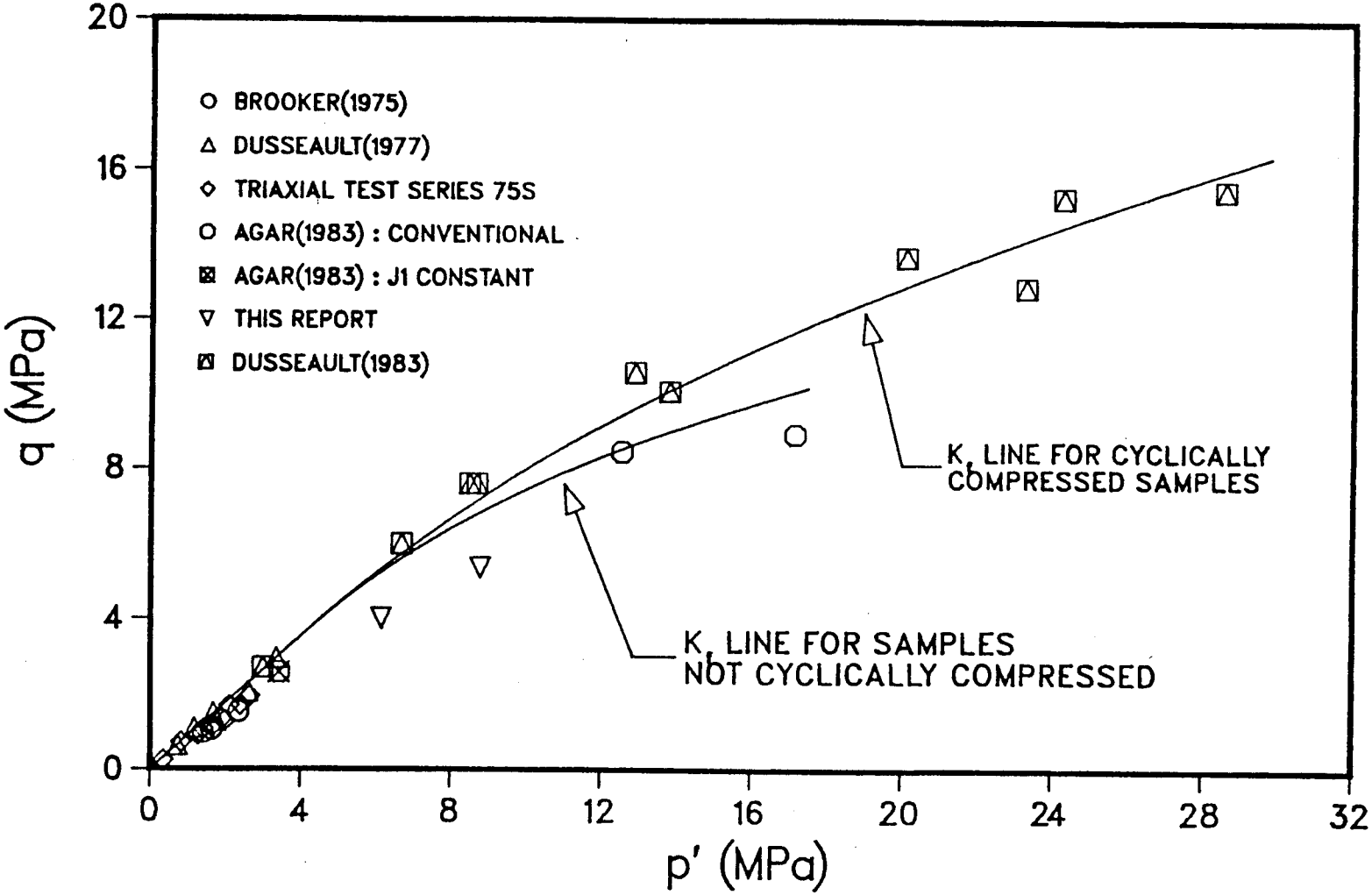

Figure 3.1 p'–q DIAGRAM FOR TRIAXIAL TEST DATA ON SAMPLES WITH BULK DENSITIES ≧ 2.0 g/cm³

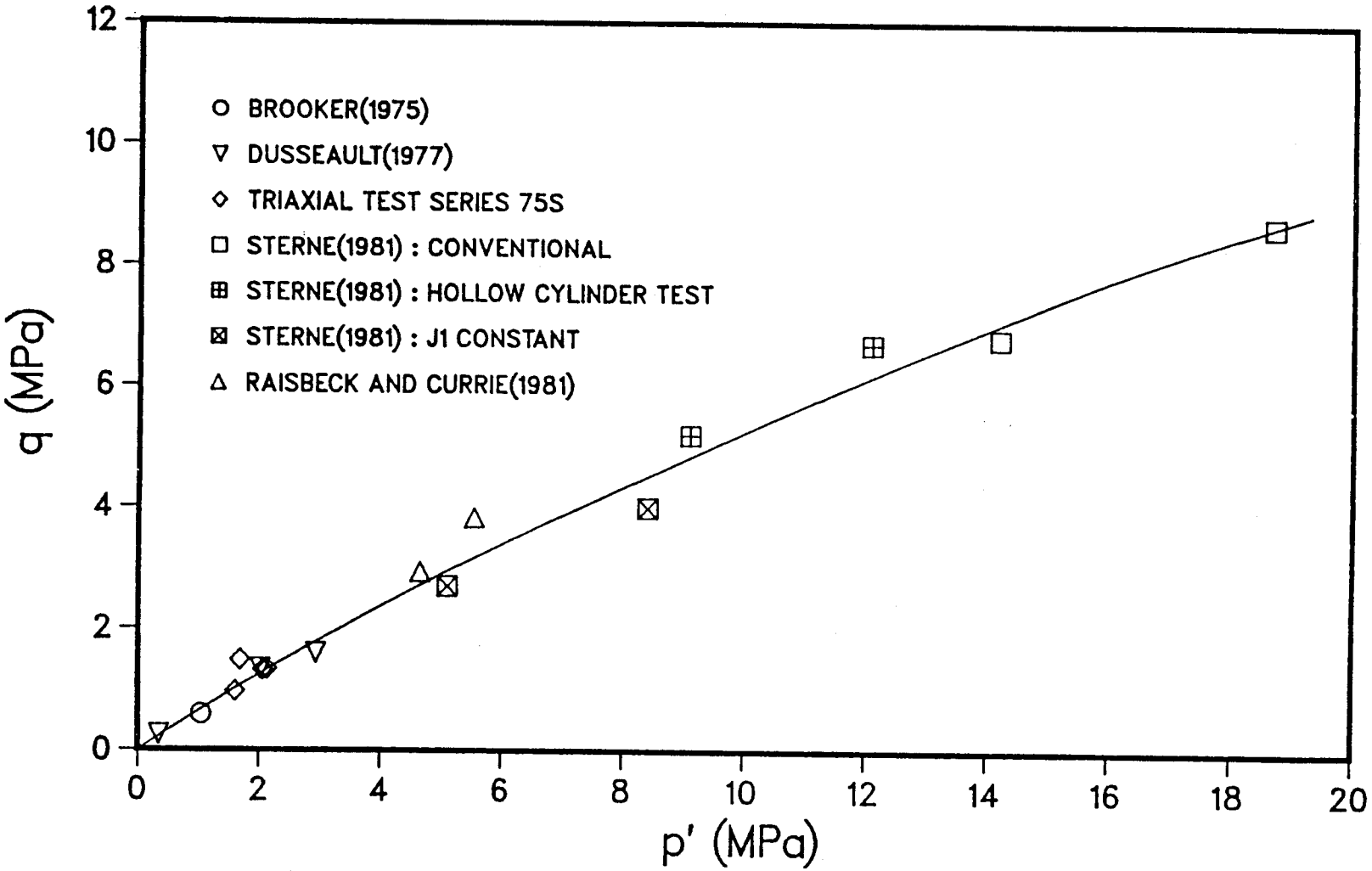

Figure 3.2 p'–q DIAGRAM FOR TRIAXIAL TESTS DATA ON SAMPLES WITH BULK DENSITIES < 2.0 g/cm³

triaxial tests with pore pressure measurements. The rest of the data included in Figures 3.1 and 3.2 were almost all derived from consolidated drained triaxial tests. Test series Dusseault(1983) were consolidated drained tests where the confining pressure for some of the samples was cycled several times, resulting in well consolidated dense samples.

Figure 3.1 is a p'-q diagram plotting the triaxial peak strength test data of samples with bulk densities ≥ 2.0 g/cm³. The average density of the non-cyclically compressed samples is about 2.08 g/cm³, whereas that of the cyclically compressed samples is slightly higher than 2.08 g/cm³.

A separate failure line (K -line) is plotted for the cyclically compressed tests as this test procedure appears to give significantly higher strength values than the normal test procedure. In figure 3.1, the K -lines are clearly non-linear above p' = 4 MPa. This common action of dense granular soils reflects the suppression of the dilatant tendency of the oil sands and subsequent breaking of sand grains during shear under high confining stresses. The K -lines for the normal and the cycled tests are similar below p' = 6 MPa indicating that cycling does not have a significant effect for these lower confining pressures. Figure 3.3 is a separate plot of the tests with p' < 4 MPa. A linear failure line can be drawn through the higher test values for this stress range and gives a ϕ' = 60°. The K -lines appear to pass through the origin which means the

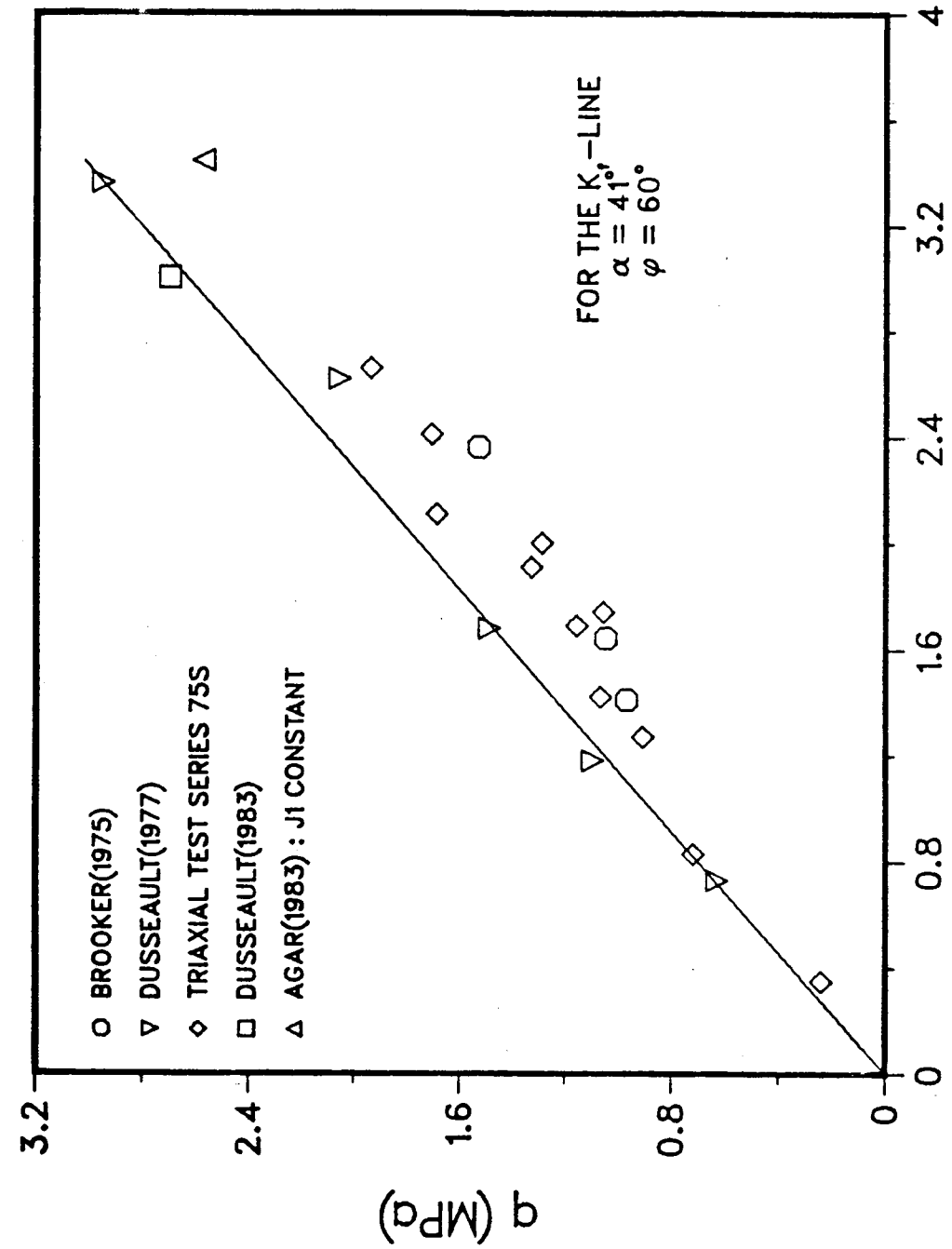

Figure 3.3 p'–q DIAGRAM FOR TRIAXIAL TESTS SAMPLES WITH BULK DENSITIES ≥ 2.0 g/cm^3 FOR p' < 4.0 MPa.

oil sands have negligible real cohesive strength. There is considerable scatter in the data points. The main reason for the scatter may be that each of the test samples has experienced a different amount of disturbance and therefore each of them has suffered a differing amount of strength loss.

The fact that the samples came from different locations presumably contributes to the scatter of the data points. However, it is probably not a major factor since the in-situ densities, grain size distributions and mineral contents of the oil sands from various locations of the McMurray Formation are usually fairly similar.

Agar(1983) has worked experimentally with the Athabasca oil sand from Saline Creek and has found that the effect of stress path on the strength of Saline Creek oil sand is small compared with that of sample disturbance. The strength of Saline Creek oil sand appears to decrease at elevated temperatures; however, the effect of temperature appears to be much smaller than that of sample disturbance. Reference is made to the location of the Saline Creek sampling site in Appendix A.

Figure 3.2 is a p'-q diagram plotting the triaxial test data on sample with bulk densities less than 2.0 g/cm^3. The average density of this set of samples is approximately 1.94 g/cm^3. It should be noted that no information could be found on the bulk densities for the data points derived from Raisbeck and Currie(1981). However, as indicated in section

5.1.1, the bulk densities are suspected to be less than 2.0 g/cm³.

The normal test K -line from Figure 3.1 and the K -line from Figure 3.2 are compared in Figure 3.4. It can be seen that the shear strength of oil sands decreases with the bulk density of the samples. The curvature of the failure line is less for the lower bulk density samples. In terms of strength, the difference between the two K -lines is approximately 25% on average whereas the difference in density between the two sets of data points in Figures 3.1 and 3.2 (2.08 and 1.94 g/cm³ respectively) is 0.14 g/cm³. By extrapolation to the approximate in-situ density of 2.15 g/cm³, the in-situ strength of the Athabasca oil sands could perhaps be 20% higher than what is represented by the K -line in Figure 3.1.

To express the shear strength of oil sands more directly, Mohr-Coulomb failure envelopes are given in Figure 3.5. The K -lines in Figure 3.1 have been used graphically to develop the Mohr envelopes. In Figure 3.5, the Mohr envelopes show the effect of confining pressure on the dilatant disposition of oil sands even more markedly. In addition, the Mohr envelopes are linear for confining pressures up to 0.5 MPa for triaxial testing.

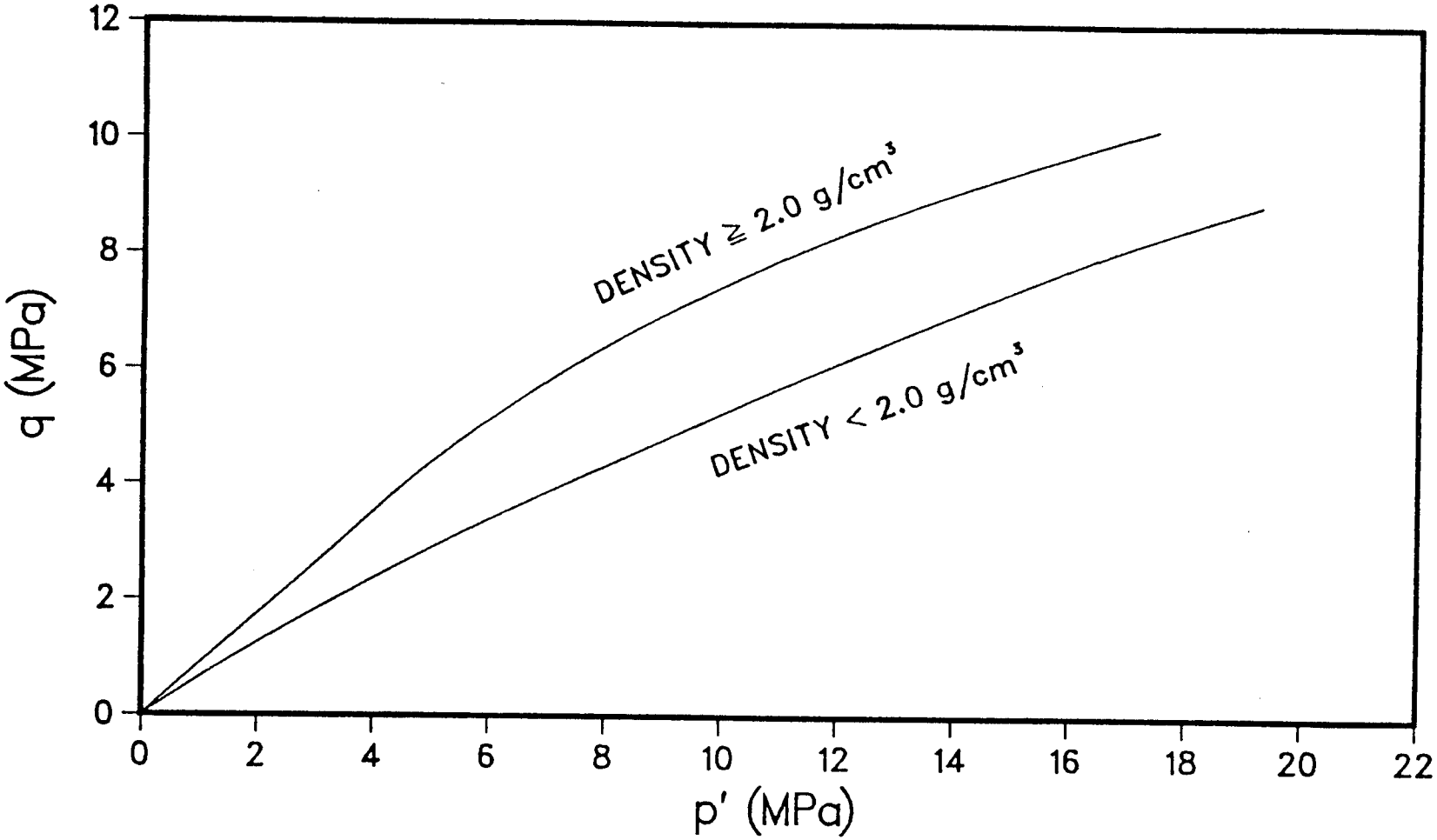

Figure 3.4 COMPARISON OF THE K_f LINES CORRESPONDING TO BULK DENSITIES ≧ 2.0 g/cm³ AND BULK DENSITIES < 2.0 g/cm³

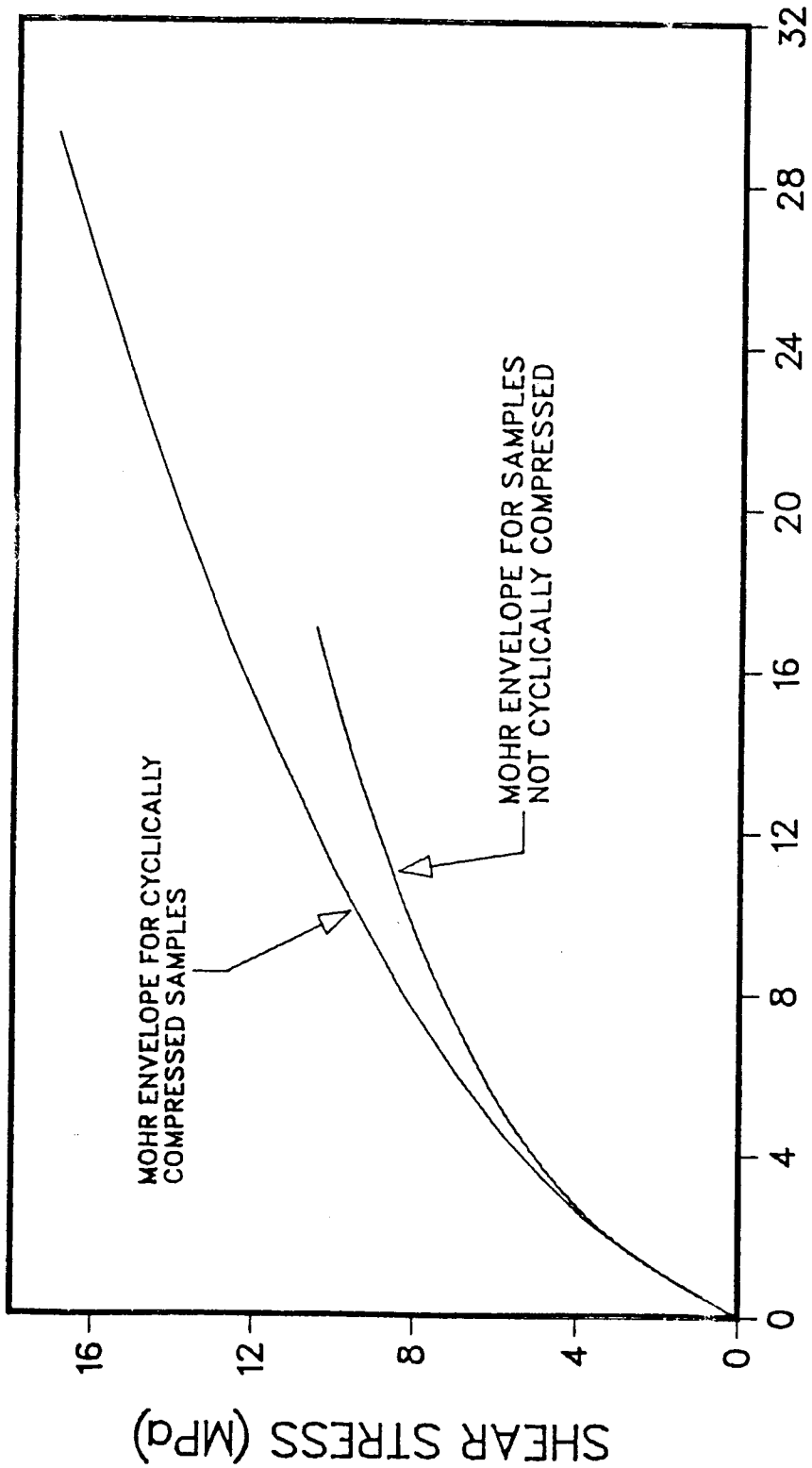

Figure 3.5 THE MOHR ENVELOPES FOR TRIAXIAL TEST SAMPLES WITH BULK DENSITIES ≧ 2.0 g/cm³

3.3 Shear Strength as Measured in Direct Shear Tests

Compared to triaxial tests, direct shear tests allow better control over the orientation of the failure plane in the sample. In addition, it is much more convenient to measure the residual shear strength in direct shear tests. The disadvantage is that direct shear tests cannot provide stress-strain information on the test samples. It should be noted that all the direct shear tests referred to in this section were drained tests.

3.3.1 Peak Shear Strength

3.3.1.1 The Athabasca Oil Sands

The strength data are categorized into groups according to the bulk density and are plotted in Figures 3.6 to 3.9. The fitted lines to the data are, in effect, the average strength envelopes of the oil sand samples in various bulk density ranges. The sample sizes were 6.35 cm diameter by 2.54 cm high for Dusseault(1977), 5.08 cm diameter by 3.00 cm high for Barnes(1980) and 5.07 cm diameter by 5.00 cm high for Test Series 79G.

Figure 3.10 contains a set of large direct shear test results on 12 inch square samples. It is copied directly from Brooker and Khan(1980). Unfortunately, no bulk density information relating to that set of test results was reported. If the variable of bulk density is disregarded, the data points in Figure 3.10 appear to

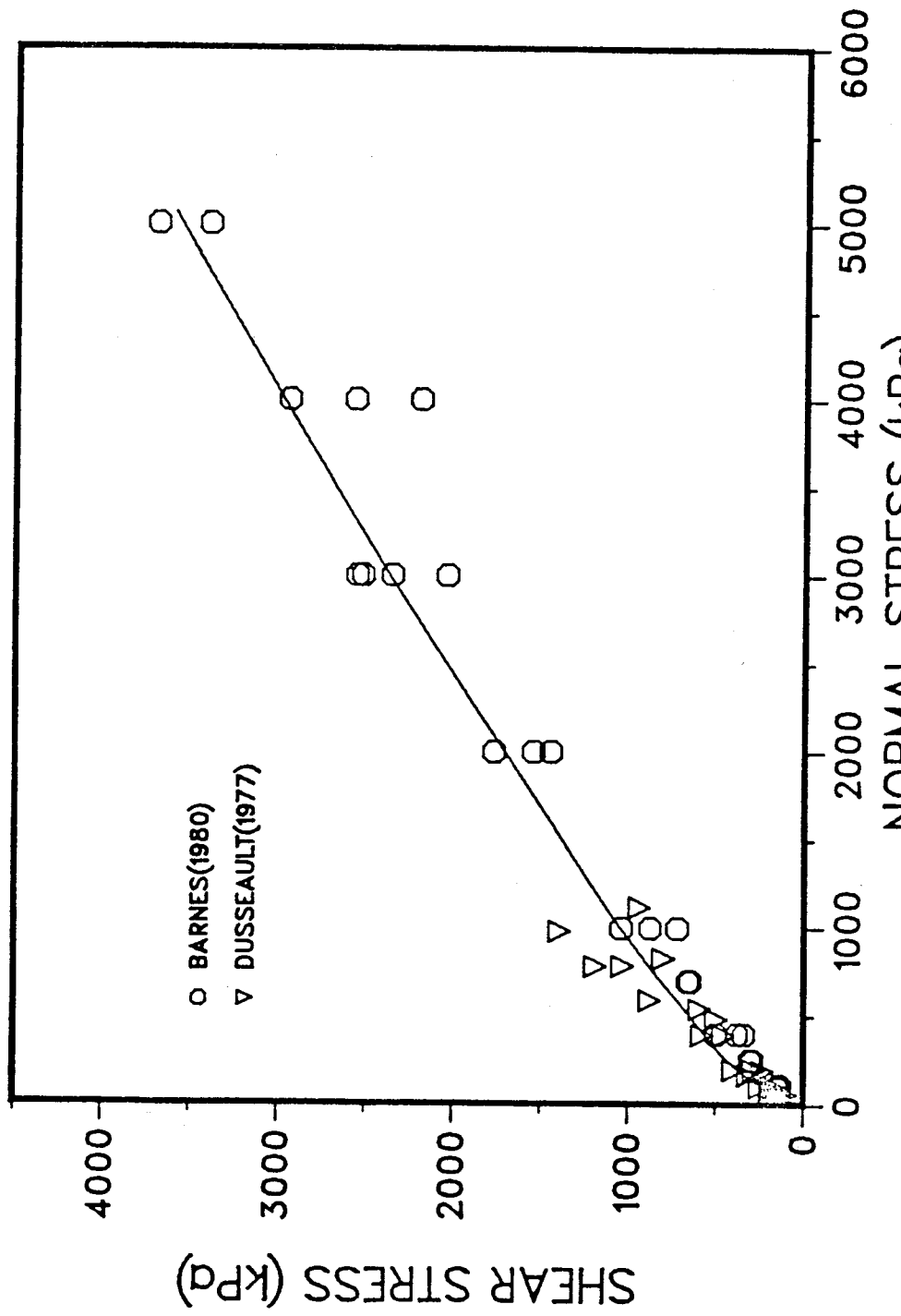

Figure 3.6 DIRECT SHEAR TEST DATA ON SAMPLES WITH SATURATED BULK DENSITIES < 2.17 g/cm³, AND ≥ 2.00 g/cm³

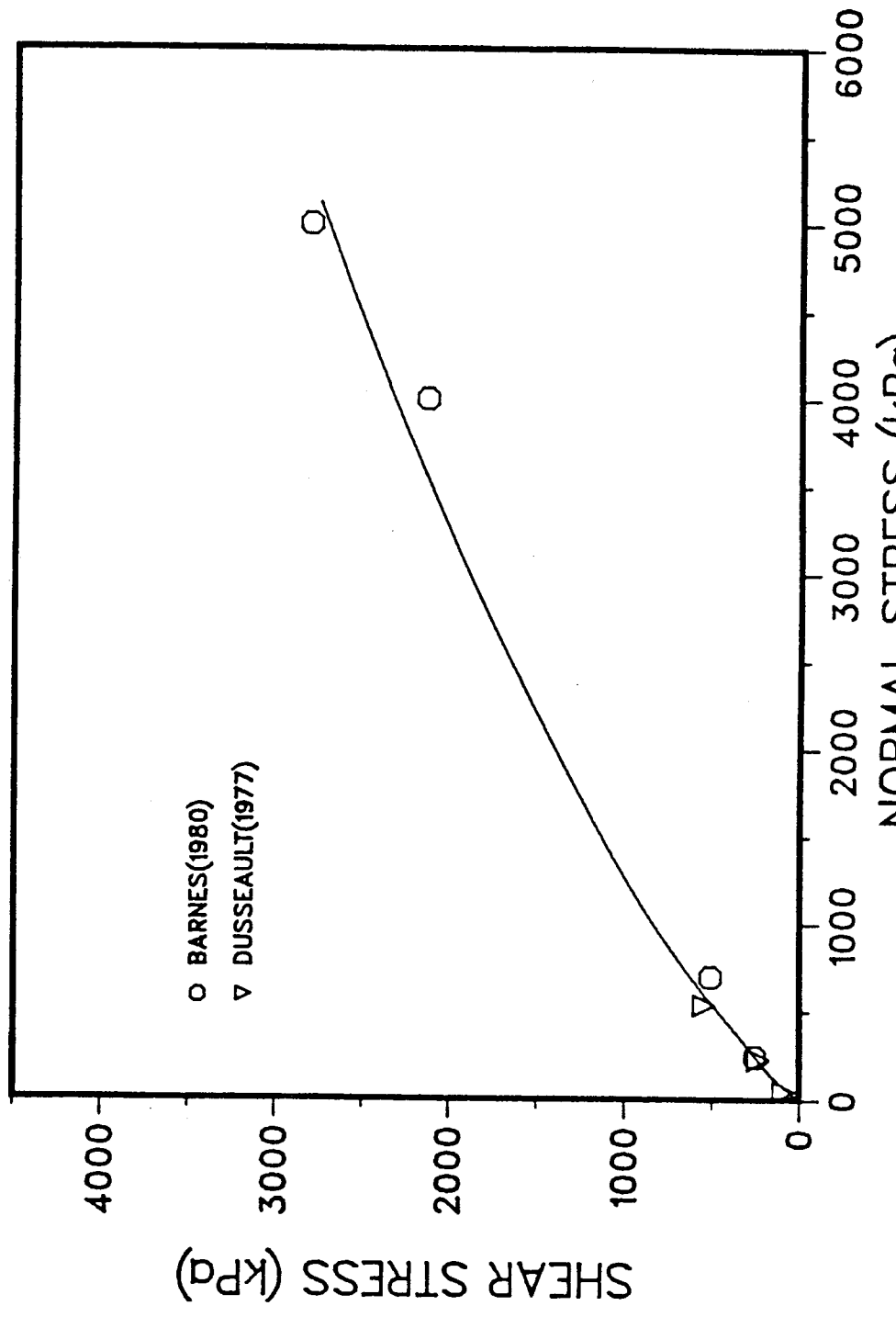

Figure 3.7 DIRECT SHEAR TEST DATA ON SAMPLES WITH SATURATED BULK DENSITIES < 2.00 g/cm³, AND ≥ 1.97 g/cm³

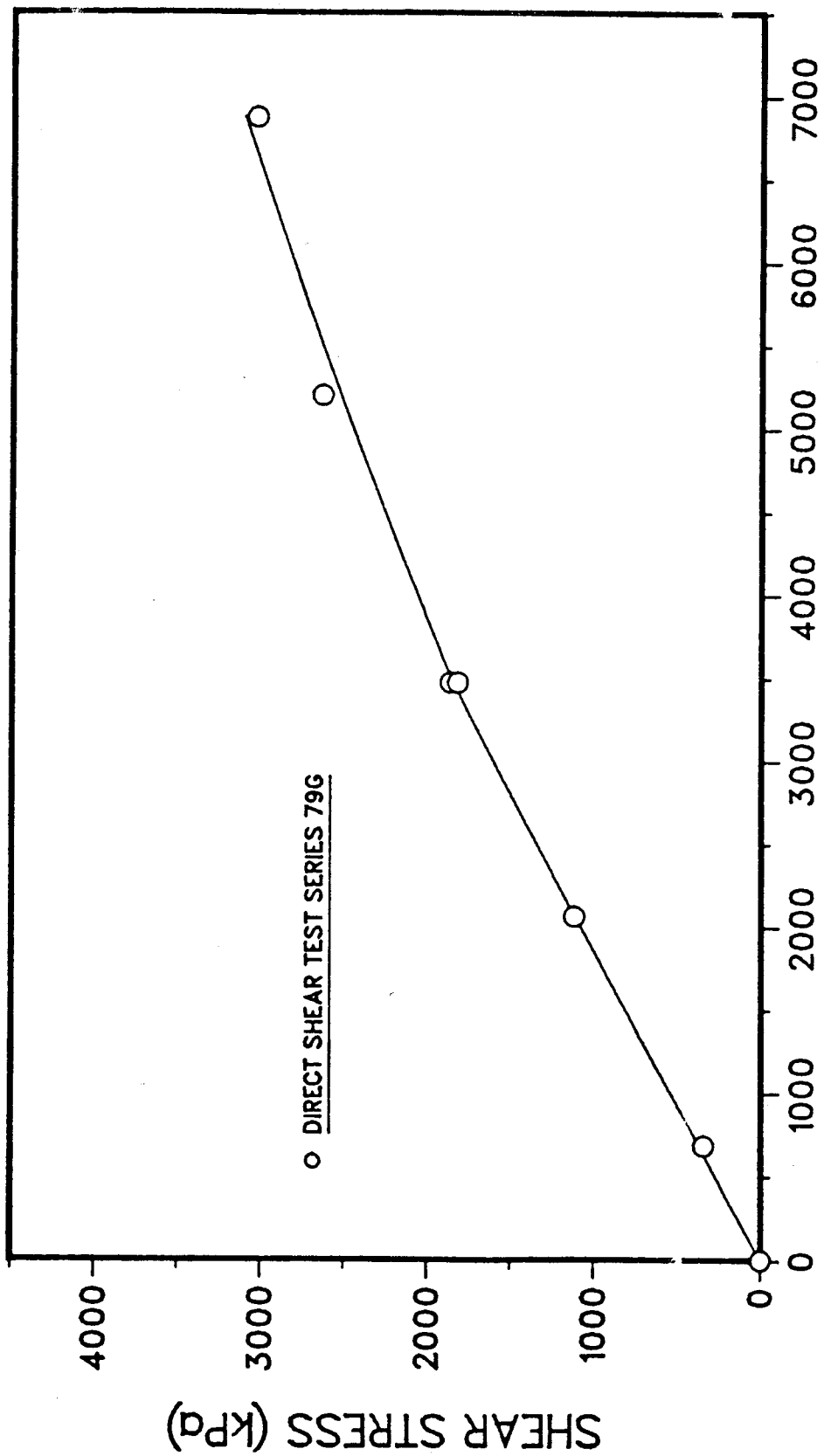

Figure 3.8 DIRECT SHEAR TEST DATA ON SAMPLES WITH SATURATED BULK DENSITIES < 1.71 g/cm³ AND ≥ 1.80 g/cm³

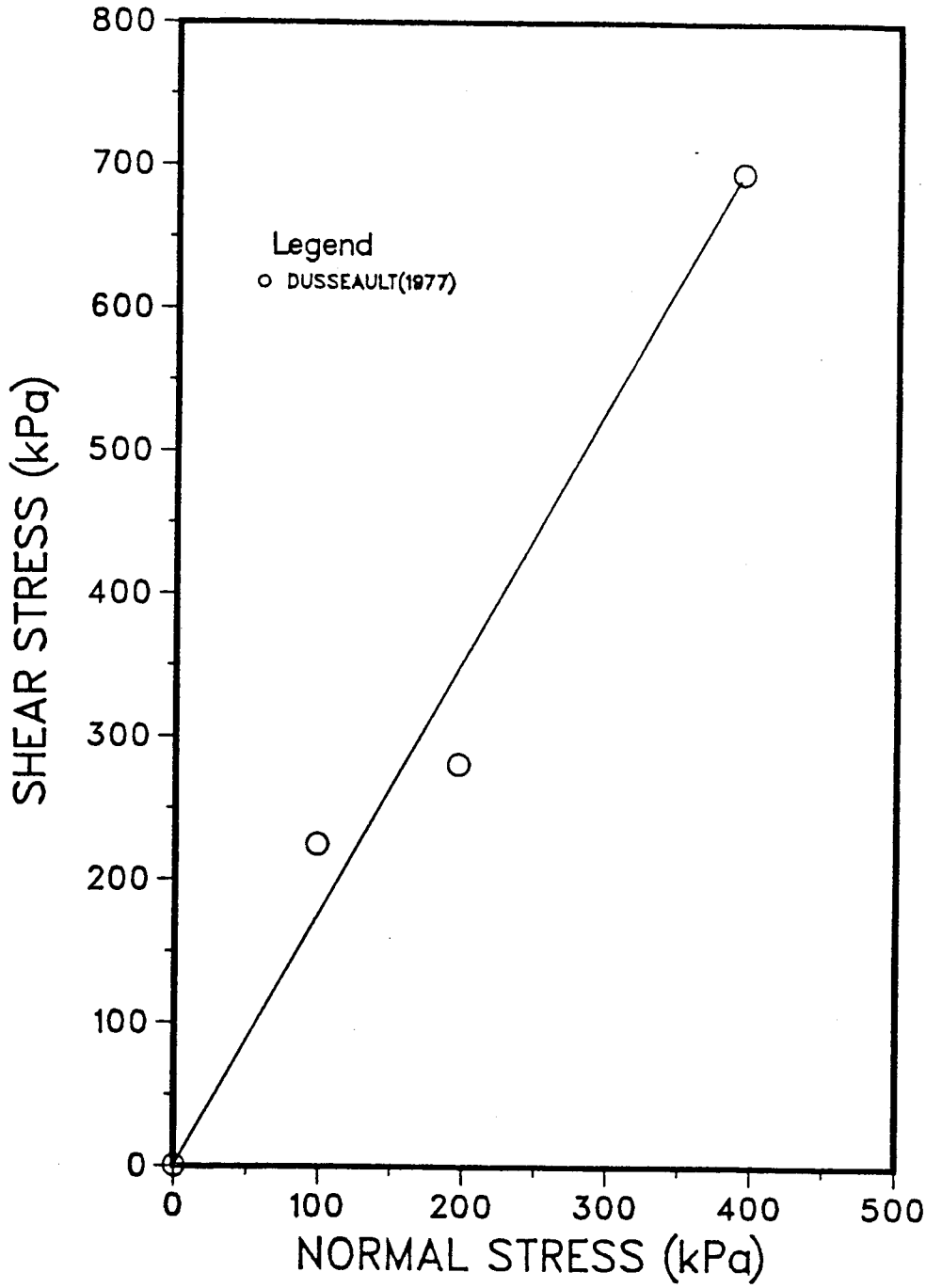

Figure 3.9 DIRECT SHEAR TEST DATA ON SAMPLES WITH SATURATED BULK DENSITIES BETWEEN 2.25 – 2.36 g/cm^3

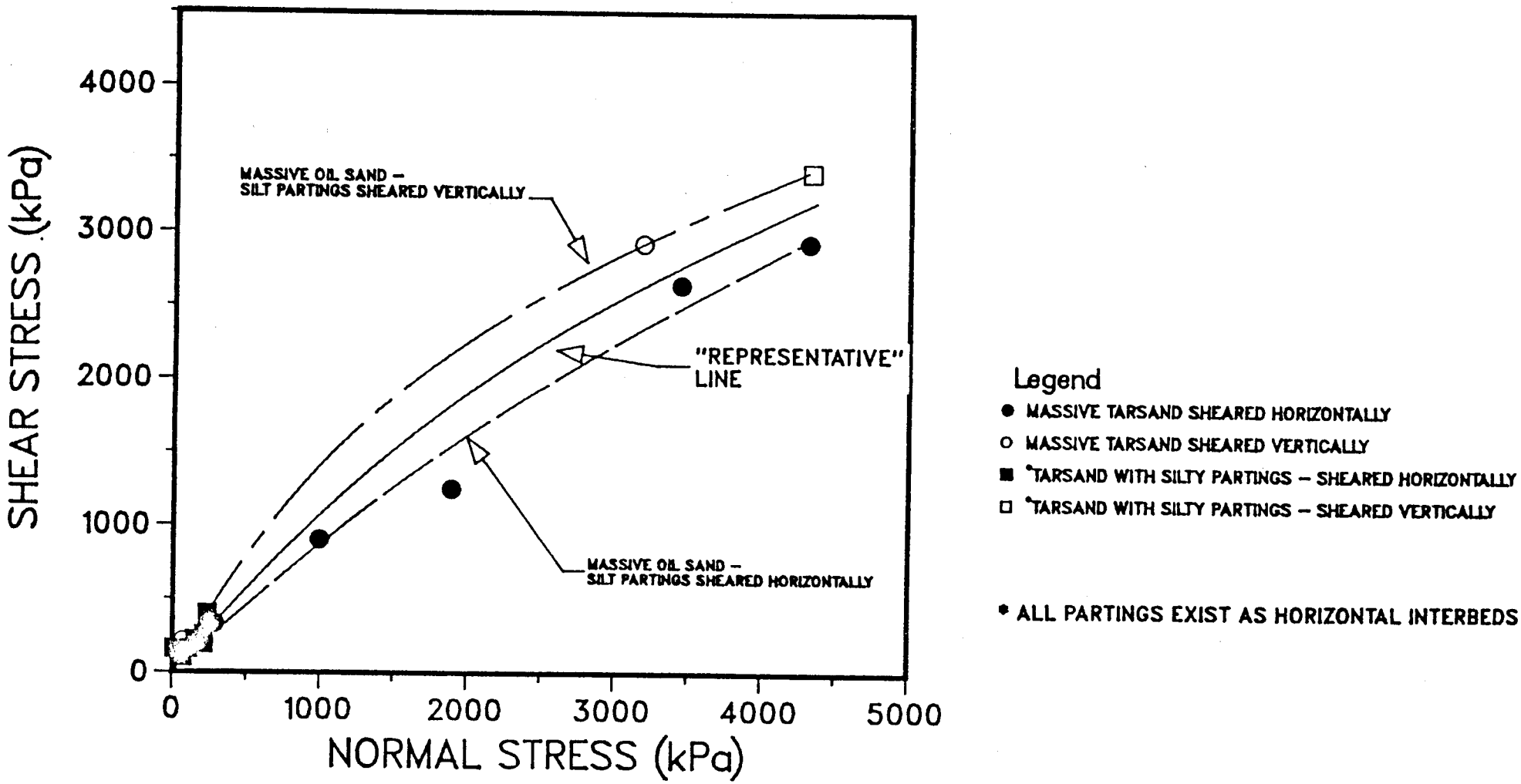

Figure 3.10 LARGE DIRECT SHEAR TEST RESULTS (BROOKER & KHAN, 1980)

indicate that the shear strength of the Athabasca oil sands is anisotropic. It seems that when sheared vertically, oil sands with horizontal silt partings are stronger than similar oil sands sheared horizontally. Despite the apparent anisotropy in the shear strength a "representative" line has been drawn in Figure 3.10. That facilitates later comparison of the test data.

Comparison of the strength envelopes is shown in Figure 3.11. The direct shear test data indicate similar trends to those indicated by the triaxial test data: the oil sands exhibit a curved failure envelope when the bulk density is above 2.0 g/cm^3 and the shear strength increases with the bulk density.

3.3.1.2 The Grand Rapids Formation

The Cold Lake Deposit consists of four separate bitumen-containing intervals: two in the Grand Rapids Formation, one in the Clearwater Formation[1] and one in the McMurray Formation.

Barnes(1980) performed two series of direct shear tests on oil-free outcrop specimens collected from the Grand Rapids "A" and "C" zones. The results are presented in Figure 3.12. The average saturated bulk density of the samples from zone "A" is 2.01 g/cm^3 whereas that of the samples from zone "C" is 2.00 g/cm^3.

---

[1]Dusseault(1980) speculated that the shear strength of the oil sands in the Clearwater Formation is around 2.5 to 3.5 MPa at a normal effective stress of 5 MPa and that visual core examination does not suggest significant anisotropy in strength or in stress-strain behaviour.

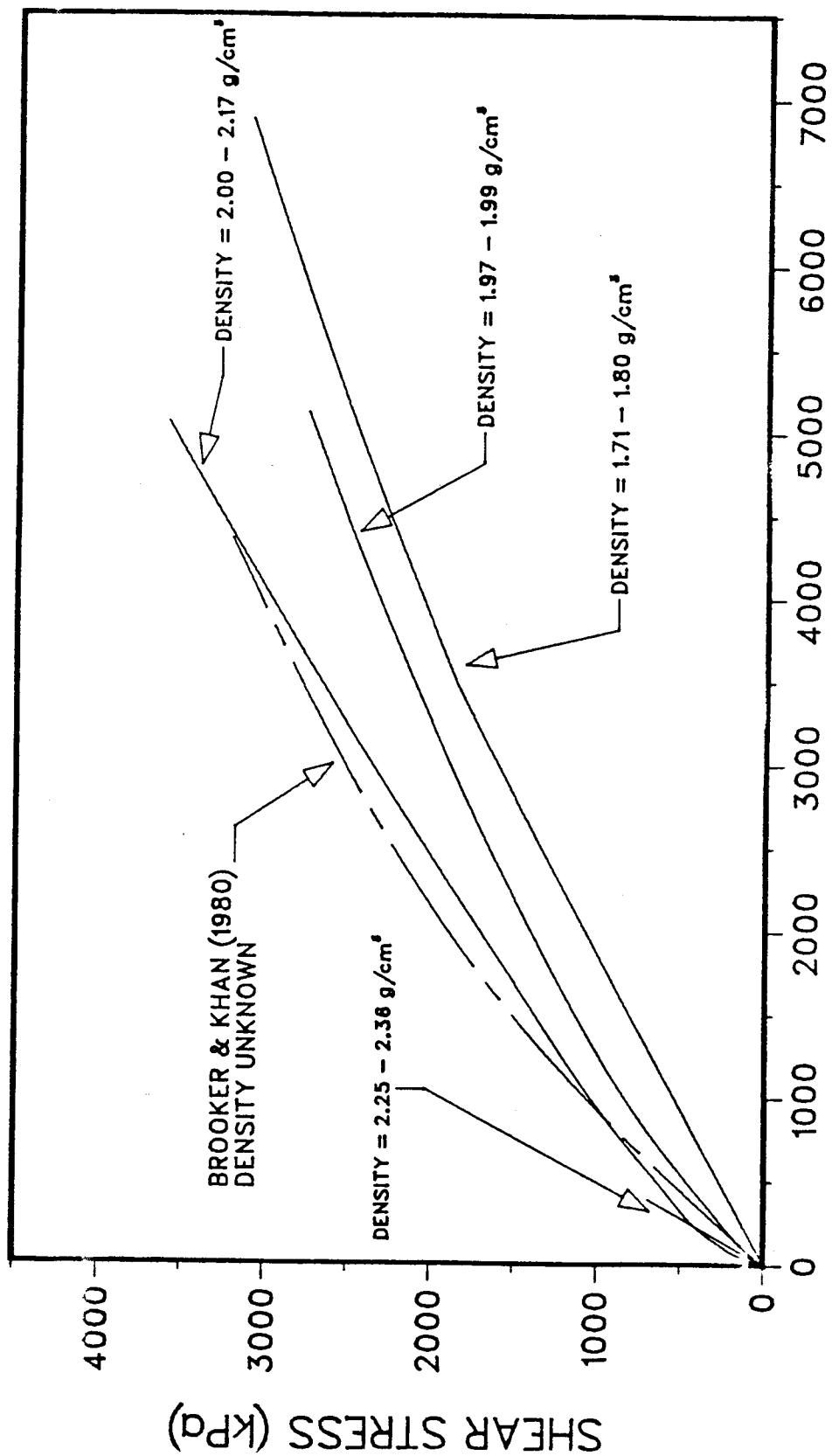

Figure 3.11 COMPARISON OF STRENGTH ENVELOPES FOR DIFFERENT BULK DENSITY RANGES

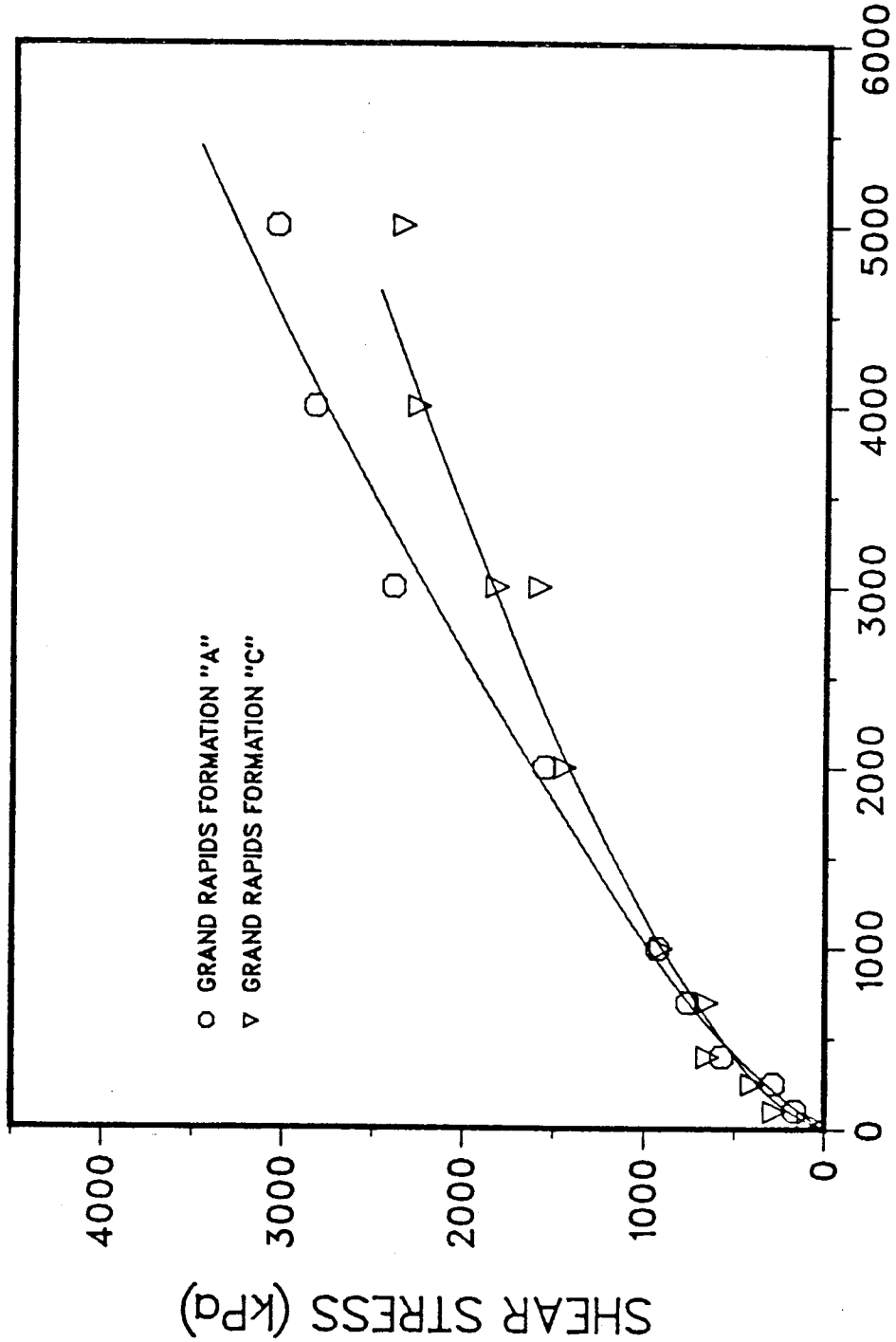

Figure 3.12 DIRECT SHEAR TEST DATA ON OIL-FREE SAMPLES FROM GRAND RAPIDS FORMATIONS "A" AND "C"

Since the two average bulk densities are so similar, the difference in strength between the two zones indicated in Figure 3.12 is probably real: the Grand Rapids Formation "A" generally has a higher shear strength than the Grand Rapids Formation "C".

There is no indication of what the in-situ saturated bulk density might be in the Grand Rapids Formation. Thus it is difficult to estimate how close to the actual in-situ strength are the strength data shown in Figure 3.12.

3.4 Comparison of Results of Direct Shear Tests and Triaxial Tests

To assess the validity of the results obtained in direct shear tests and triaxial tests, it is useful to compare the strength data provided by the two types of tests. Such a comparison is made in Figure 3.13 for the higher bulk density samples.

Figure 3.13 indicates that the shear strength as measured in triaxial tests is significantly higher than that measured in direct shear tests over the entire confining stress range. There could be a number of reasons for such an observation: in general, the sample size used for direct shear tests are smaller than those employed in triaxial tests. So relatively speaking, the direct shear test samples could on average receive more disturbance than the triaxial test samples during the assembling process of the

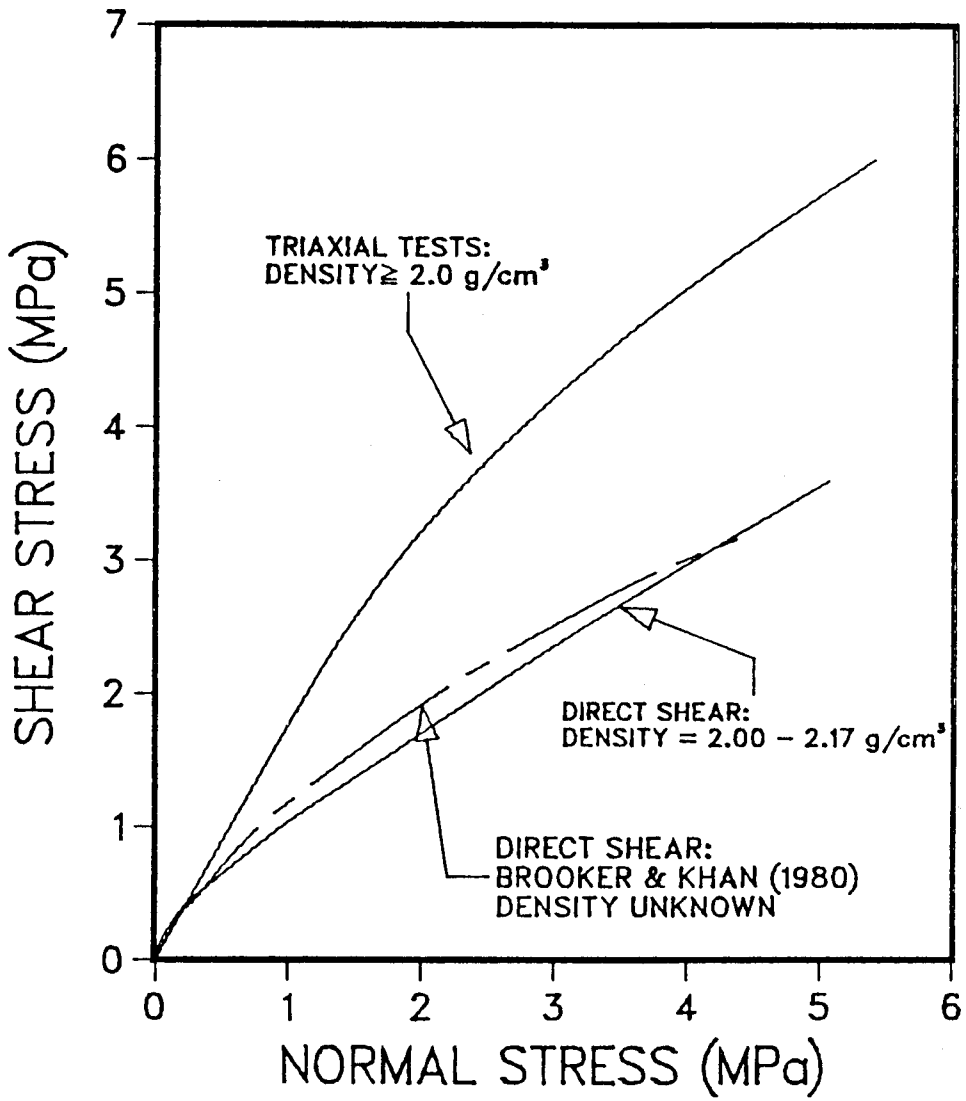

Figure 3.13 COMPARISON OF THE FAILURE ENVELOPES OF OIL SANDS OBTAINED BY TRIAXIAL TESTS AND DIRECT SHEAR TESTS

test set-up. In the case of oil sands, sample disturbance as indicated by a slight decrease of the bulk density could mean a significant reduction in strength.

In addition, the direct shear test is often criticized for effecting a non-uniform condition on the sample which leads to progressive failure across the sample. Both the normal stress and the shear stress are not uniform in a direct shear test, and the lateral (confining) stresses on the sample are unknown and most probably not constant during shear. Because of their locked structure, the oil sands tend to strain-weaken after failure. So they are vulnerable to the effect of progressive failure. As a result, the maximum shear strength of the oil sands as measured in the direct shear test could be considerably lower than the true peak shear strength.

Interestingly, Lambe and Whitman(1979) noted that the friction angle from direct shear tests is generally greater (by perhaps 2°) than the friction angle from triaxial tests, especially for dense sands. The comparison of data upon which this conclusion was drawn was most probably confined to the lower range of normal stress which is of interest to conventional soil mechanics and may not apply to the high normal stress range shown here. For example, Lambe and Whitman quoted the comparison performed by Taylor(1939). In Taylor's paper, the highest normal stress used was only 0.41 MPa (60 psi).

When the factors discussed above are put together, the trends observed in Figure 3.13 appear to be reasonable. However, it must be cautioned that the observation is based on a limited amount of data (especially direct shear test data at high confining pressures). The data correspond to samples from different locations. That means variation in mineralogy, lithology, and stress history are factors to be considered also. Therefore, the observed difference shown in Figure 3.13 should be considered tentative.

3.5 Unconfined Compression Tests

Since the oil sands have negligible real cohesive strength, they consequently should have relatively small unconfined shear strength. When sheared in an undrained manner in an unconfined compression test, negative pore pressures caused by dilation pull the sand grains together and result in an apparent uniaxial shear strength. However, because the confining pressure on the sand structure has such a dominant effect ($\phi' = 60°$) on the oil sand strength, the undrained unconfined shear strength of oil sands is of little real practical importance.

Figure 3.14 plots the undrained unconfined shear strength of Athabasca oil sands against the bulk density. No discernible pattern could be found in Figure 3.14 and this is by no means unexpected. The uniaxial shear strength depends on the disturbance to the sand structure, the magnitude of the negative pore pressure caused by dilation

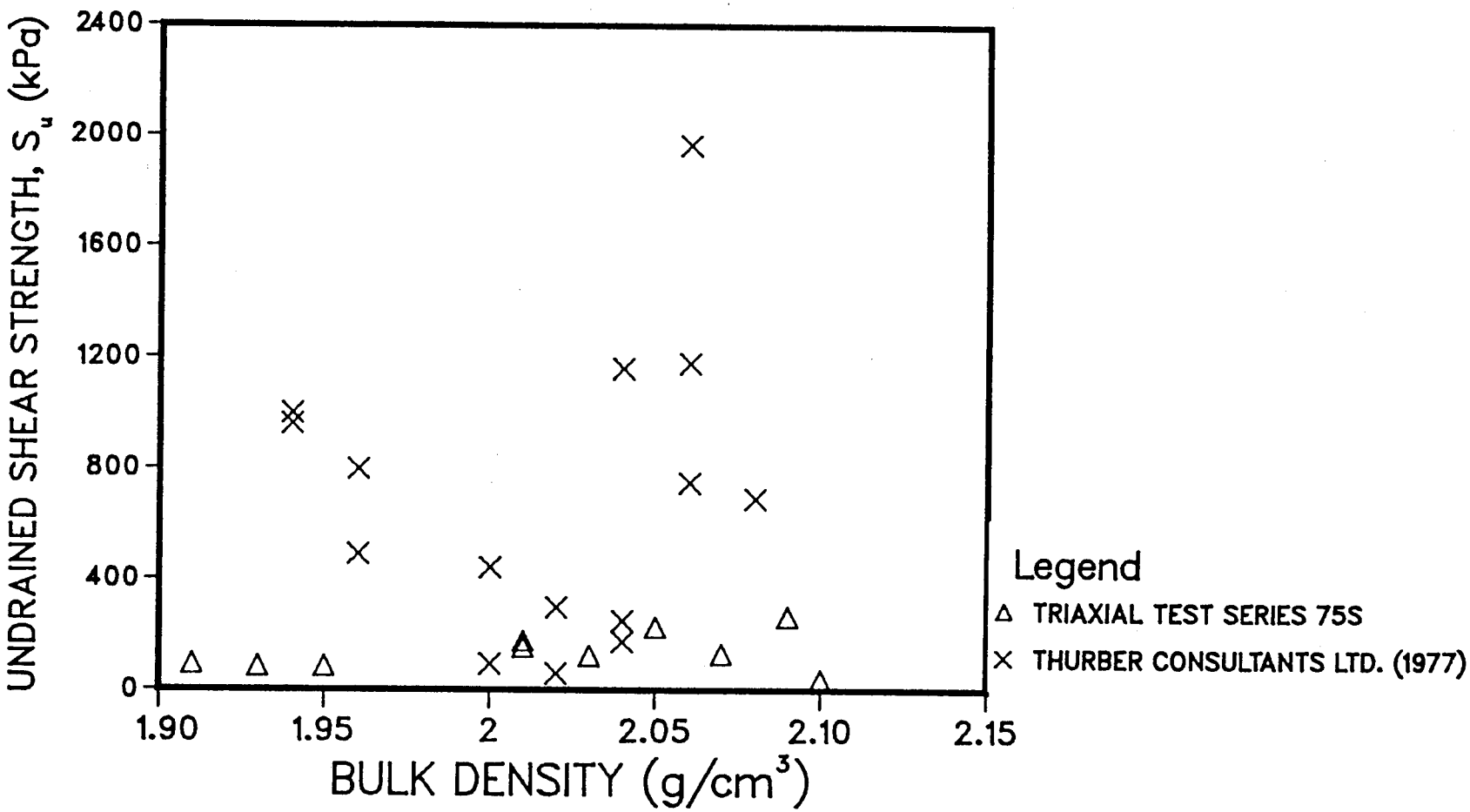

Figure 3.14 UNDRAINED SHEAR STRENGTH OF ATHABASCA OIL SANDS DERIVED FROM UNCONFINED COMPRESSION TESTS AS A FUNCTION OF THE BULK DENSITY

in the sample and the bulk density. Since the negative pore pressure attainable is a function of a number of variables such as dilation, the water and bitumen content (and therefore permeability) and temperature, it is insufficient to express the uniaxial shear strength of oil sands solely as a function of the bulk density.

Figure 3.15 depicts the variation of undrained uniaxial shear strength with depth. It appears that the uniaxial shear strength decreases with increasing depth. That is probably because deeper oil sands experience a larger magnitude of stress relief during the coring process. Consequently, the dissolved gases in the pore fluid have a greater tendency to come out of solution and impose a severer disruption on the locked fabric of the oil sand matrix. Actually, as shown by the triaxial tests, the effect of confining pressure results in a large increase of shear strength with depth.

3.6 Correlation of Strength with Bulk Density

Figure 3.16 illustrates an attempt to correlate the strength of the Athabasca oil sands with the bulk density. Clearly, there is considerable scatter among the data points. While it may be possible to draw approximate upper and lower bounds to the data, such an approach is probably not of any practical use except to show the influence of disturbance.

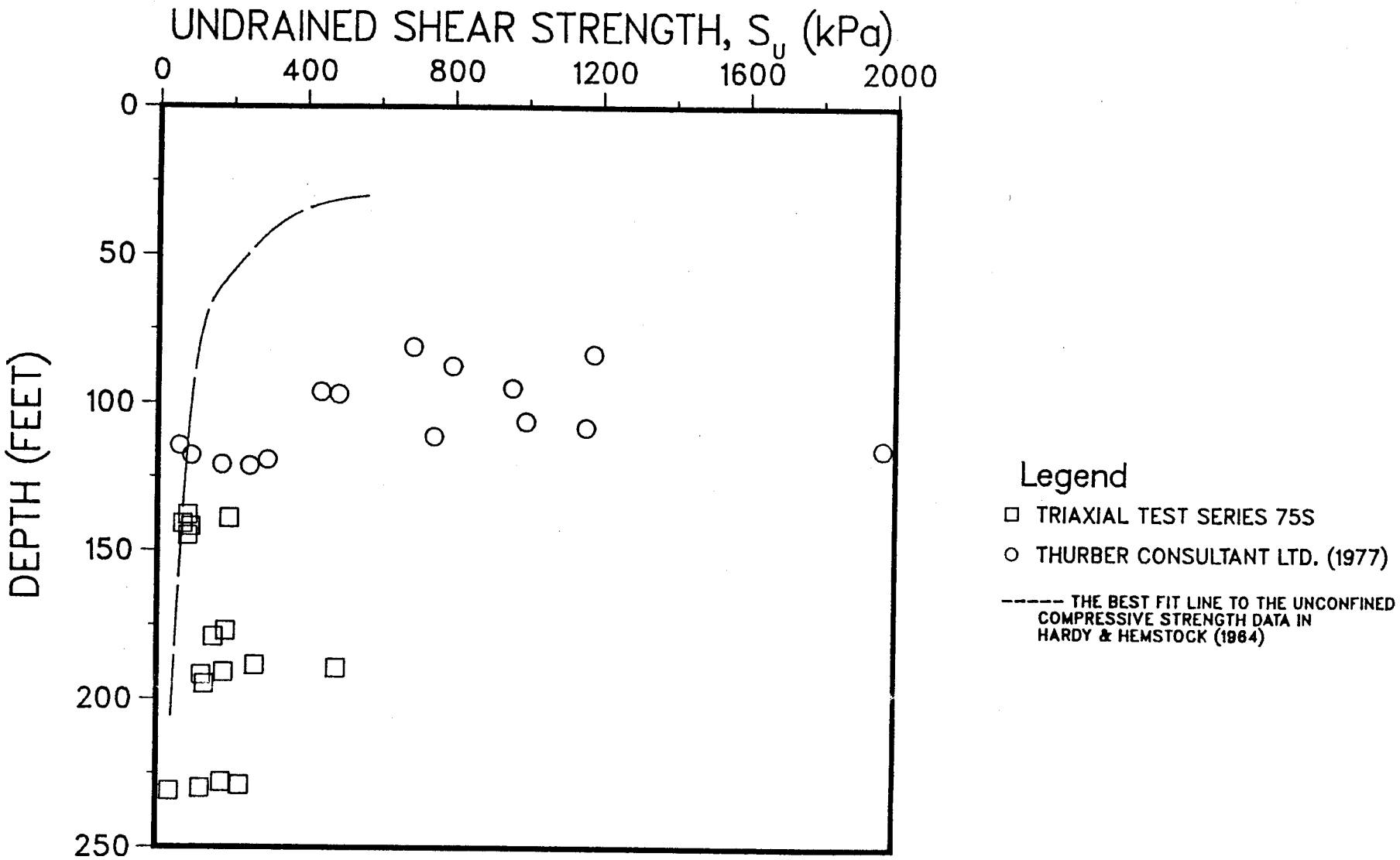

Figure 3.15 A SUMMARY OF THE UNCONFINED COMPRESSION TEST RESULTS AS A FUNCTION OF DEPTH

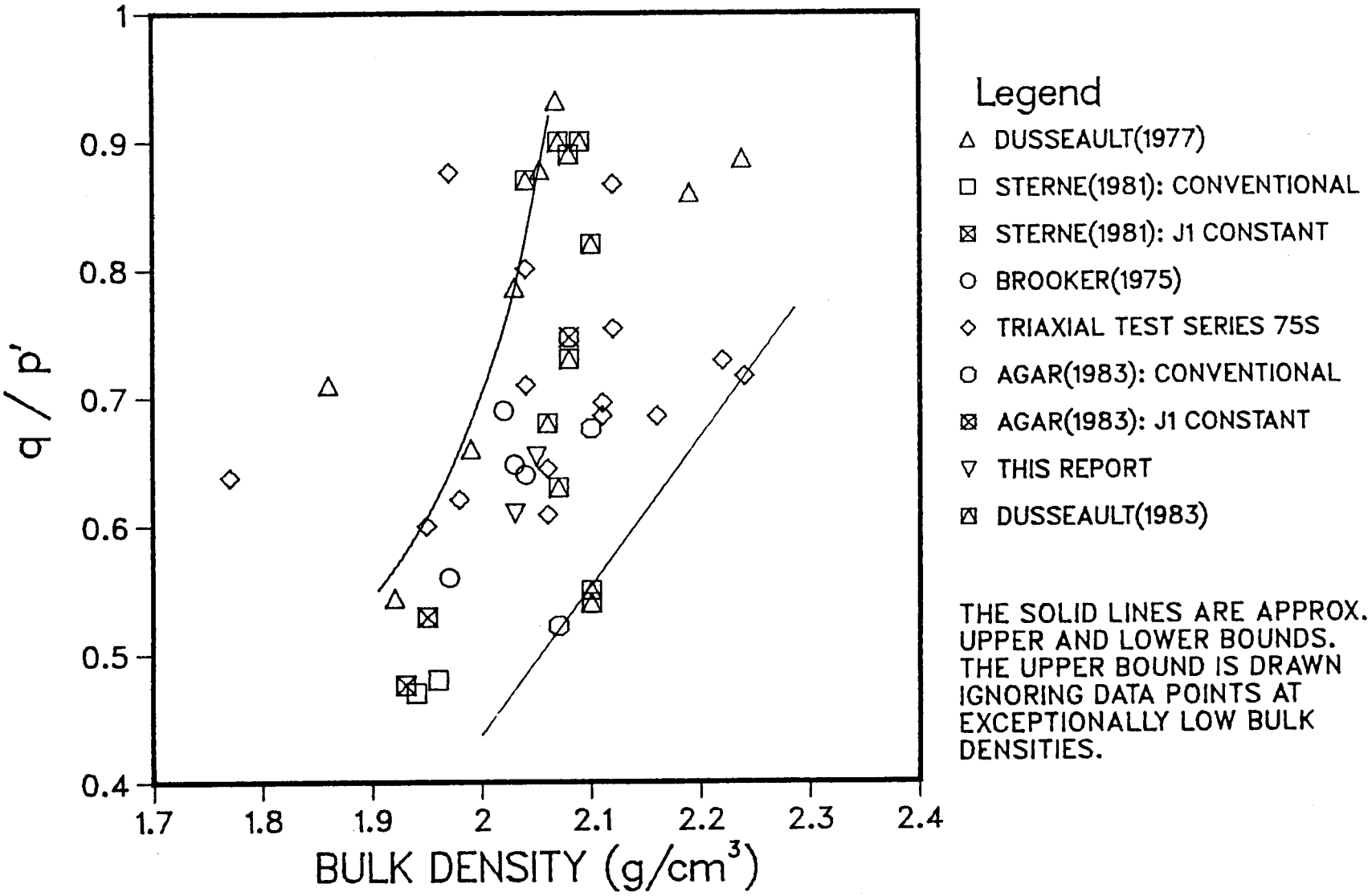

Figure 3.16 CORRELATION OF q / p' WITH BULK DENSITY

3.7 Notion of "Tensile Strength" in Oil Sands

To answer the question of the real source of strength in Athabasca oil sands, Dusseault(1977) investigated a number of possibilities. He discovered that cementation agents such as carbonates, silica, siderite, pyrite and iron oxide occur predominantly on a local basis. Clay minerals generally are present only in small quantities. While the factors of bitumen viscosity, pore pressure, and pore fluid surface tensions may be relevant, they could not possibly contribute significantly to the strength of Athabasca oil sands. It follows that Athabasca oil sands should have relatively little to no real tensile strength. Furthermore, the tensile strength of Athabasca oil sands is expected to be unpredictable since the factors mentioned above can vary within a very wide range.

These conclusions are consistent with the shear strength data shown in Figures 3.1 to 3.11. Extrapolating these data to zero normal stress, the Athabasca oil sands could probably have a maximum tensile strength of 20 kPa caused by the interlocked sand structure. While the majority of the test data is on Athabasca oil sands, the limited amount of data on the Grand Rapids Formation shown in figure 3.11 also suggests that the oil sands in the Grand Rapids Formation zones "A" and "C" have small to no tensile strength.

Chapter 4

RESIDUAL SHEAR STRENGTH OF OIL SANDS

4.1 Residual Strength based on Direct Shear Tests

The residual shear strength of the Athabasca oil sands and the Grand Rapids Formation "A" obtained in direct shear tests is presented in Figures 4.1 to 4.3. Although the Athabasca oil sands have a different mineral content from the Grand Rapids sand zone "A", it appears that the residual friction angle of oil sands varies within a fairly narrow range. As shown in Figure 4.4, the residual friction angle ranges from 30° to 33°.

This is consistent with the observation that the residual friction angle of sand in general stays within a relatively limited range. For example, the residual friction angle of "medium fine sand" is approximately 31.7° (Lambe and Whitman, 1979).

4.2 Residual Strength based on Triaxial Tests

The residual shear strength of Athabasca oil sands as measured in the triaxial tests is plotted in Figure 4.5 using the p'-q quantities at the residual stage of the triaxial tests. The "residual" K -line is translated to the corresponding Mohr-Coulomb failure envelope in Figure 4.6. This plot shows that the "residual" Mohr envelope of Athabasca oil sands is linear when the normal stress is below approximately 7 MPa. The slope of that portion of the

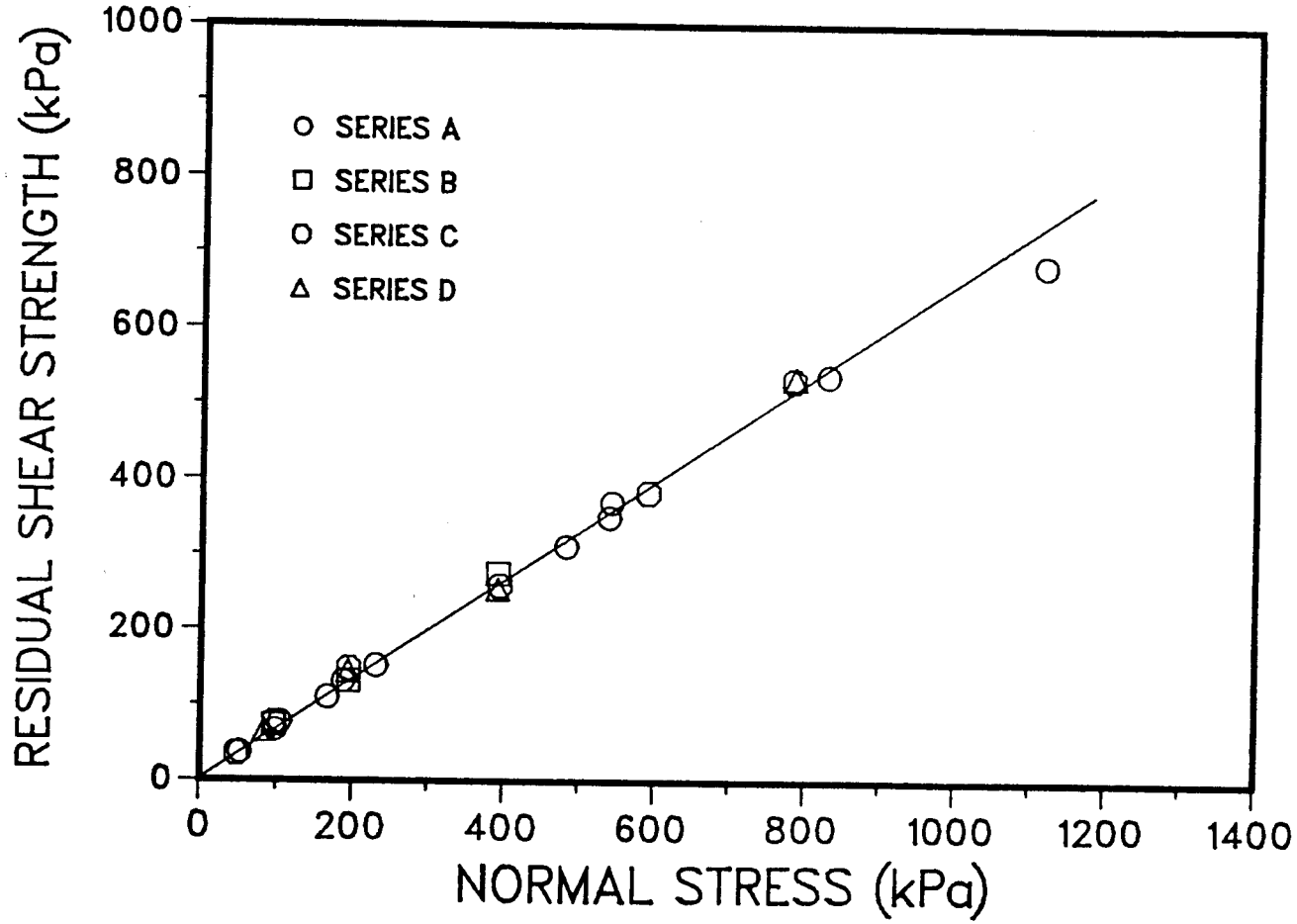

Figure 4.1 RESIDUAL SHEAR STRENGTH DATA FROM DIRECT SHEAR TESTS BY DUSSEAULT(1977)

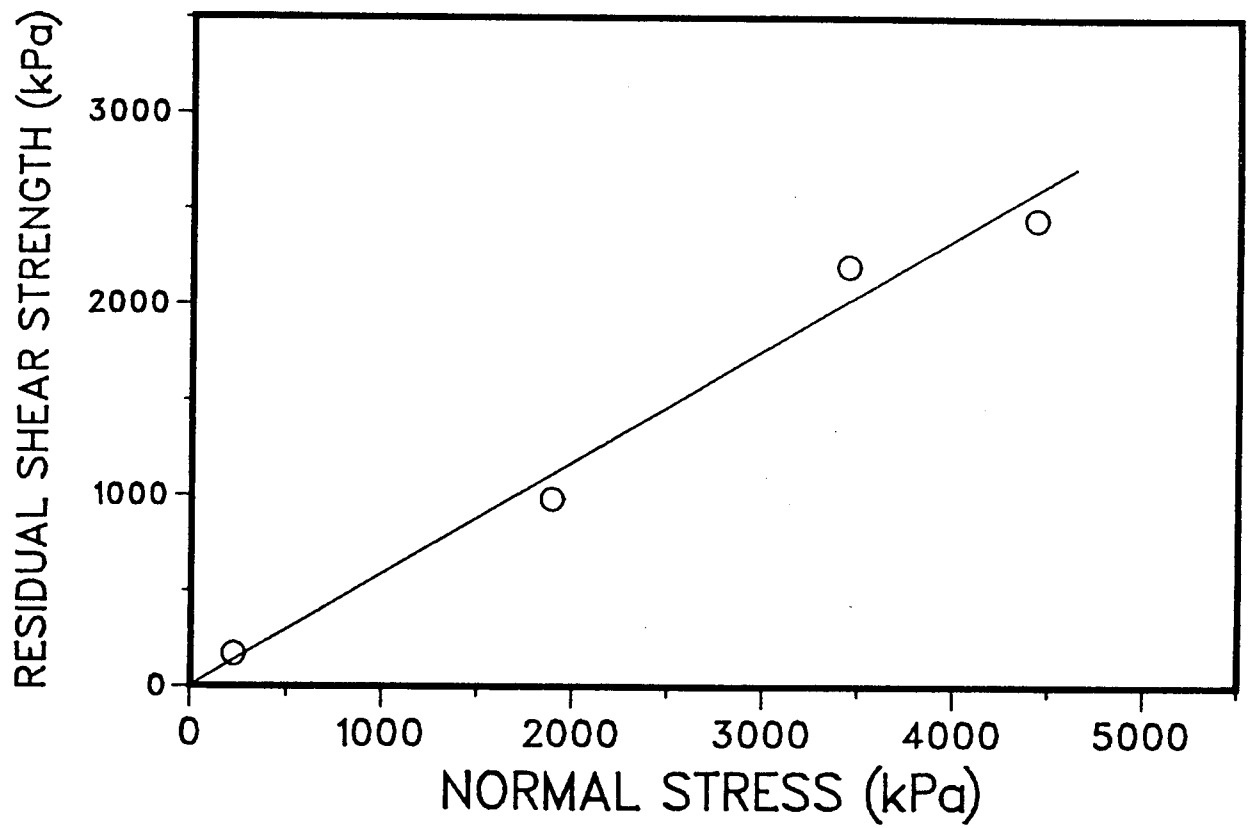

Figure 4.2 RESIDUAL SHEAR STRENGTH OF MASSIVE TARSAND – SHEARED HORIZONTALLY IN LARGE DIRECT SHEAR TESTS (BROOKER & KHAN, 1980)

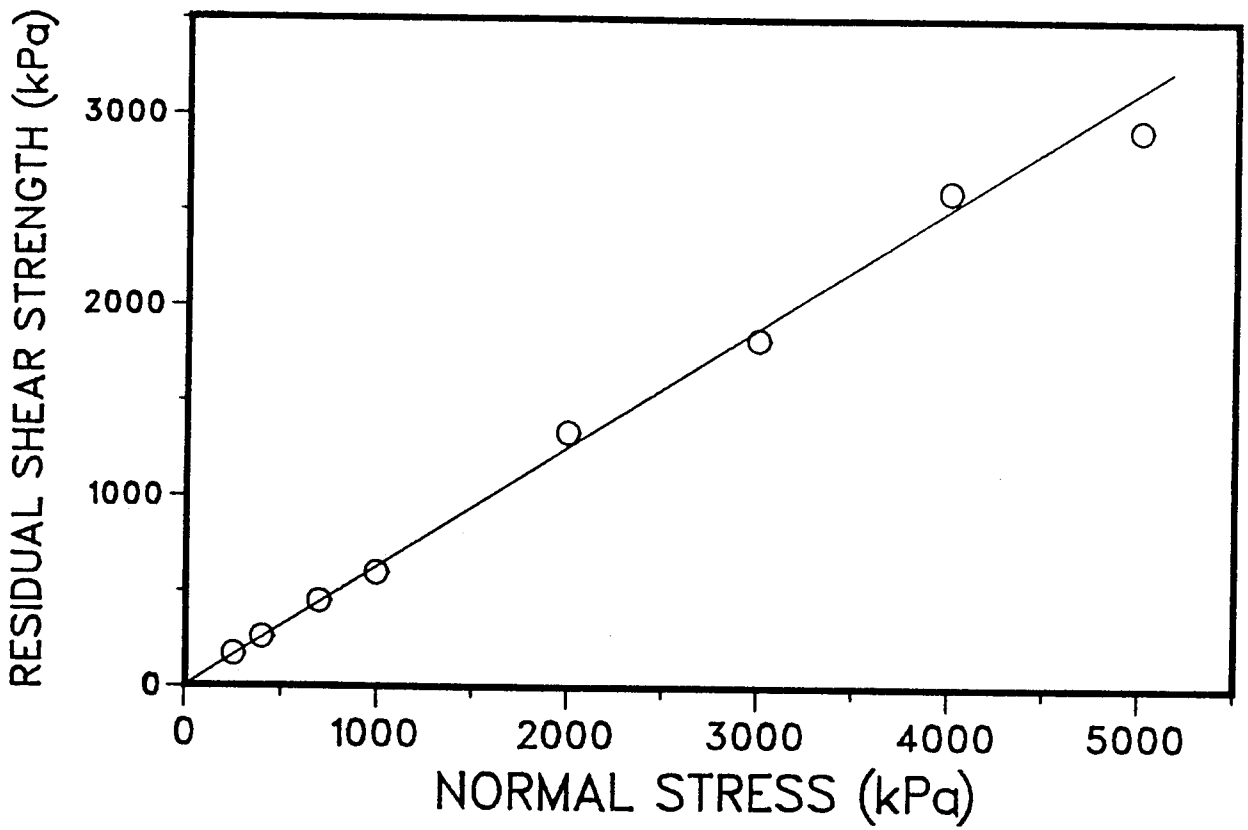

Figure 4.3 RESIDUAL SHEAR STRENGTH DATA FROM DIRECT SHEAR TESTS FOR GRAND RAPIDS FORMATION A BY BARNES(1980)

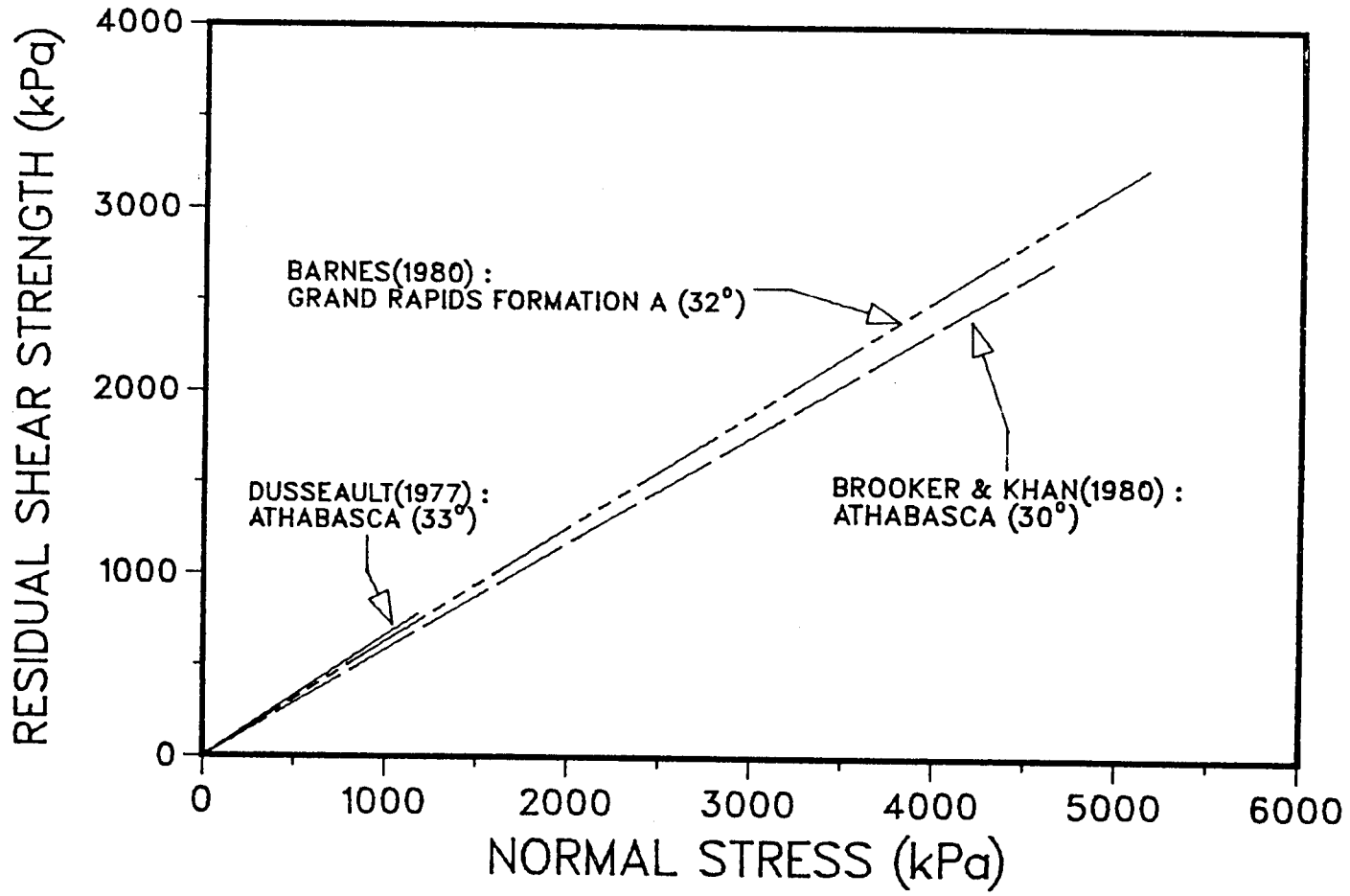

Figure 4.4 COMPARISON OF THE DIRECT SHEAR TEST ENVELOPES FOR THE RESIDUAL STRENGTH OF ALBERTA OIL SANDS

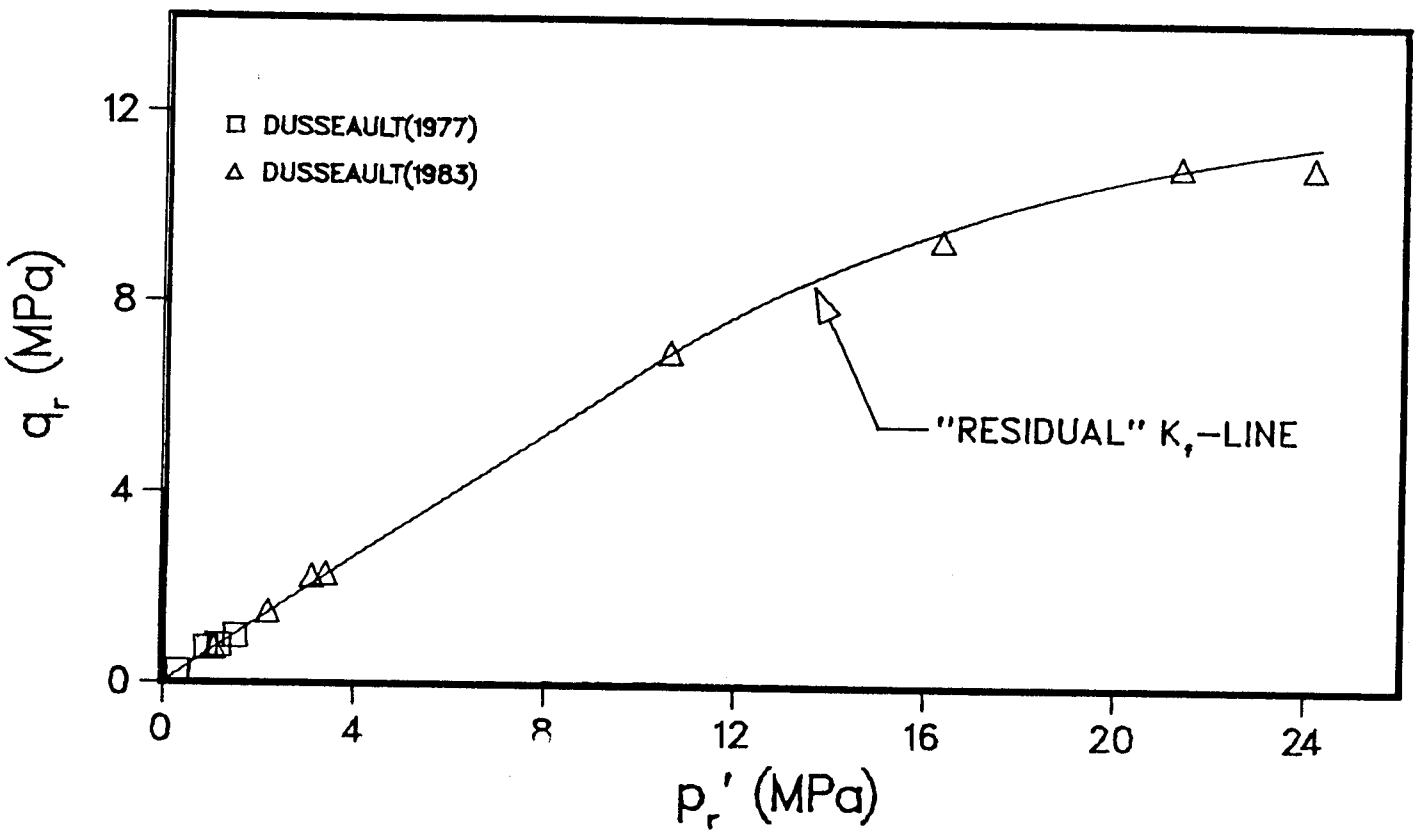

Figure 4.5 RESIDUAL SHEAR STRENGTH OF ATHABASCA OIL SANDS AS MEASURED BY TRIAXIAL TESTS

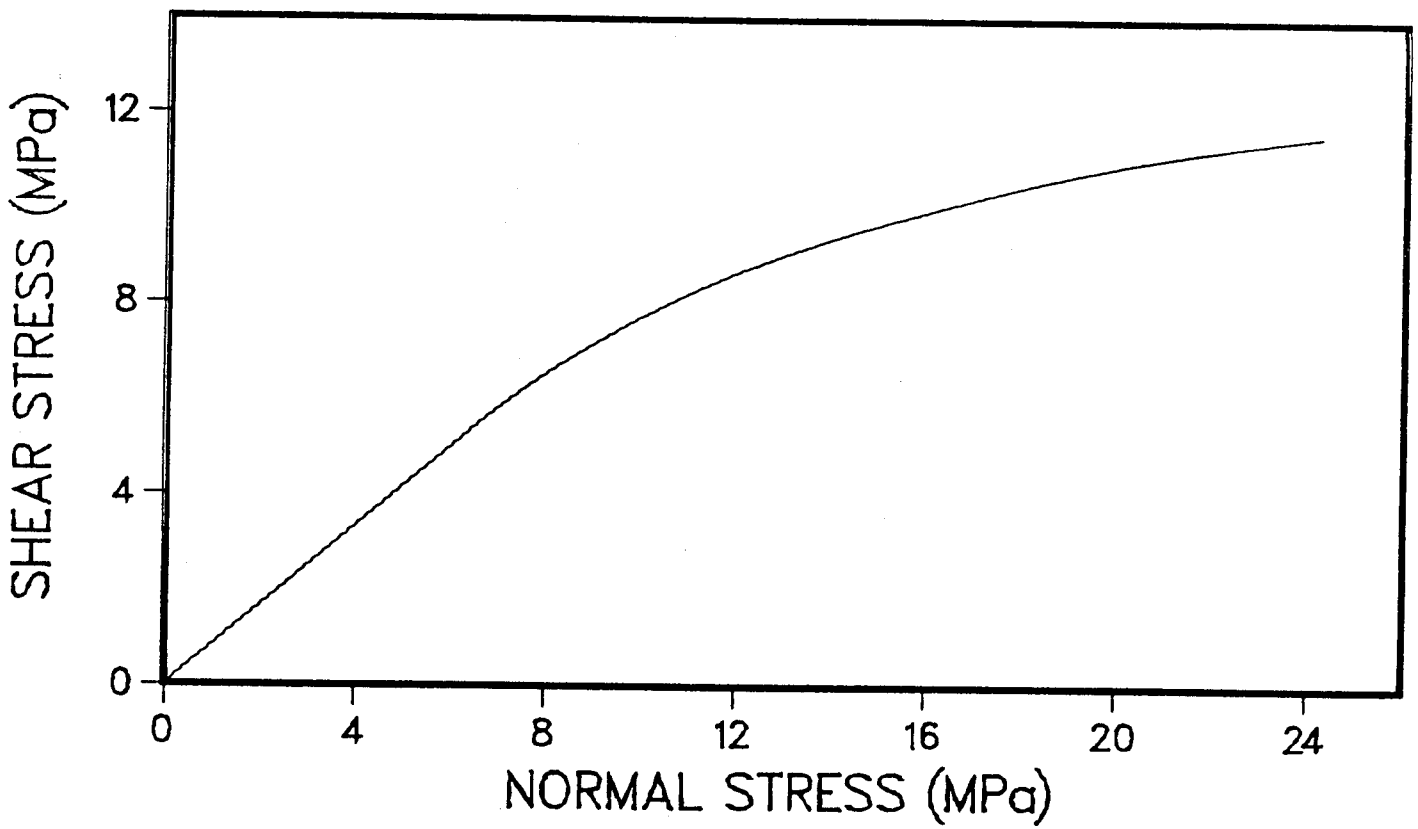

Figure 4.6 MOHR ENVELOPE FOR THE RESIDUAL SHEAR STRENGTH OF ATHABASCA OIL SANDS BASED ON TRIAXIAL TESTS

envelope is about 40°. Above 7 MPa, the slope of the residual envelope, that is, ϕ ', starts to decrease. At the normal stress of 24 MPa, the slope of the curve is no more than 10°.

The decrease of the ϕ ' angle with increasing normal stress could be attributed to the crushing of the sand grains. As explained previously, the oil sands have a dense, interlocked structure. At low normal stresses, the sand grains tend to roll over each other when put under a shear stress. The amount of grain crushing is relatively small. However, as the normal stress increases, it reduces the dilatant tendency of the oil sands. Consequently, when the shear stress forces the oil sand to deform, the straining would have to be achieved increasingly by grain-crushing of the oil sand. Breaking of the grains means a reduction of the effective grain size. At the residual stage of a triaxial test under high normal stress, the crushing of the grains must have significantly reduced the effective grain size of the sand matrix in the failure zone. As a result, the ϕ ' angle decreases.

This phenomenon had not been observed in direct shear tests on oil sands. Presumably, that is because the normal stress in those tests had not been carried to a level high enough to cause significant grain-crushing.

4.3 Comparison of the Residual Failure Envelopes derived by Triaxial and Direct Shear Tests

The residual Mohr envelope obtained from triaxial tests is compared with the residual envelope obtained from direct shear tests in Figure 4.7. Clearly, the triaxial test results show a greater residual strength than that obtained by direct shear testing.

Several factors might contribute to such a discrepancy. First of all, to reach the residual strength in a direct shear test on oil sands, multi-reversal of the shearing action along the failure plane is required. That is very different from the uni-directional shearing action in a triaxial test where the amount of strain on the failure plane is limited. Furthermore, the stress field obtained in a triaxial test can be considerably different from that in a direct shear test. It has been demonstrated in section 3.4 that the difference between the stress-strain conditions in the triaxial test and the direct shear test could lead to considerable differences in the measured peak shear strength of the oil sands. In the case of the peak strength, the triaxial test also provided higher estimations of the strength. Perhaps, the same factors are at work in both cases. Although the triaxial residual strength is considerably greater than residual strength values for sands quoted in the literature (Lambe and Whitman, 1979), these literature values have generally been obtained by direct shear testing on subrounded to subangular sand grains. The

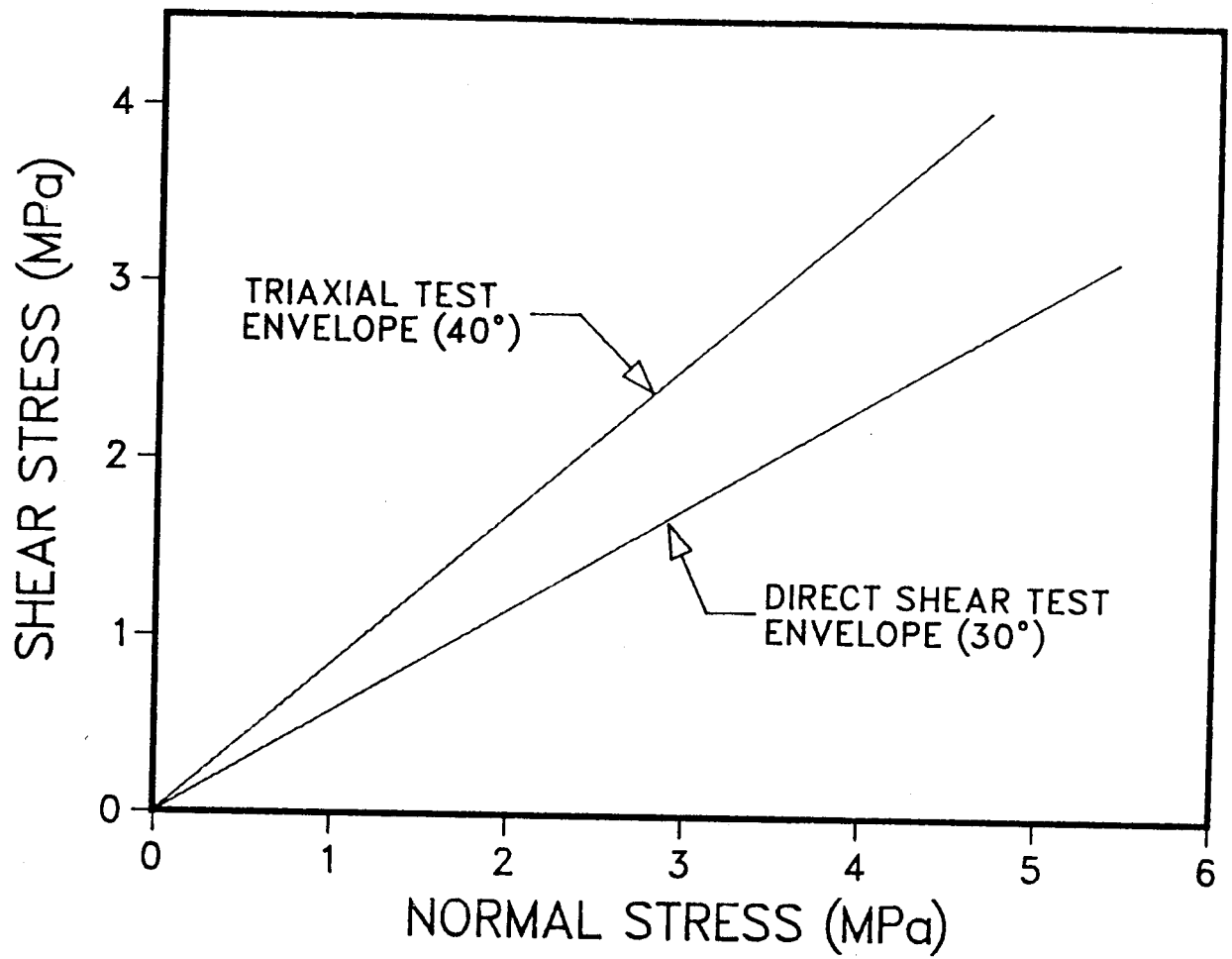

Figure 4.7 COMPARISON OF THE RESIDUAL FAILURE ENVELOPES OF ATHABASCA OIL SANDS

highly angular shape of oil sand grains may be the cause of the high residual strength found in triaxial tests.

4.4 Strain-Weakening of the Oil Sands

As shear-straining is continually imposed on oil sands, the locked sand structure is gradually disrupted. At a certain stage, the sand matrix starts to become less competent strength-wise, and the shear strength of the oil sand drops. In other words, the oil sand has a tendency to strain-weaken.

This tendency is examined in Figure 4.8 which shows the ratio of the residual strength to the peak strength against the effective confining pressure in triaxial tests on Athabasca oil sands. Apparently, the higher the confining pressure, the smaller is the tendency of the oil sands to strain-weaken.

In numerical analysis or simulation of the behaviour of oil sands, the strain-weakening phenomenon needs to be modelled. That requires not only the post-peak modulus values and the residual shear strength, but also the strain at which the residual strength is reached.

The triaxial test provides a means to estimate the "residual" strain, that is, the strain required to bring the shear strength of oil sands to the residual level. However, since triaxial testing on oil sands is usually not carried to the residual stage, there are only scanty data on the residual strain. All the available test results are on

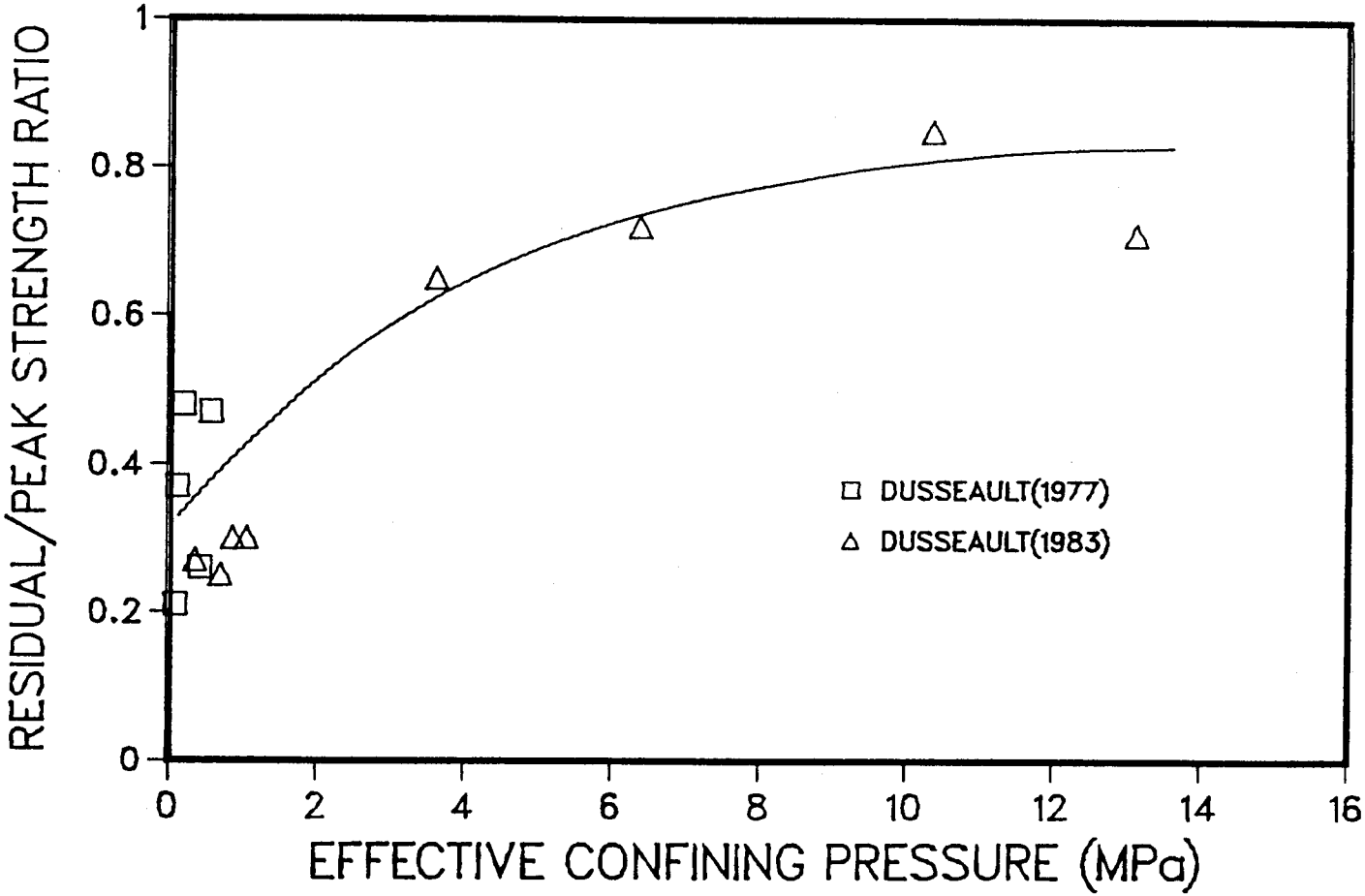

Figure 4.8 THE STRAIN–WEAKENING TENDENCY OF THE ATHABASCA OIL SANDS AS INDICATED BY THE RATIO OF q_r/q_p

Athabasca oil sands and are plotted in Figure 4.9. The residual axial strain increases with the effective confining pressure in a triaxial test. On the other hand, there is no indication from examination of the stress-strain curves that the axial strain at peak failure depends on the effective confining pressure. That means as the effective confining pressure becomes higher, it takes more straining to reach the residual strain from the peak failure strain.

Since the tendency of the oil sands to strain-weaken diminishes and the strain required to reach the residual strength increases as the mean stress level increases, the overall picture is that the Athabasca oil sands become more ductile with higher confining stress. This observation is by no means unusual. For example, it is well-known that carbonate rocks and sandstones tend to be more ductile as the confining stress becomes higher.

Direct shear testing of oil sands is often carried to the stage where the residual strength is reached. Unfortunately, that requires multi-reversals in the shearing action. As a result, the direct shear test results only provide displacements along the shear surface not strains. That makes it difficult to obtain other than qualitative stress-strain data from the direct shear test and for this reason, the direct shear test results have not been included in this discussion on strain-weakening.

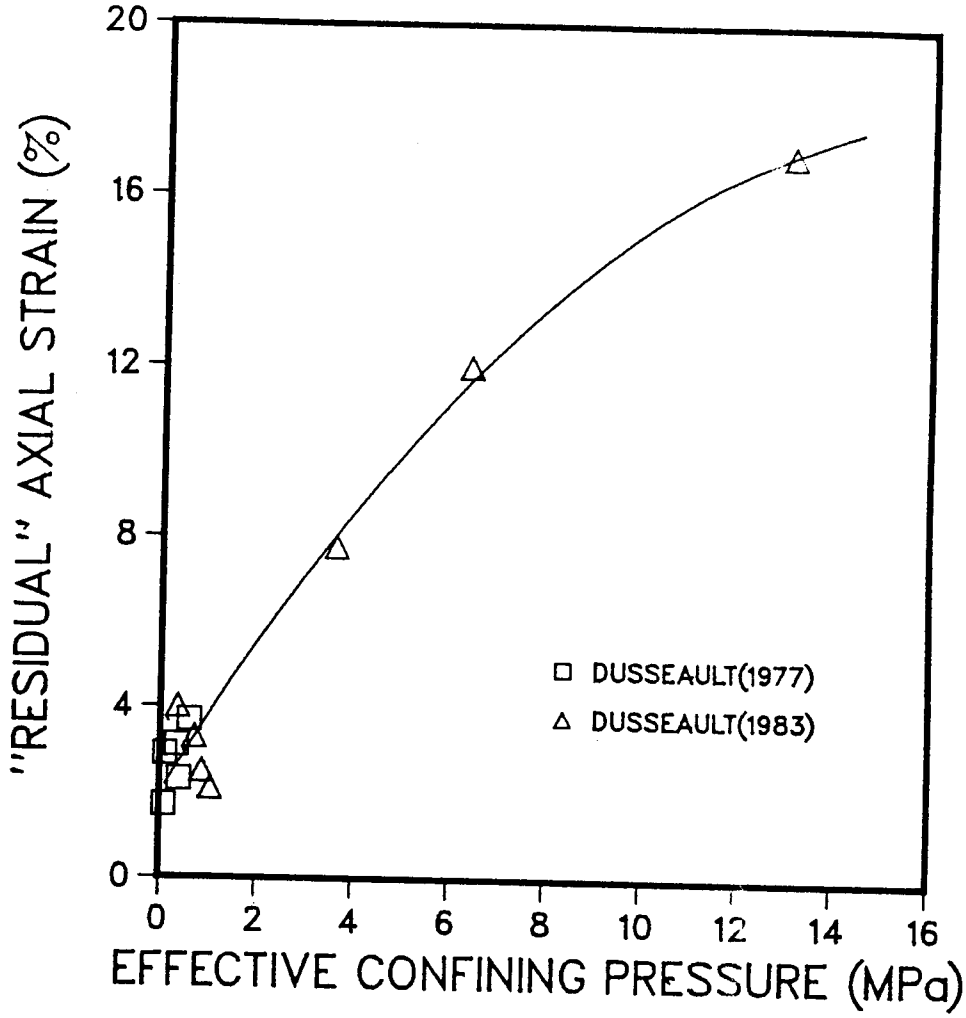

Fig 4.9 THE AXIAL STRAIN AT WHICH RESIDUAL STRENGTH IS REACHED IN TRIAXIAL TESTS ON ATHABASCA OIL SANDS

Chapter 5

DEFORMATION PROPERTIES

5.1 Modulus of Elasticity

The modulus of elasticity can be expressed in terms of the tangent modulus or the secant modulus. In this report, the tangent modulus is used predominantly because it is deemed more appropriate for stress-strain analysis. Therefore, unless stated otherwise, the modulus of elasticity of oil sands as discussed in this report refers to the tangent modulus.

The measurement of the modulus of elasticity may be done by a number of methods. Depending on the test method used, the modulus of elasticity derived may be the drained modulus, the undrained modulus, or the dynamic modulus. The results obtained by these methods are discussed in the following.

5.1.1 Drained Triaxial Tests

Based on the theory of elasticity, the modulus of elasticity (E) can be calculated from measurements of the axial stress and strain in a triaxial shear test. For a standard triaxial test,

$$E = \frac{\partial \sigma_z}{\partial \epsilon_z} \qquad (1)$$

where σ_z = axial stress

and ϵ_z = axial strain.

If ϵ_n = radial strain

ϵ = volumetric strain

and the Poisson's ratio is defined as

$$\nu = - \frac{\partial \epsilon_n}{\partial \epsilon_z} \qquad (2)$$

then citing conservation of volume,

$$\partial \epsilon_z + 2 \cdot \partial \epsilon_n = \partial \epsilon \qquad (3)$$

Substituting equation (2) into (3) and rearranging,

$$\nu = \frac{1}{2} \left(1 - \frac{\partial \epsilon}{\partial \epsilon_z} \right) \qquad (4)$$

Employing equations (1) and (4), the data of the triaxial tests retrieved from the literature were analysed.

The modulus of elasticity values are shown in Figure 5.1 for consolidated-drained triaxial tests. Clearly, the drained elastic modulus of the Athabasca oil sands increases markedly with the confining pressure. The rate of increase of the modulus however decreases with increasing confining pressure. Two envelopes for E are shown, one for normal triaxial tests and another for tests where the confining pressure was cycled on the sample at the beginning of the test. It appears that cycling results in denser samples with higher E values. By extrapolation, the drained modulus of elasticity is apparently zero or

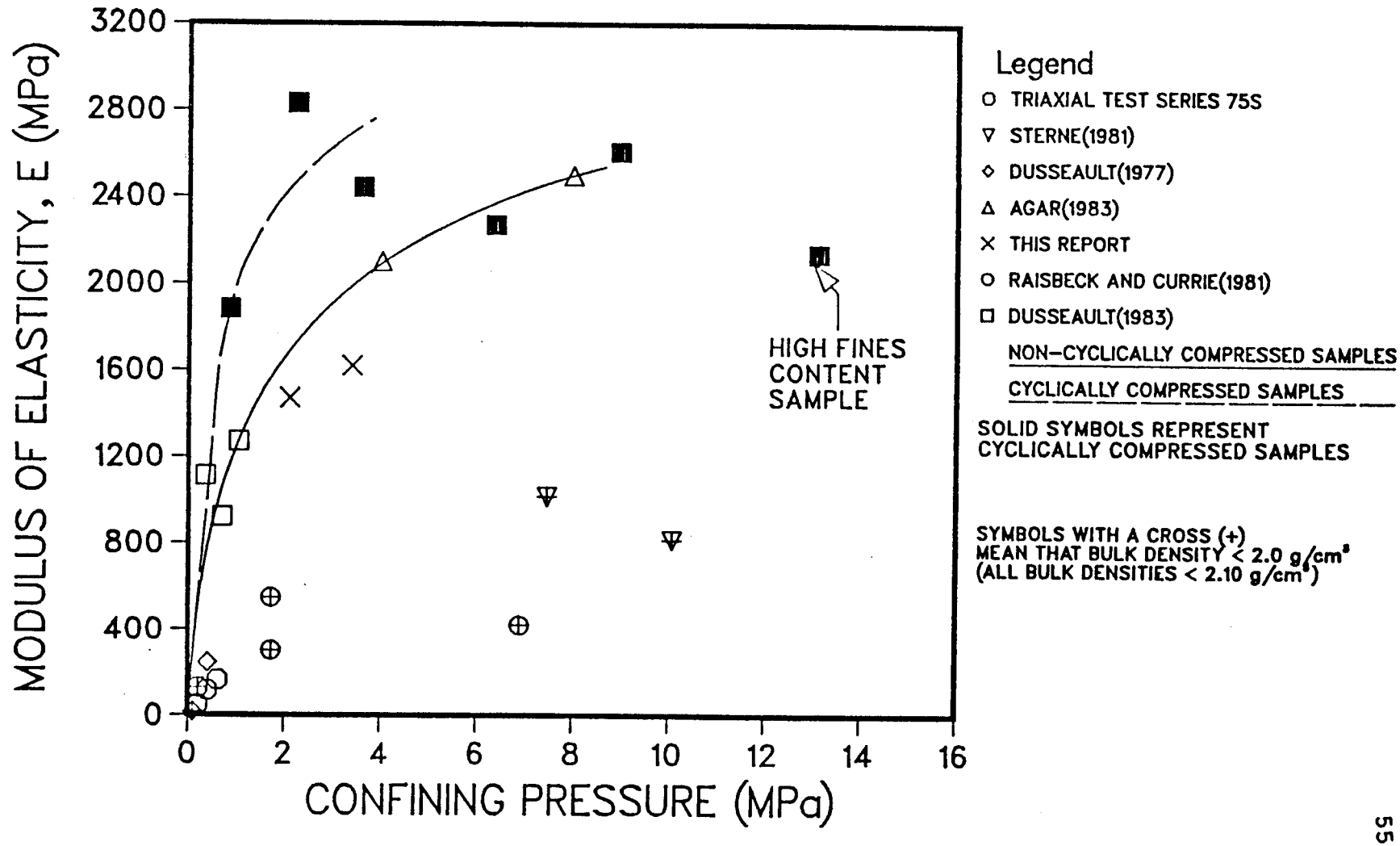

Figure 5.1 VARIATION OF E WITH CONFINING PRESSURE AT AXIAL STRAIN ε_a = 0.25%

negligible at zero confining pressure. This agrees with the description that oil sands are cohesionless materials and they have negligible real cohesive strength (Dusseault, 1977).

It may be noted that those data points with a cross marked inside indicates that these oil sand samples had an initial bulk density less than 2.0 g/cm³. These data points show that sample disturbance has a large effect on the drained modulus of elasticity of oil sands. To obtain representative values of the elastic modulus, undisturbed samples carefully handled are required. Even though the bulk densities were not reported in Raisbeck and Currie(1981), the position of the data points in Figure 5.1 suggests that their samples had bulk densities less than 2.0 g/cm³.

Figure 5.2 shows the K -line for samples with bulk densities greater than 2.0 g/cm³. It also shows the data points derived from Stern(1981) and Raisbeck and Currie(1981) for samples with bulk densities less than 2.0 g/cm³. If Figure 5.2 is contrasted with Figure 5.1, it can be seen that proportionally sample disturbance on oil sands does not reduce the shear strength as much as it reduces the drained modulus of elasticity. In other words, compared with the shear strength the drained modulus of elasticity is more sensitive to sample disturbance.

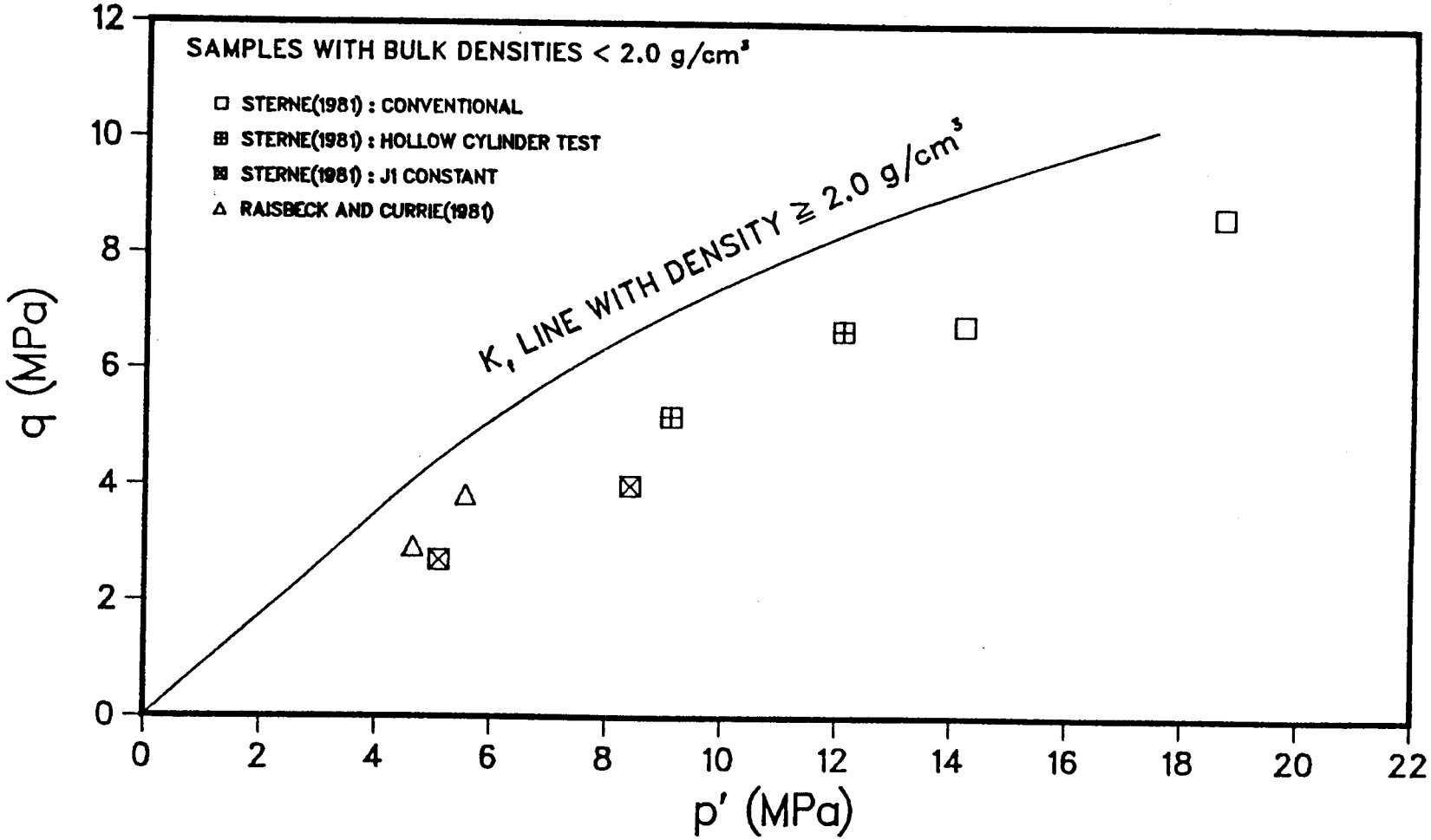

Figure 5.2 POSITION OF DATA POINTS WITH DENSITIES < 2.0 g/cm³ WITH RESPECT TO THE K_f LINE WITH BULK DENSITIES ≧ 2.0 g/cm³

5.1.1.1 Variation of E with Strain

Generally, the measured drained modulus of elasticity of Athabasca oil sands decreases with increasing axial strain because of the curvature of the stress-strain plot. The two triaxial tests performed for this report and shown in detail in Appendix A are typical examples (Figures A.2 and A.3). Consequently, it is necessary to specify the axial strain at which the elastic modulus is calculated.

In Figure 5.1, an axial strain of 0.25% is used. The choice of a suitable axial strain value deserves some consideration. At small strains, for example 0.1%, measurement errors could be caused by problems in the triaxial test such as seating of the end porous stones and the top loading cap in the triaxial cell. Therefore, when the stress and strain are small, even small experimental errors can result in significant uncertainty in the estimation of the tangent elastic modulus. On the other hand, for the modulus to be in the elastic range the chosen strain value has to be considerably smaller than the failure strain. A reasonably good sample of oil sand could have a failure axial strain in the area of 0.8% and most stress-strain curves are linear up to 0.3 to 0.4% strain. Therefore the tangent modulus should be measured between 0.15% and 0.3%. The choice of 0.25% axial strain in Figure 5.1 is therefore arbitrary but a reasonable value for most

tests.

That the modulus of elasticity of Athabasca oil sands is a function of the deviator stress or axial strain is exemplified in Figures 5.3 and 5.4 for the two tests reported in Appendix A. To illustrate the relationship better, the secant modulus has been used in these two diagrams and for the purpose of comparison, the tangent modulus values are plotted in Figures 5.5 and 5.6. The secant values show considerable change at very small percent strains while the tangent values do not significantly decrease until after 0.25% strain. The low strain secant values are much more affected by the experimental errors noted above and are therefore not as reliable.

It is worth noting that the hyperbolic model (Duncan, 1980) appears to describe satisfactorily the stress-strain behaviour of Saline Creek oil sand before failure in conventional triaxial tests (Agar, 1983).

5.1.2 Undrained Triaxial Tests

Consolidated-undrained triaxial tests provide a means to estimate the undrained modulus of elasticity. Because the sample cannot change volume during shear in the undrained test, it would be expected that the stress-strain behaviour would differ from that in drained tests. For this reason, these modulus of elasticity values have been considered separately. In Figure 5.7 , the undrained

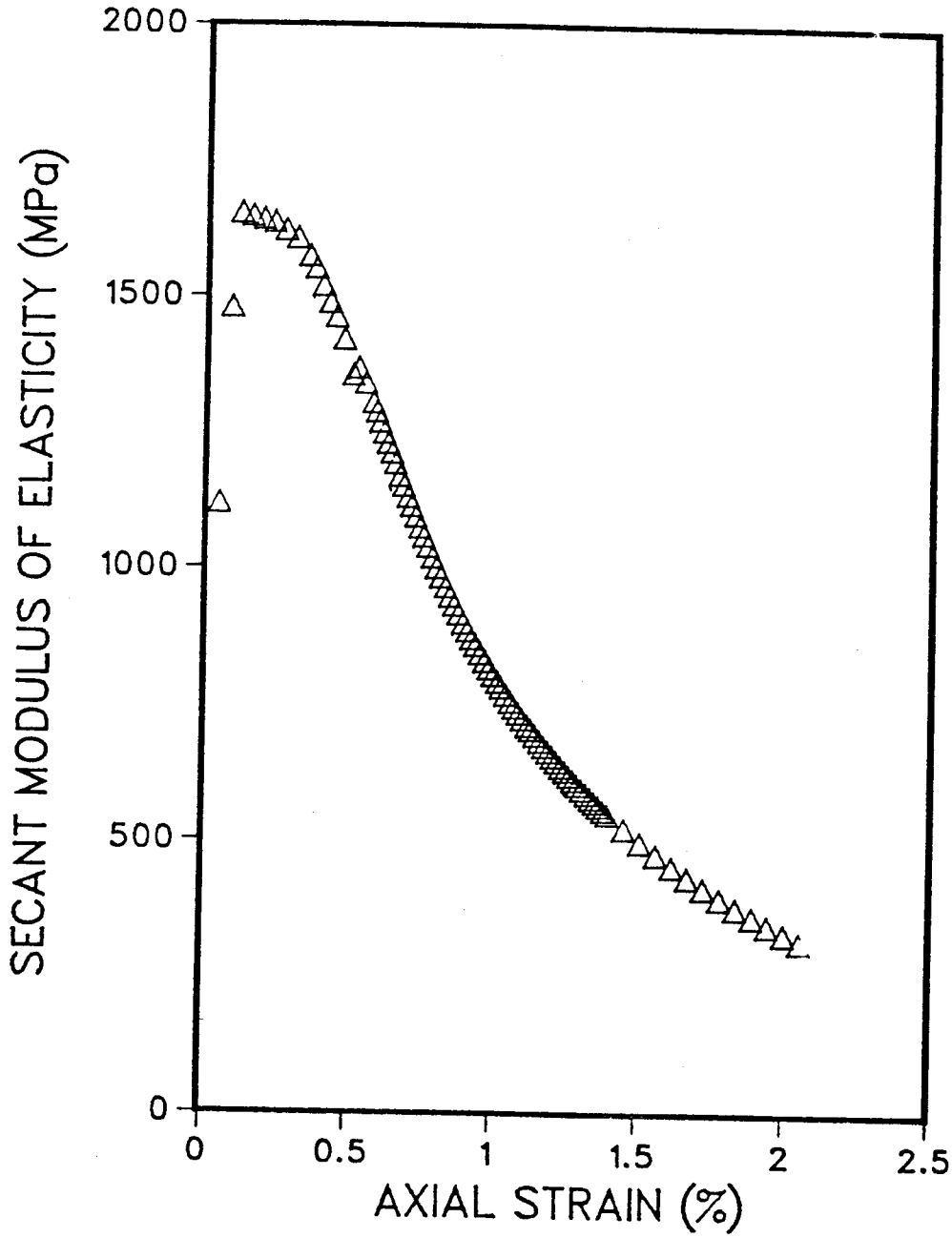

Figure 5.3 The secant modulus of Saline Creek oil sand at a confining pressure of 2.1 MPa

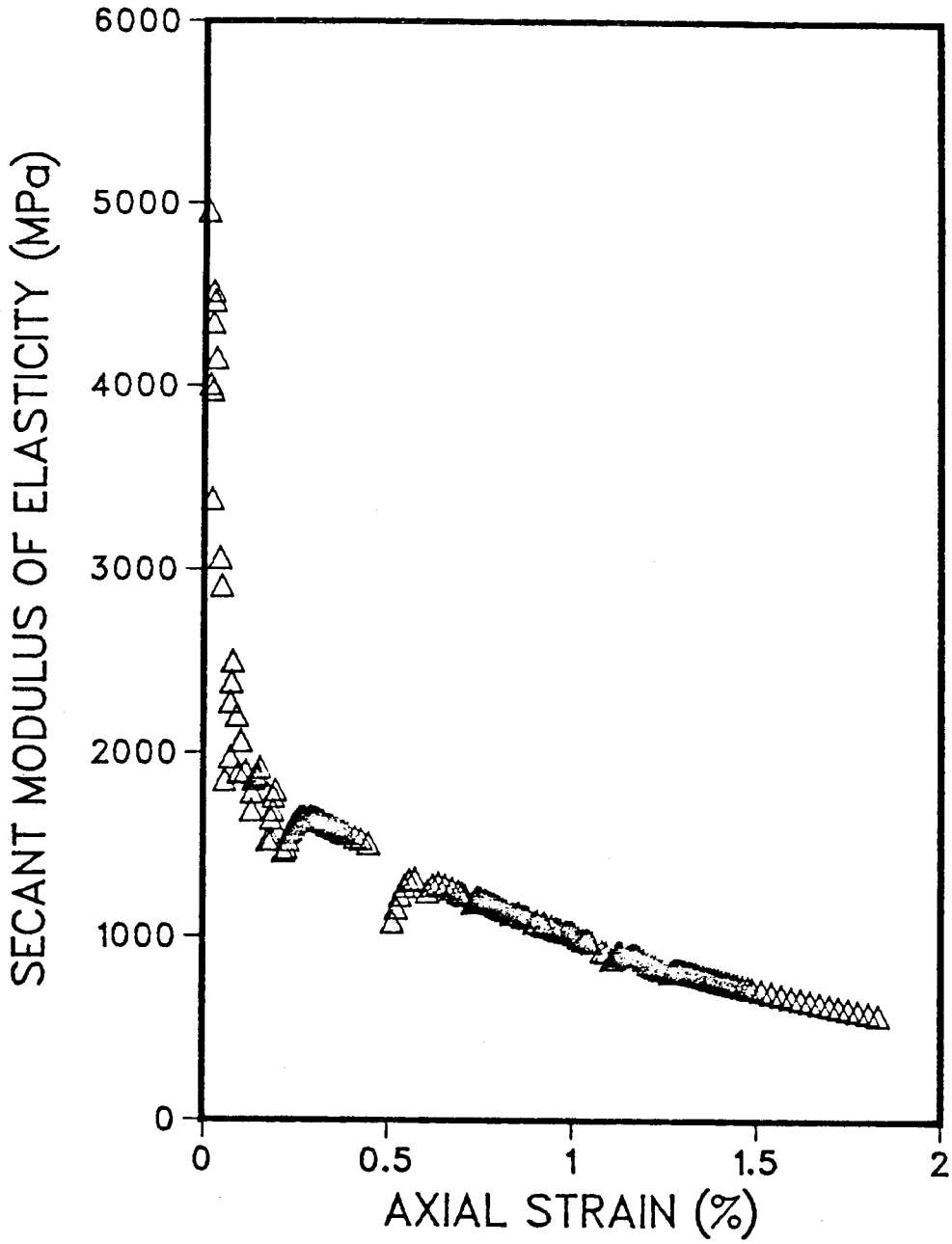

Figure 5.4 The secant modulus of Saline Creek oil sand at a confining pressure of 3.4 MPa

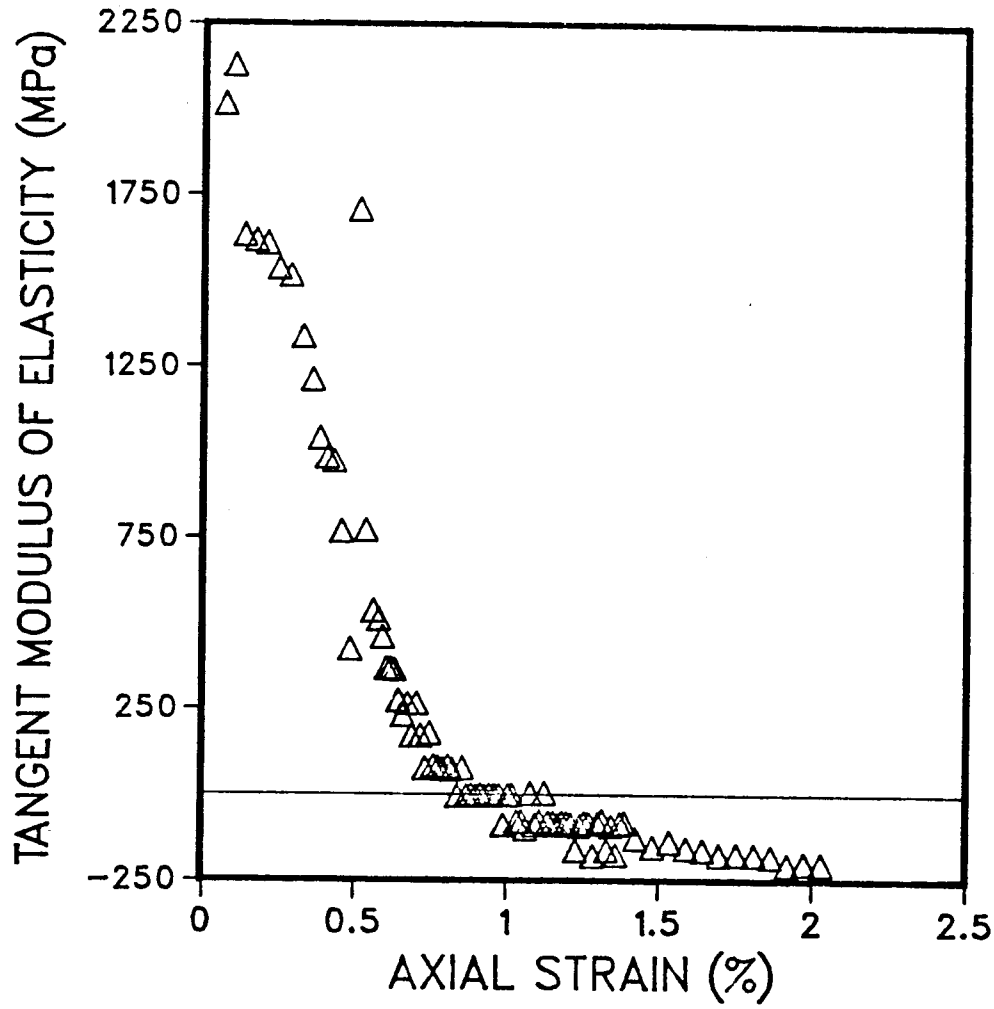

Figure 5.5 VARIATION OF THE MODULUS OF ELASTICITY OF SALINE CREEK OIL SAND WITH AXIAL STRAIN UNDER A CONFINING PRESSURE OF 2.1 MPa

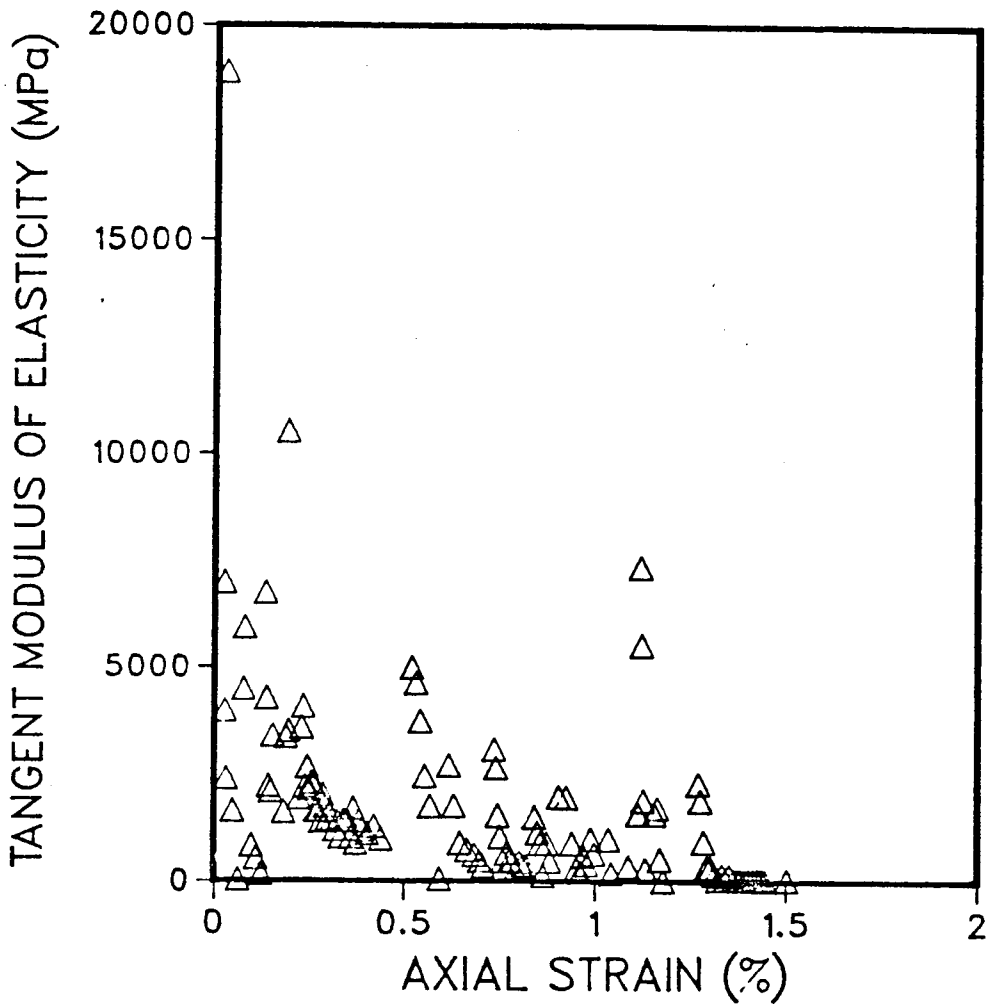

Figure 5.6 VARIATION OF THE MODULUS OF ELASTICITY OF SALINE CREEK OIL SAND WITH AXIAL STRAIN UNDER A CONFINING PRESSURE OF 3.4 MPa

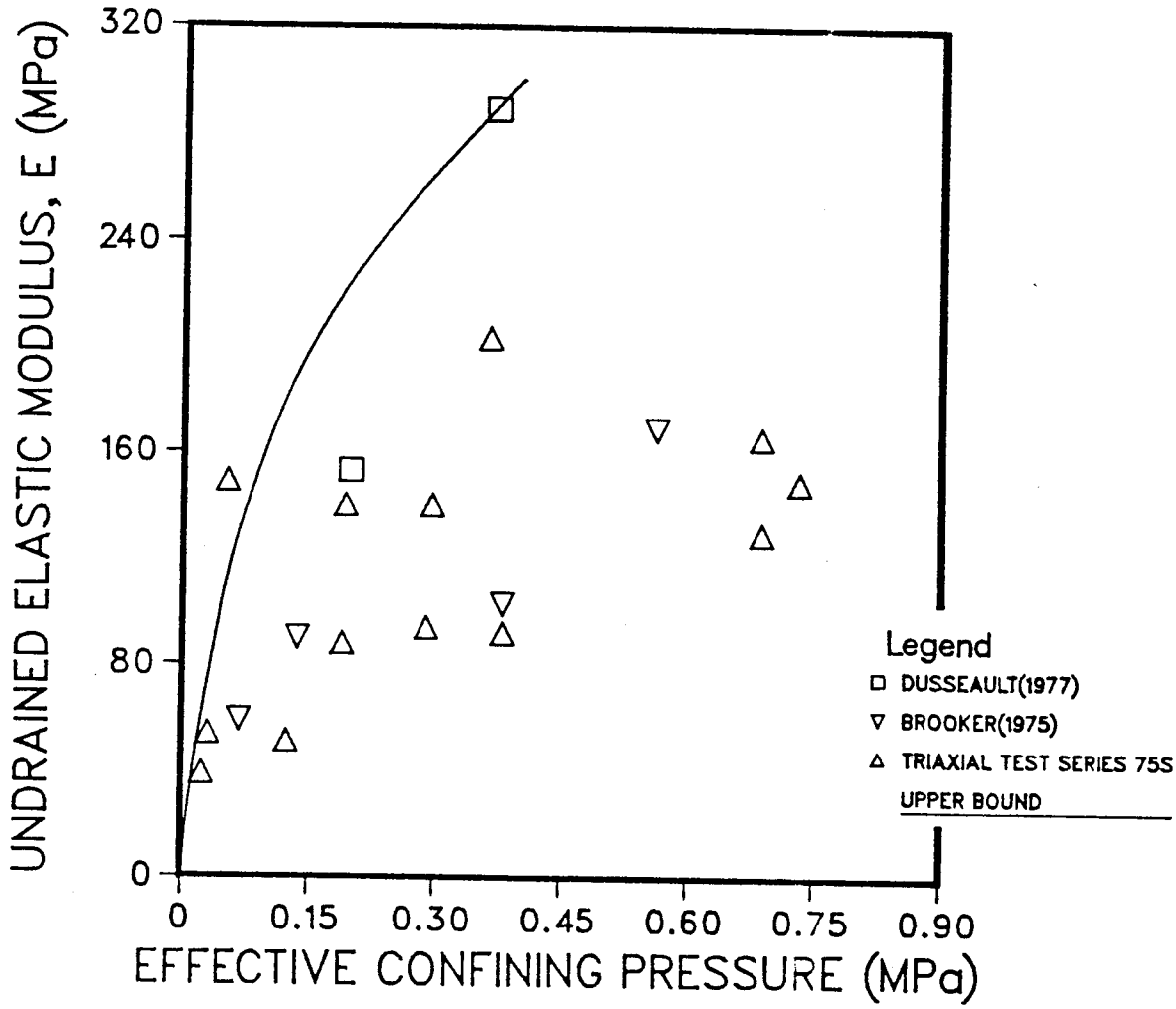

Figure 5.7 VARIATION OF THE UNDRAINED TANGENT MODULUS OF ATHABASCA OIL SANDS WITH THE EFFECTIVE CONFINING PRESSURE AT AXIAL STRAIN $\varepsilon_a = 0.25\%$ AS MEASURED IN UNDRAINED TRIAXIAL TESTS

modulus is plotted against the effective confining stress at an axial strain of 0.25%. The modulus data available are limited to the low confining stress range (σ_3' < 0.8 MPa). Although there is considerable scatter in the data because of variations in bulk density and fines content of the samples, Figure 5.7 shows that the undrained modulus of the Athabasca oil sands also increases with the confining effective pressure. A maximum envelope is shown for the modulus and a comparison with the drained modulus of elasticity in Figure 5.1 shows that even the maximum undrained modulus is considerably smaller. The undrained modulus should be somewhat smaller than the drained modulus because in the undrained test the pore pressure is increasing in the strain range considered which reduces the effective confining pressure and therefore the modulus. Also, in the drained test the density increases during testing which would tend to increase the modulus. The large difference shown here, however, may be more due to scatter and lack of data.

5.1.3 Unconfined Compression Tests

As explained in section 3.5, there are uncertainties associated with the stress state in an unconfined compression test on oil sands. As a result, the validity of the elastic modulus derived from the unconfined compression test is dubious at best.

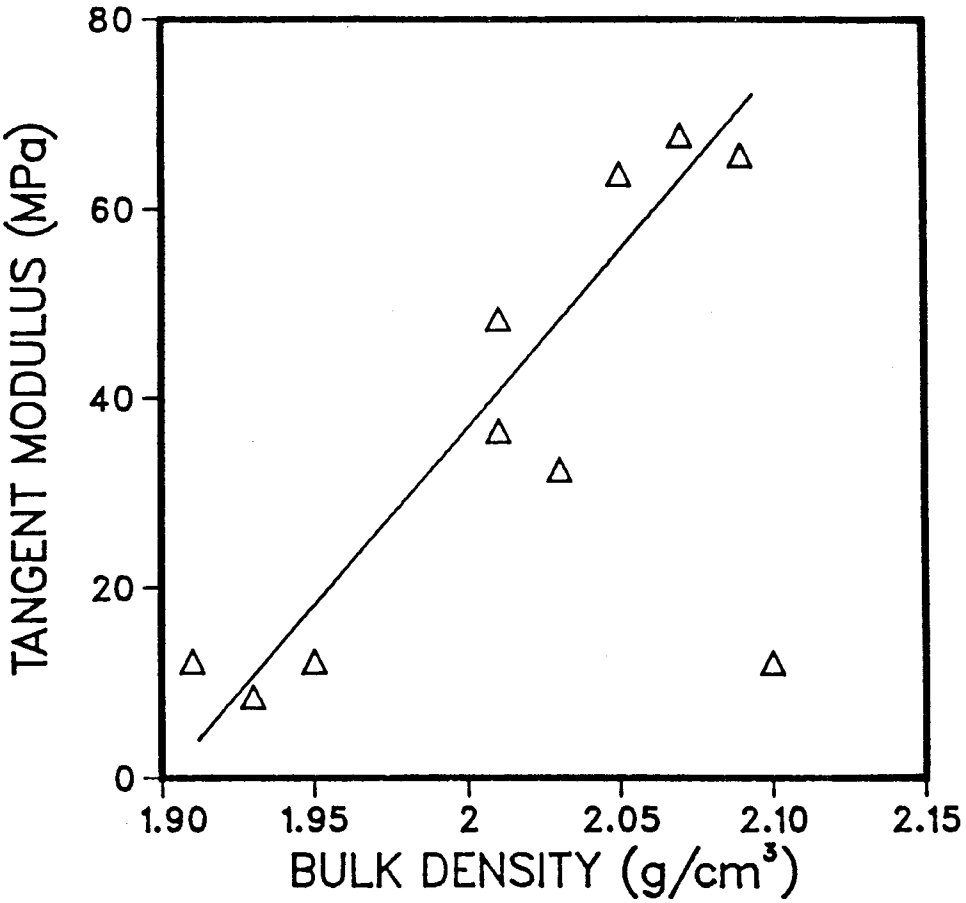

Figure 5.8 TANGENT MODULUS OF ELASTICITY OF ATHABASCA OIL SANDS AS A FUNCTION OF BULK DENSITY (DERIVED FROM UNCONFINED COMPRESSION TEST RESULTS IN TRIAXIAL TEST SERIES 75S)

Nevertheless, an effort had been made to plot the tangent modulus against the bulk density in Figure 5.8. The limited amount of data in Figure 5.8 seem to indicate that the unconfined tangent modulus of Athabasca oil sands increases with the bulk density. Indeed, if all other variables are kept constant, the unconfined tangent modulus should increase with the bulk density. The very low modulus values are an indication of the lack of practical significance of the results of unconfined compression tests.

5.1.4 Sonic Method

Basing on elastic theories, strain waves could be used to log various geologic formations in the field. For example, the dynamic modulus of elasticity may be computed from P-wave data (Jaeger and Cook, 1979) as

$$E = \frac{(1+\nu)(1-2\nu)\rho C^2}{(1-\nu)} \qquad (5)$$

where C = velocity of P-wave propagation

ν = Poisson's ratio

ρ = density of material

Dusseault(1982) reported some sonic velocity data for the strata in the Cold Lake oil sands area. Generally, the ratio between dynamic and static moduli is commonly from 1.5 to 3.0 for non-cemented strata at the effective stress levels of interest. Accordingly, Dusseault suggested some static modulus values for the various formations at Cold Lake. These values are listed in Table 3.

TABLE 3. MODULI OF ELASTICITY AS DERIVED BY THE SONIC METHOD FOR THE COLD LAKE OIL SAND AREA. (AFTER DUSSEAULT, 1982)

MATERIAL	MEAN IN-SITU SONIC VELOCITY (m/s)	ASSUMED POISSON'S RATIO	DYNAMIC YOUNG'S MODULUS (GPa)	STATIC YOUNG'S MODULUS (GPa)
Glacial Overburden (0 - 100 m)	1700	0.25	4.8	2.0
Colorado Clay Shales (100 - 320 m)	2050	0.45	2.6	1.5
Grand Rapids Formation (320 - 425 m)	2250	0.35	6.8	4.0
Clearwater Reservoir Section (425 - 455 m)	2300	0.35	7.1	4.5
McMurray Formation (455 - 515 m)	2650	0.32	11.0	6.0

Table 4. Moduli of elasticity derived by the sonic method for the Fort McMurray Formation at Athabasca and the Clearwater Formation at Cold Lake

	McMurray Formation (Probable in-situ value at 300-m depth)	Clearwater Formation (Probable in-situ value at 450-m depth)	McMurray Formation from Fig. 5.1 for a confining stress at a depth of 300 m.
In-situ static moduli of elasticity (assuming $\nu = 0.28$)	5 to 8 GPa	4 GPa	2 to 3 GPa

Using the same approach, Dusseault(1980) suggested an elastic modulus for the McMurray Formation at Athabasca. The modulus value is shown in Table 4. For the purpose of comparison, the modulus for the Clearwater Formation is also included in Table 4.

The geophysical sonic method avoids the problem of sample disturbance. In addition, it can cover larger areas and provide average values of the geomechanical properties under investigation. However, it should be noted that the relationship between the static and dynamic elastic moduli of oil sands has not been established with any certainty. The ratio of the dynamic modulus to the static modulus is a function of several variables including the confining pressure. That means the modulus values tabulated in Tables 3 and 4 have considerable uncertainty associated with them. As a comparison the static modulus of elasticity from Figure 5.1 for a confining stress equivalent to a depth of 300m is shown on Table 4. The laboratory measurement is less than 50% of the value calculated from the sonic field measurement.

5.2 Poisson's Ratio

Equipped with the volume change data during shear in consolidated drained triaxial tests the Poisson's ratio may be calculated according to equation (4) in section 5.1.1. Figure 5.9 illustrates the variation of Poisson's ratio of Athabasca oil sands as a function of the confining pressure

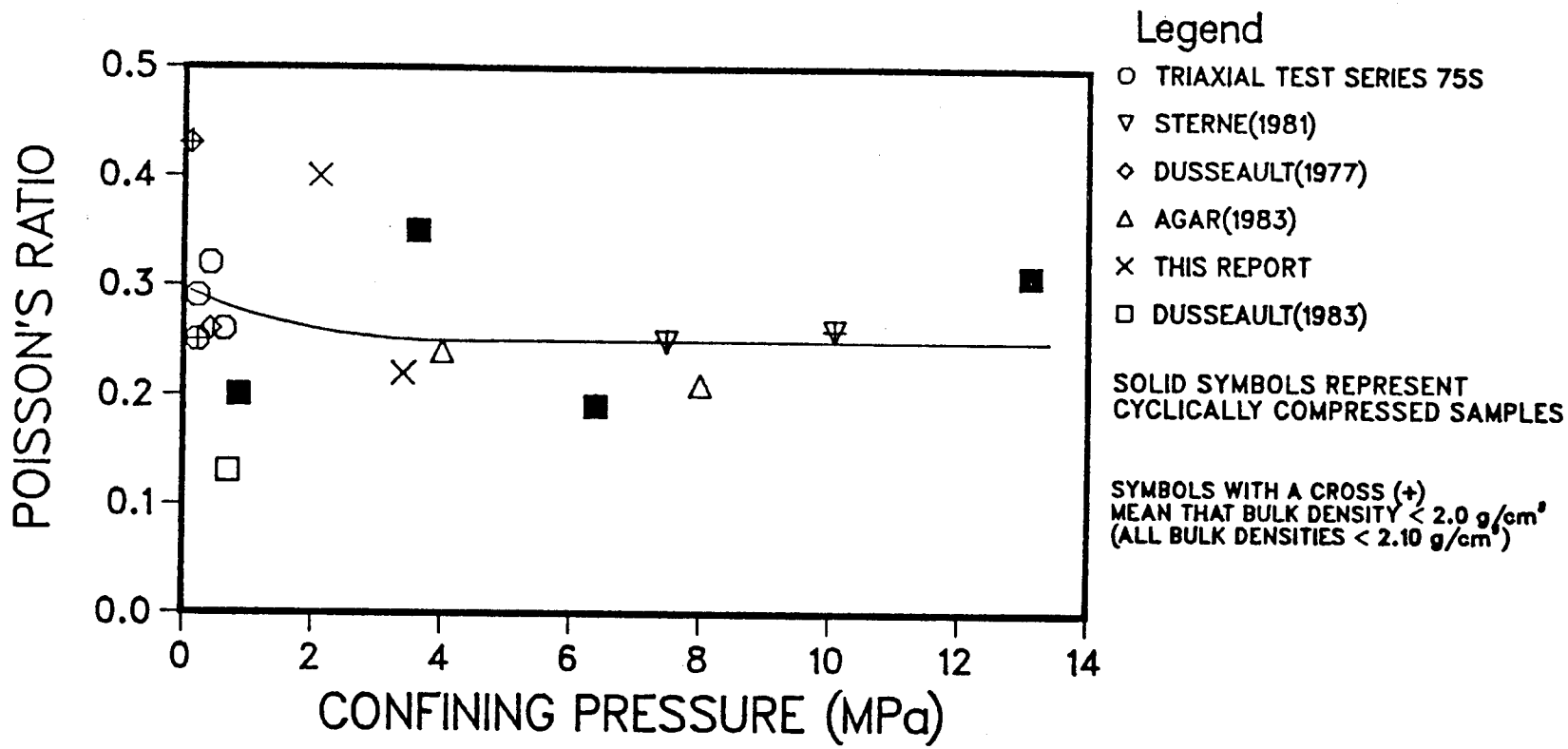

Figure 5.9 VARIATION OF THE POISSON'S RATIO WITH CONFINING PRESSURE AT AXIAL STRAIN ε_a = 0.25%

at an axial strain of 0.25%. It indicates that the Poisson's ratio is fairly constant around 0.25 over a wide range of confining pressure. At a low confining pressure, the Poisson's ratio could be around 0.3.

In Figure 5.9, the data points with a cross marked inside them signify that the oil sand sample used in the test had a bulk density less than 2.0 g/cm^3. If the bulk density reflects the degree of disturbance, then this amount of sample disturbance appears to have little effect on the Poisson's ratio of the Athabasca oil sand samples.

Like the Poisson's ratio of other cohesionless materials the Poisson's ratio of oil sand is a function of the axial strain in drained tests where volume change is taking place. Figures 5.10 and 5.11 illustrate this point. These two figures are based on the two triaxial tests on Saline Creek oil sand reported in Appendix A. Both of the figures indicate that the Poisson's ratio of Saline Creek oil sand increases with the axial strain in a triaxial test. At about the failure strain, the Poisson's ratio peaks and starts to decrease as the axial strain increases further. Because of its locked structure, the oil sand has a strong tendency to dilate under shear loading. Typical volumetric strain behaviour is shown in Figures A.2 and A.3. As the compressive stress is applied to the sample, there is an initial period of volume decrease when the increase in the applied stresses on the sample dominates the volume change behaviour. As the compressive stress continues to increase,

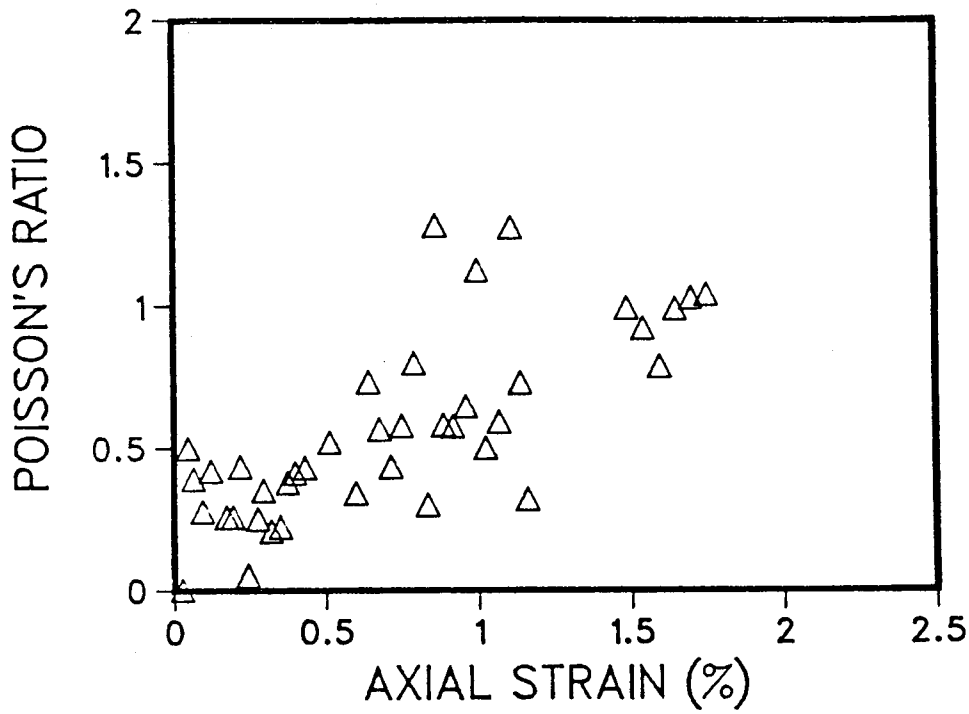

Figure 5.10 VARIATION OF THE POISSON'S RATIO OF SALINE CREEK OIL SAND WITH AXIAL STRAIN UNDER A CONFINING PRESSURE OF 2.1 MPa

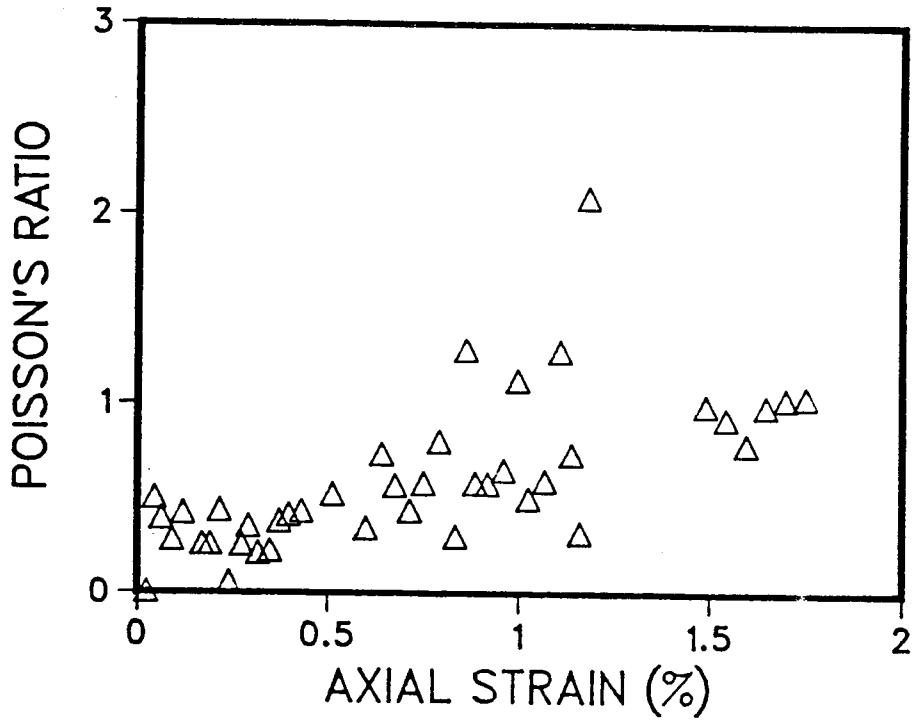

Figure 5.11 VARIATION OF THE POISSON'S RATIO OF SALINE CREEK OIL SAND WITH AXIAL STRAIN UNDER A CONFINING PRESSURE OF 3.4 MPa

the change in volume due to shear stresses starts to dominate and the sample dilates. This dilatant tendency results in the Poisson's ratio becoming larger than 0.5 as increasing shear load is applied on the oil sand. In fact, the Poisson's ratio can increase to beyond unity. An examination of the volume change data in other triaxial tests reveals that the behaviour described above applies as well to Athabasca oil sands as it does to dense granular media in general.

Because of the above volumetric change behaviour, the Poisson's ratio should only be calculated at low values of strain when the sample is compressing in a fairly linear manner. For high quality oil sand samples this linear compressive behaviour generally occurs up to at least 0.25% axial strain.

5.3 Shear Modulus

Collecting the data on the modulus of elasticity and the Poisson's ratio together, the shear modulus may be calculated as

$$G = \frac{E}{2\ (\ 1 + \nu\ )} \qquad (6)$$

Concentration is first placed on the set of results derived from the drained triaxial tests. If equation (6) is applied to the data on the modulus of elasticity and the Poisson's ratio which are summarized in Figures 5.1 and 5.9 respectively, a set of shear modulus values may be derived.

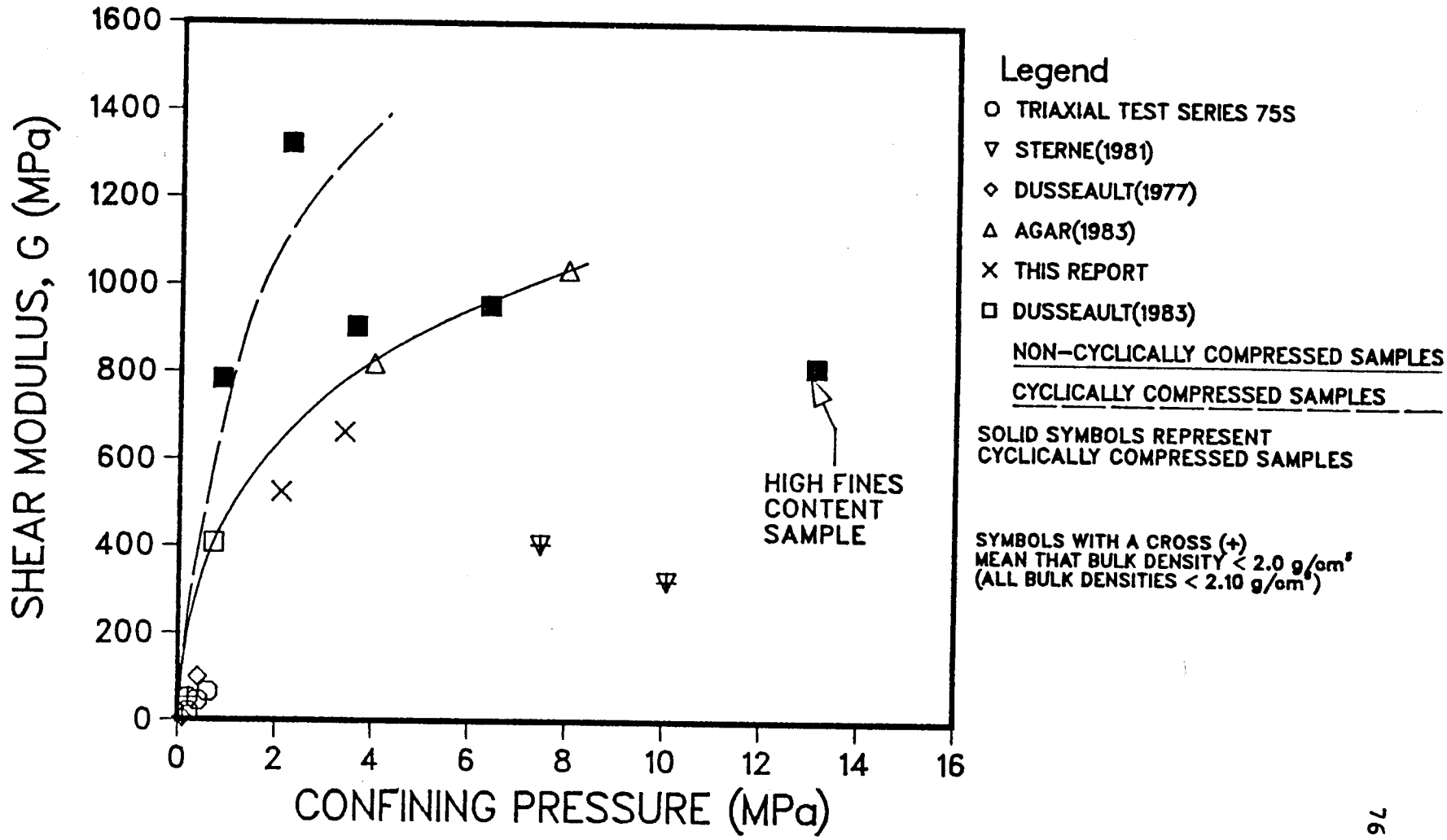

Figure 5.12 VARIATION OF G WITH CONFINING PRESSURE AT AXIAL STRAIN $\varepsilon_a = 0.25\%$

This set of values are presented in Figure 5.12 which depicts the variation of the shear modulus of Athabasca oil sands with the confining pressure at an axial strain of 0.25%. Evidently, the shear modulus increases rapidly with the confining pressure with the rate of increase tending to decrease as the confining pressure becomes higher. Extrapolating back to zero confining pressure, the shear modulus is practically zero. This variation in shear modulus is, of course, similar to the variation in modulus of elasticity as the Poisson's ratios used in the calculations are fairly constant. Therefore, all the variables which affect the modulus of elasticity will have a similar effect on the shear modulus. No direct measurements of the shear modulus of oil sand were found in the literature. Therefore the applicability of Equation (6) for oil sand cannot be verified.

For the condition of undrained triaxial tests, the Poisson's ratio is equal to 0.5. In that case, equation (6) becomes

$$G = \frac{E}{3} \qquad (7)$$

Applying equation (7) to the undrained modulus data shown in Figure 5.7, the corresponding shear modulus values can be obtained. These shear modulus values are plotted in Figure 5.13 against the effective confining pressure. The variation is, of course, similar to the variation of E.

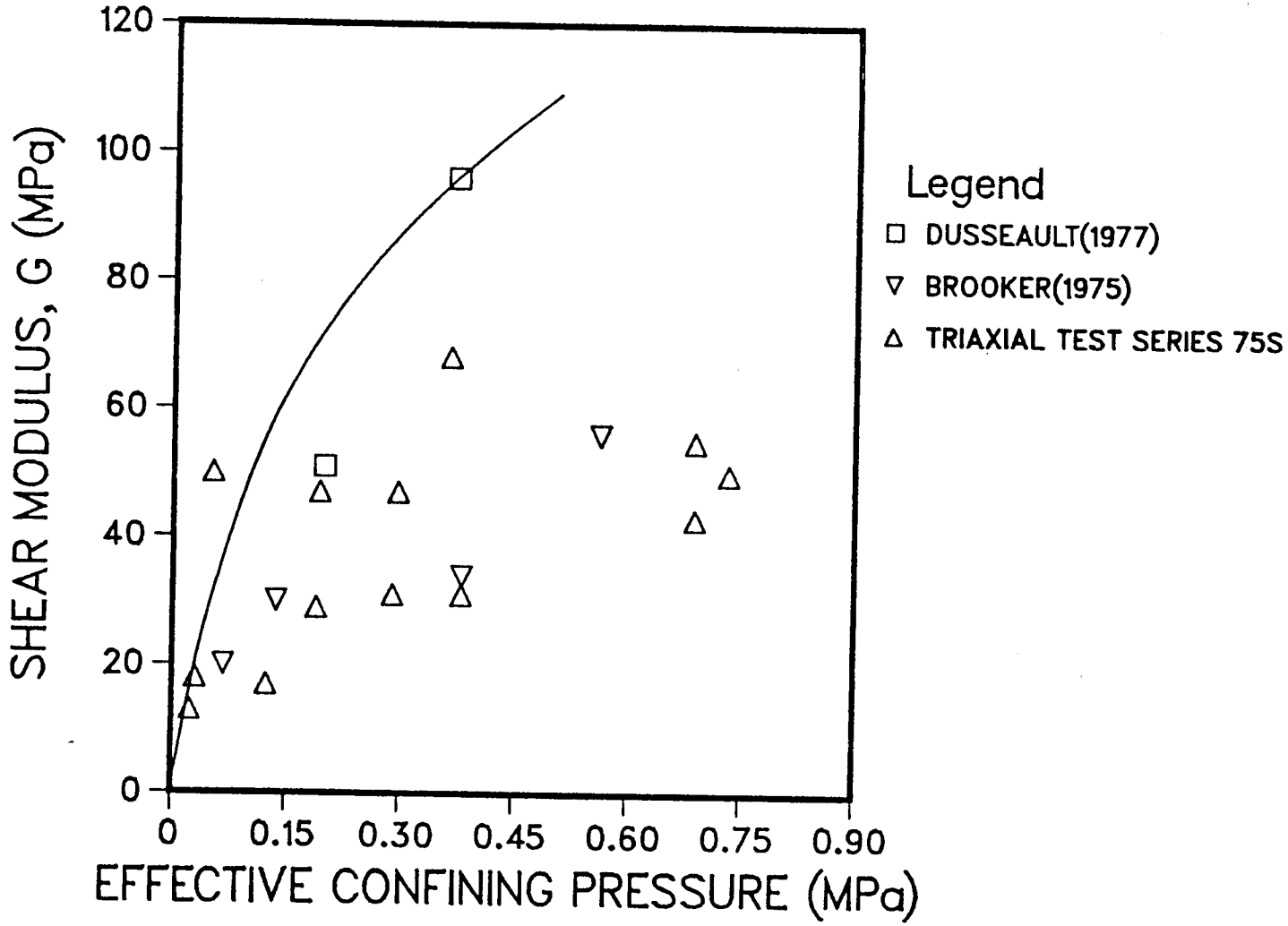

Figure 5.13 VARIATION OF G WITH THE EFFECTIVE CONFINING PRESSURE AT AXIAL STRAIN ε_a = 0.25% AS MEASURED IN UNDRAINED TRIAXIAL TESTS

5.4 Compressibility of Oil Sands

One method to estimate the compressibility of oil sands is to put a sample of oil sand under confined compression in an oedometer test. From the oedometer test results, the compressibility may be expressed in terms of:

a = coefficient of compressibility

$$= - \frac{\partial e}{\partial \sigma} \qquad (8)$$

or m = coefficient of volume compressibility

$$= - \frac{\partial \epsilon}{\partial \sigma} \qquad (9)$$

A typical stress-strain response of oil sands in an oedometer test is shown in Figure 5.14. Usually, the compressibility of oil sands is much higher on initial loading. The compressibility quickly converges to much lower values in subsequent loading and unloading cycles. Because all the test samples must have inevitably experienced stress relief and some sample disturbance, the cyclic compressibility is believed to be more representative of the in-situ compressibility than the first-cycle compressibility.

The compressibility data on Athabasca oil sands as derived from oedometer tests are summarized in Tables 5a and 5b. It can be seen that for good quality samples, the cyclic coefficient of volume compressibility is generally between 0.2 and 0.6 $x10^{-4}kPa^{-1}$. On comparison, the first-cycle compressibility is not only much larger; it has

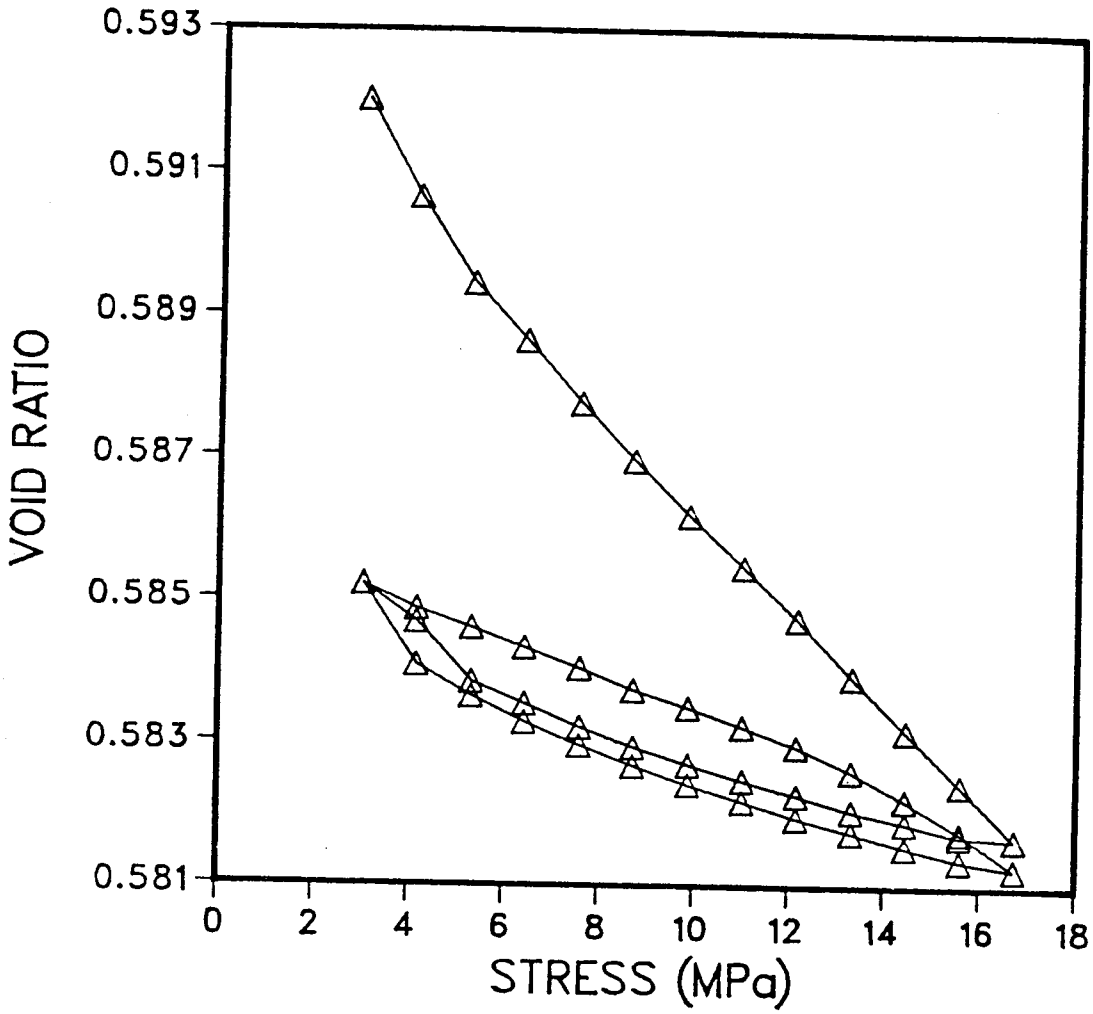

Figure 5.14 AN EXAMPLE OF THE STRESS–STRAIN RESPONSE OF OIL SANDS IN AN OEDOMETER TEST (AFTER BARNES, 1980)

TABLE 5a. COEFFICIENT OF COMPRESSIBILITY OF ATHABASCA OIL SANDS: OEDOMETER TEST RESULTS.

REFERENCE	MATERIAL	VOID RATIO	RANGE OF STRESS (MPa)	COEFFICIENT OF COMPRESSIBILITY a_v (kPa^{-1} x 10^{-6})			
				1st cycle		later cycle	
				load	unload	load	unload
Barnes (1980)	Fine-grained McMurray Formation *	0.49	3-16.7	0.80	0.33	0.35	0.28
	Medium-Grained McMurray Formation *	0.54	3-16.7	2.15	0.28	0.30	0.25
	Coarse-Grained McMurray Formation *	0.30	3-16.7	2.05	0.17	0.52	0.20
Direct Shear Test Series 79 G	Athabasca Oil Sand	0.77 - 0.95	3-17	4.0-7.0	0.5-0.8	1.4-1.7	0.5-1.0

*Sand samples were oil-free

TABLE 5b. COEFFICIENT OF VOLUME COMPRESSIBILITY OF ATHABASCA OIL SANDS: OEDOMETER TEST RESULTS

REFERENCES	MATERIALS	RANGE OF STRESS (MPa)	COEFFICIENT OF VOLUME COMPRESSIBILITY m_v (KPa $^{-1}$ x10 $^{-6}$)					
			Initial Void Ratio	1st cycle		Average Later Cycle Void Ratio	Later Cycle	
				Load	Unload		Load	Unload
Sterne (1981)	Middle McMurray Formation North of Fort McMurray	6.6 - 17	0.66	2.60	0.76	0.53	0.65	0.22
Agar (1983)	Saline Creek Oil Sand	0.5 - 4	0.59	0.92	0.88	0.53	0.90	0.80
	Saline Creek Oil Sand	2 - 18	0.56	0.7-1.4	0.49-0.61	0.53	0.57-0.58	0.52-0.53
Triaxial Test Series 64G	Athabasca Oil Sands	0 - 4.9	0.66	7.3	2.1	-	-	-

a much greater variability too. Prior to testing, each sample had experienced a differing degree of disturbance and stress relief. Therefore, depending on the exact amount of damage to the locked structure of the oil sands, the sample could be comparatively compressible or fairly incompressible on the initial cycle of loading.

Another approach to measure the compressibility of oil sands is to impose isotropic compression on the sample as at the beginning of a triaxial test and monitor the corresponding volumetric strain. Table 6 summarizes the data derived from such an approach. The quantity of data available is limited. The data indicates that the cyclic coefficient of volume compressibility is in the range of 0.2 to 0.8 $x10^{-4}kPa^{-1}$.

It should be noted that the stress path followed in the oedometer test is different from that corresponding to isotropic compression. Thus although the volumetric stress-strain relationships of oil sands are similar qualitatively during both isotropic and confined compression, quantitatively they are somewhat different. For a given change in σ_1, the change in J_1 ($= \sigma_1 + \sigma_2 + \sigma_3$) is greater during isotropic compression. Consequently, a given change in σ_1 will result in a greater volumetric strain during isotropic compression. This implies that the compressibility derived by isotropic compression should be larger than that obtained in oedometer tests. However, it seems that the data derived by isotropic

TABLE 6. ISOTROPIC COMPRESSIBILITY OF ATHABASCA OIL SANDS

REFERENCE	MATERIAL	RANGE OF STRESS (MPa)	COEFFICIENT OF VOLUME COMPRESSIBILITY m_v ($\times 10^{-6}$ x kPa $^{-1}$)					
			INITIAL VOID RATIO	1st CYCLE		AVERAGE LATER CYCLE VOID RADIO	LATER CYCLE	
				LOAD	UNLOAD		LOAD	UNLOAD
Agar (1983)	Saline Creek Oil Sand	4 - 25	0.49	1.50	0.78	0.46	0.79	0.56
Sterne (1981)	Middle McMurray Formation North of Ft. McMurray	4 - 10	0.68 - 0.69	0.55-1.61	-	-	-	-
		4 - 10	0.73 - 0.77	2.07-4.12	-	-	-	-
		4 - 10	0.76 - 0.78	2.64-3.60	-	-	-	-
Raisbeck & Currie (1981)	Oil Sands	0 - 7	-	3.11	-	-	-	-
This Report	Saline Creek Oil Sand	0 - 1.7	0.58	4.1	-	-	-	-
		0 - 3.1	0.61	4.4	-	-	-	-

TABLE 6. (cont'd) ISOTROPIC COMPRESSIBILITY OF ATHABASCA OIL SANDS

REFERENCE	MATERIAL	RANGE OF STRESS (MPa)	INITIAL VOID RATIO	AVERAGE LATER CYCLE VOID RATIO	COEFFICIENT OF VOLUME COMPRESSIBILITY m_v ($KPa^{-1} \times 10^{-6}$)			
					1st Cycle		Later Cycle	
					Load	Unload	Load	Unload
Dusseault (1981)	Athabasca Oil Sands	2.93-13.3	-	-	0.82	0.36		
		"	0.543	0.517	0.82	0.36		
		"	0.560	0.531	0.93	0.35		
		"	0.629	0.610	0.89	0.50		
		2.76-13.1	0.550	-	-	0.25		
		6.20-13.1	0.543	0.513	0.61	0.34		

compression is similar to the oedometer test results shown in Tables 5a and 5b.

Figure 5.15 sums up the compressibility data as a function of the void ratio and whether the data are from first loading or repeated cycling tests. There are no definite relationships between the void ratio and the compressibilities, although it may be fair to say that high first-cycle compressibilities usually correlate with high initial void ratios. Also, it appears that the void ratio does not have a great effect on the cyclic compressibility of Athabasca oil sands. In other words, the cyclic compressibility testing of Athabasca oil sands appears to overcome the relatively small amount of disturbance experienced by the samples shown in Figure 5.15. In light of this, extrapolation on the test data suggests that the volume compressibility of Athabasca oil sands is probably between 0.3 and 0.7 $x10^{-4}kPa^{-1}$.

So far, all the data discussed in this section are on Athabasca oil sands, for there is very little information on the oil sands at other locations in Alberta. Barnes(1980) performed a number of oedometer tests on oil-free sands from Grand Rapids Formation zones "A" and "C". The results are reproduced in Table 7. In Table 7, the compressibility is expressed in terms of a. The coefficient of volume compressibility (m) is related to a as

$$m = \frac{a}{1 + e_o} \qquad (10)$$

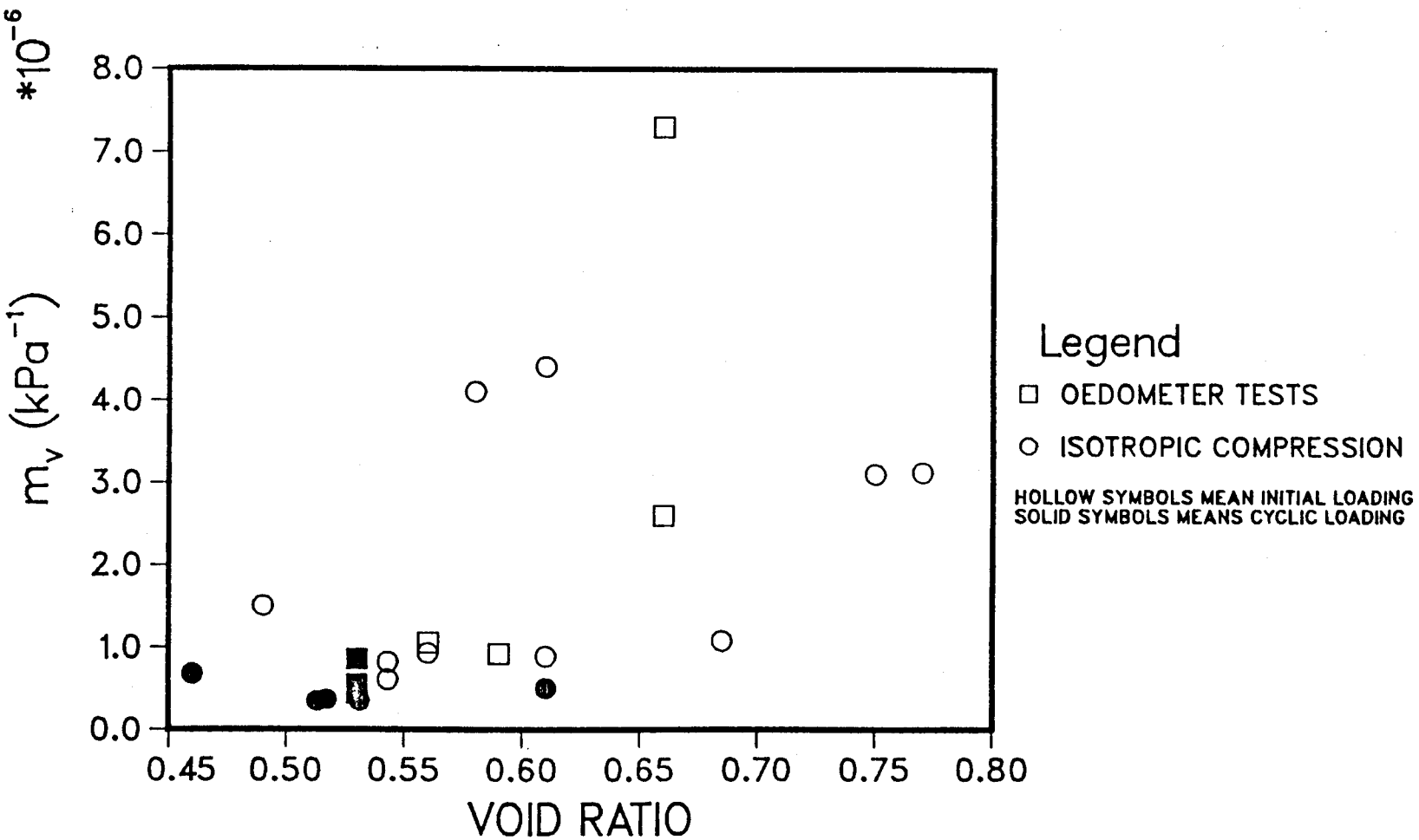

Figure 5.15 THE COEFFICIENT OF VOLUME COMPRESSIBILITY OF ATHABASCA OIL SANDS

TABLE 7. COMPRESSIBILITY OF OIL-FREE SANDS IN THE GRAND RAPIDS FORMATION
(Barnes, 1980)

MATERIAL	VOID RATIO	RANGE OF STRESS (MPa)	COEFFICIENT OF COMPRESSIBILITY a_v (KPa $^{-1}$ x 10 $^{-6}$)			
			1st CYCLE		LATER CYCLE	
			LOAD	UNLOAD	LOAD	UNLOAD
Grand Rapids Formation "A"	0.57	3 - 16.7	0.96	0.32	0.28	0.27
Grand Rapids Formation "C"	0.60	3 - 16.7	6.13	0.17	0.51	0.17

Although the initial void ratio (e_o) is not known exactly, equation (9) shows that for $e_o \simeq 0.6$, m could be between 0.1 and 0.3 $x10^{-4}kPa^{-1}$. Apparently, the sands of the Grand Rapids Formation have a compressibility comparable to or possibly smaller than the compressibility of the Athabasca oil sands. Also, Dusseault(1980) suggested that the compressibility of the oil sands in the Clearwater Formation at Cold Lake could be between 0.4 and 1.0 $x10^{-4}kPa^{-1}$.

To sum up the discussion in this section, the probable values of the coefficient of volume compressibility of oil sands are listed in Table 8.

5.5 Axial Strain at Failure based on Triaxial Tests

To investigate what the strain at failure would likely be for a completely undisturbed sample, the failure strains in all the triaxial test examined in this study are plotted against the bulk density of the oil sand samples in Figure 5.16. There is considerable scatter in the data points. However, a definite trend is discernible: the failure strain decreases with increasing bulk density of the samples. Extrapolating to the in-situ bulk density between 2.1 and 2.3 g/cm^3, the axial strain at failure is probably 0.8% to 1.5% under axisymmetric boundary conditions.

Since the bulk density of an oil sand sample partly reflects the quality of that sample, the trend indicated in Figure 5.15 suggests that the axial strain at failure could also be considered to be an indicator of the quality of the

TABLE 8. PROBABLY IN-SITU VALUES OF THE COEFFICIENT OF VOLUME COMPRESSIBILITY UNDER CONFINED COMPRESSION FOR THE MCMURRAY FORMATION AT ATHABASCA, THE CLEARWATER FORMATION AT COLD LAKE, AND THE GRAND RAPIDS FORMATION 80 km SOUTHWEST OF FORT MCMURRAY.

	MCMURRAY FORMATION	CLEARWATER FORMATION	GRAND RAPIDS FORMATION
Coefficient of Volume Compressibility, m_v (kPa $^{-1}$ x 10 $^{-6}$)	0.3 to 0.7 (stress range ≈ 3 - 17 mPa)	0.4 to 1.0 (stress range ≈ 7 - 13 mPa)	0.3 to 0.5 (stress range ≈3 - 17 mPa)

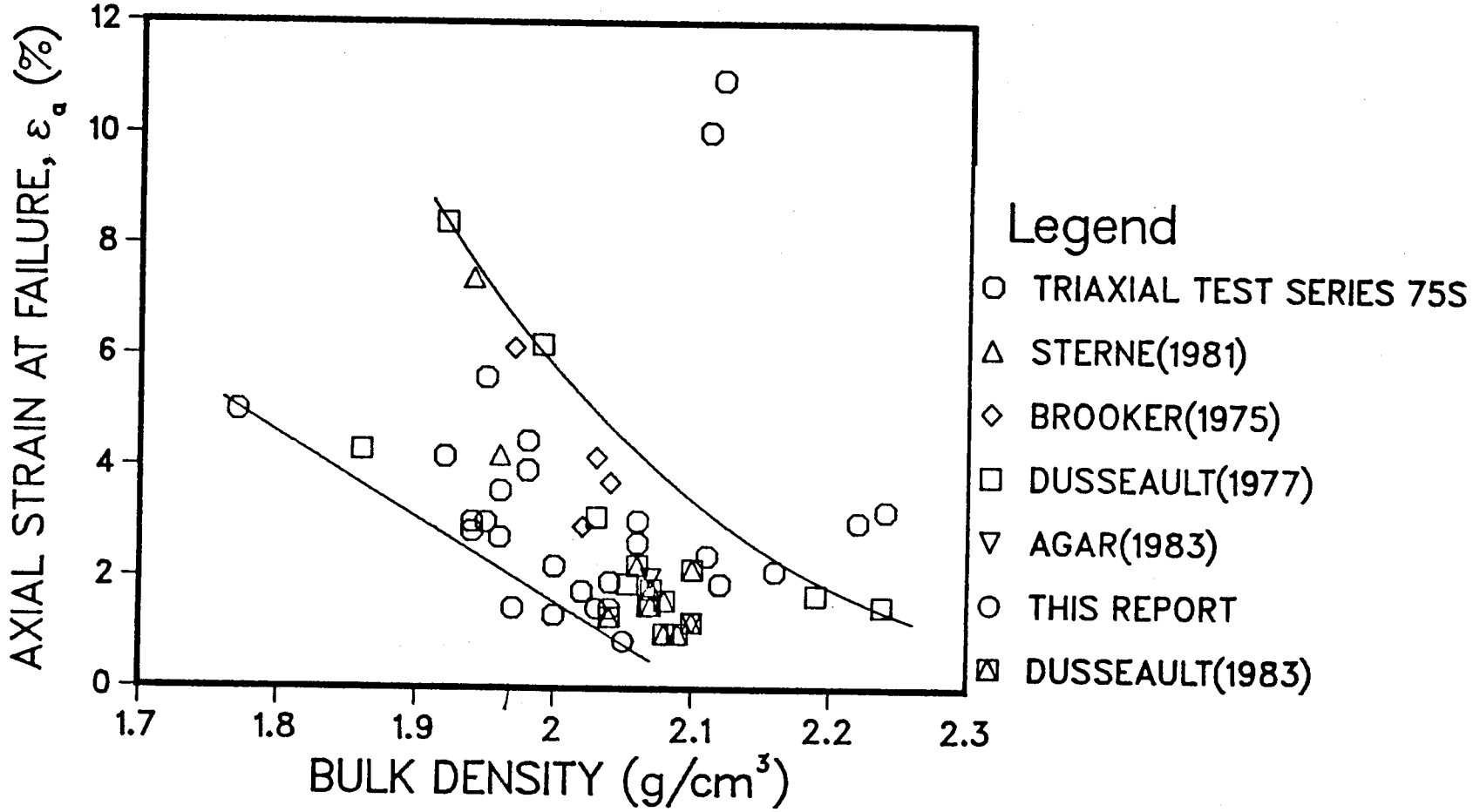

Figure 5.16 AXIAL STRAIN AT FAILURE IN TRIAXIAL TESTS AS A FUNCTION OF THE BULK DENSITIES OF THE SAMPLES

sample.

Chapter 6

PORE PRESSURE PARAMETERS "$\bar{A}$ " AND "B"

Assuming the principle of superposition, the pore pressure change Δu may be expressed in terms of the corresponding changes in the principal stresses $\Delta\sigma_1$ and $\Delta\sigma_3$ (Skempton, 1954):

$$\Delta u = B.\Delta\sigma_3 + \bar{A}\ (\Delta\sigma_1 - \Delta\sigma_3) \qquad (11)$$

where $\bar{A}$ and B are the pore pressure parameters.

6.1 The B Parameter

It can be shown that

$$B = \frac{1}{1 + \dfrac{n_w C_w + n_b C_b}{C_s}} \qquad (12)$$

where n_w = water porosity

n_b = bitumen porosity

C_w = compressibility of water

C_b = compressibility of bitumen

C_s = compressibility of soil skeleton.

The variable C is equivalent to the coefficient of volume compressibility m as discussed in section 5.4.

The B parameter is measured in triaxial tests by applying an isotropic stress to a saturated sample and measuring the increase in pore pressure. The smaller the increase in pore pressure, the smaller must be the compressibility of the soil skeleton.

Agar(1983) found that based on pore pressure parameter B tests on Saline Creek oil sand, the B parameter was measured to be in the range of 0.8 to 0.9. The testing on Saline Creek oil sand in the present study showed that the B parameter of the samples was approximately 0.5 to 0.7.

When dealing with ordinary soil materials, the compressibility of the soil structure is usually much larger than that of the pore fluid in the case of fully saturated soils. Therefore the B parameter is usually very close to unity. In this respect, the B value of the Saline Creek oil sand is relatively low which deserves some consideration. Turning attention to equation (12), it is useful to adopt some representative figures for the variables in that equation to calculate a value for B for comparison purposes. For a reasonably good oil sand sample, the composition of the oil sand is typically 11% bitumen, 6.5% water, and 82.5% sand by mass. These would give

$n \simeq 14\%$

$n \simeq 22\%$

$C \simeq 0.8 \times 10^{-4} kPa^{-1}$ (for isotropic compression)

$C \simeq 0.46 \times 10^{-4} kPa^{-1}$ for water

$C \simeq 2.0 \times 10^{-4} kPa^{-1}$ for bitumen.

(The compressibility values of water and bitumen are quoted from Kosar, 1983). Substituting these values into equation (12),

$B \simeq 0.6.$

Good grade oil sand typically has an in-situ composition of

11% bitumen, 4% water, and 85% sand. So assuming

n_w = 8.5%

n_a = 23.3%

C_s = 0.3 x10^{-4}kPa^{-1}

C_w = 0.46 x10^{-4}kPa^{-1}

C_a = 2.0 x10^{-4}kPa^{-1}

to be representative in-situ values, it may be reasonable to expect B $\simeq$ 0.4 in the field. Clearly, the low compressibility of oil sands is the reason why the B parameter is not close to unity. It would appear that pore pressure parameter B tests would be a better indicator of sample quality than bulk density values. The lower the measured value of B, the better the quality of the sample must be. The B value would be little influenced by fines content of the sample in contrast to the bulk density.

The B parameter is not constant during undrained triaxial shear testing since the compressibility of the sand skeleton varies with the stress level. However, this change is small and only of interest when estimating change in pore pressure during undrained shearing.

6.2 The $\bar{A}$ Parameter

The $\bar{A}$ parameter is measured during undrained shear testing. The $\bar{A}$ parameter changes with the axial strain and reflects the tendency of the sample to change volume from shear strains. During an undrained shear test a saturated sample cannot change volume and the pore pressure must

change with shear strains. An increase in pore pressure indicates the sample is attempting to compress and a decrease in pore pressure indicates an attempt to dilate. Figure 6.1 shows a typical undrained triaxial test result from Dusseault(1977). Typically, the $\bar{A}$ parameter starts with a positive value and peaks at a very low strain (at around 0.2% axial strain). Thereafter, it decreases with increasing axial strain. The decrease usually carries it to some negative values before the peak strength is reached.

Interestingly, undrained triaxial test results show that the parameter at failure, $\bar{A}_f$, seems to decrease when the axial strain at failure increases. This observation is illustrated in Figure 6.2 and indicates that there is a tendency for greater dilation at higher strains. Such volume changes can be observed in drained tests. But $\bar{A}$ does not correlate well with the bulk density for these tests. That suggests two points. Firstly, $\bar{A}$ is susceptible to the effect of sample disturbance and it depends upon the quality of the oil sand samples. Secondly, the bulk density may not satisfactorily reflect the quality of the sample. For example, a high fines content in an oil sand sample can result in a deceivingly high bulk density but fail to increase the shear strength of the sample. It is for this reason that little weight has been put on the data point which has a positive $\bar{A}$ value in Figure 6.2. That data point corresponds to a sample with a high clay content.

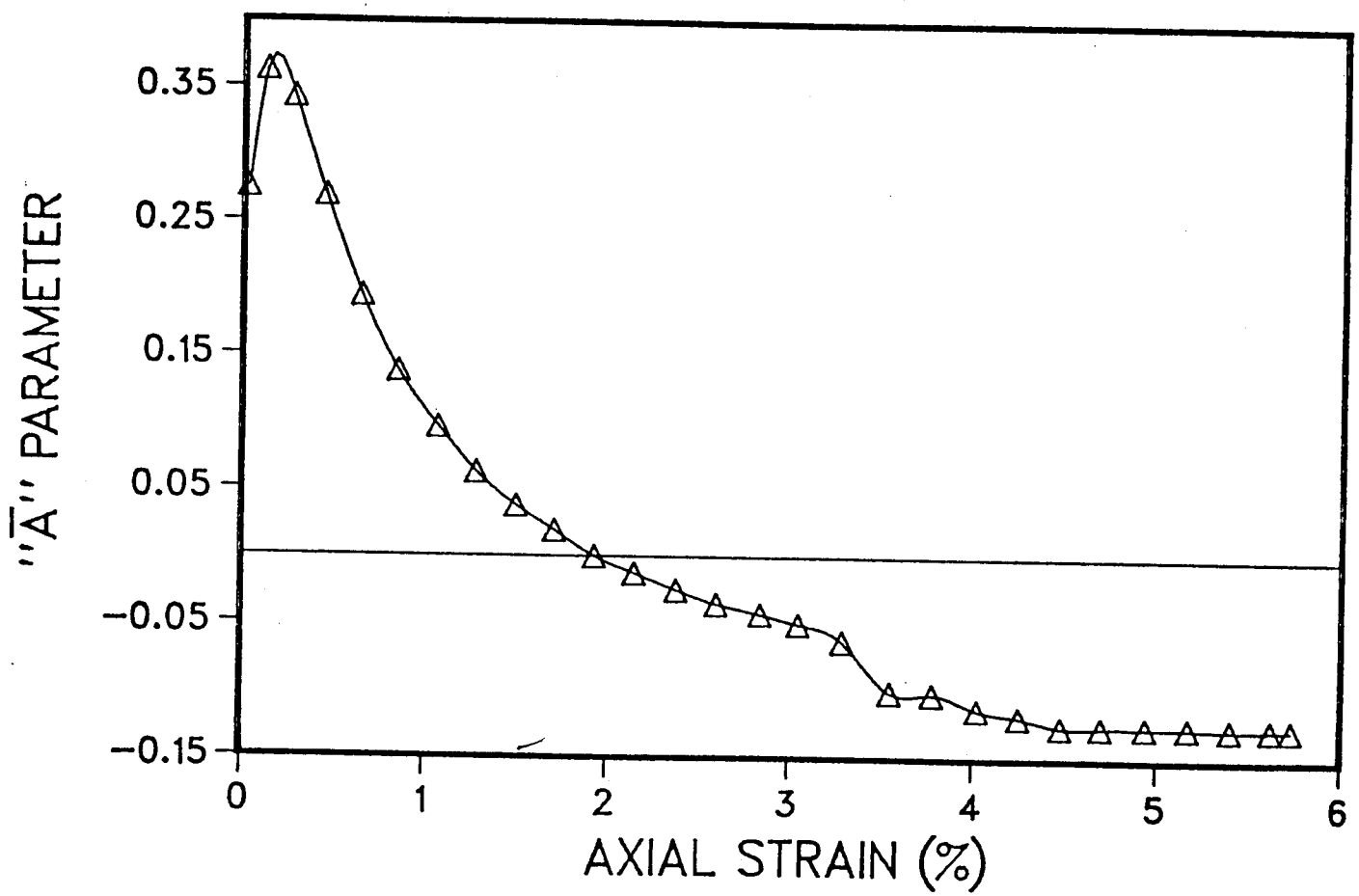

Figure 6.1 VARIATION OF PORE PRESSURE PARAMETER $\bar{A}$ WITH AXIAL STRAIN IN AN UNDRAINED TRIAXIAL TEST ON ATHABASCA OIL SANDS AS A TYPICAL EXAMPLE OF THE PORE PRESSURE RESPONSE DURING LOADING (AFTER DUSSEAULT, 1977)

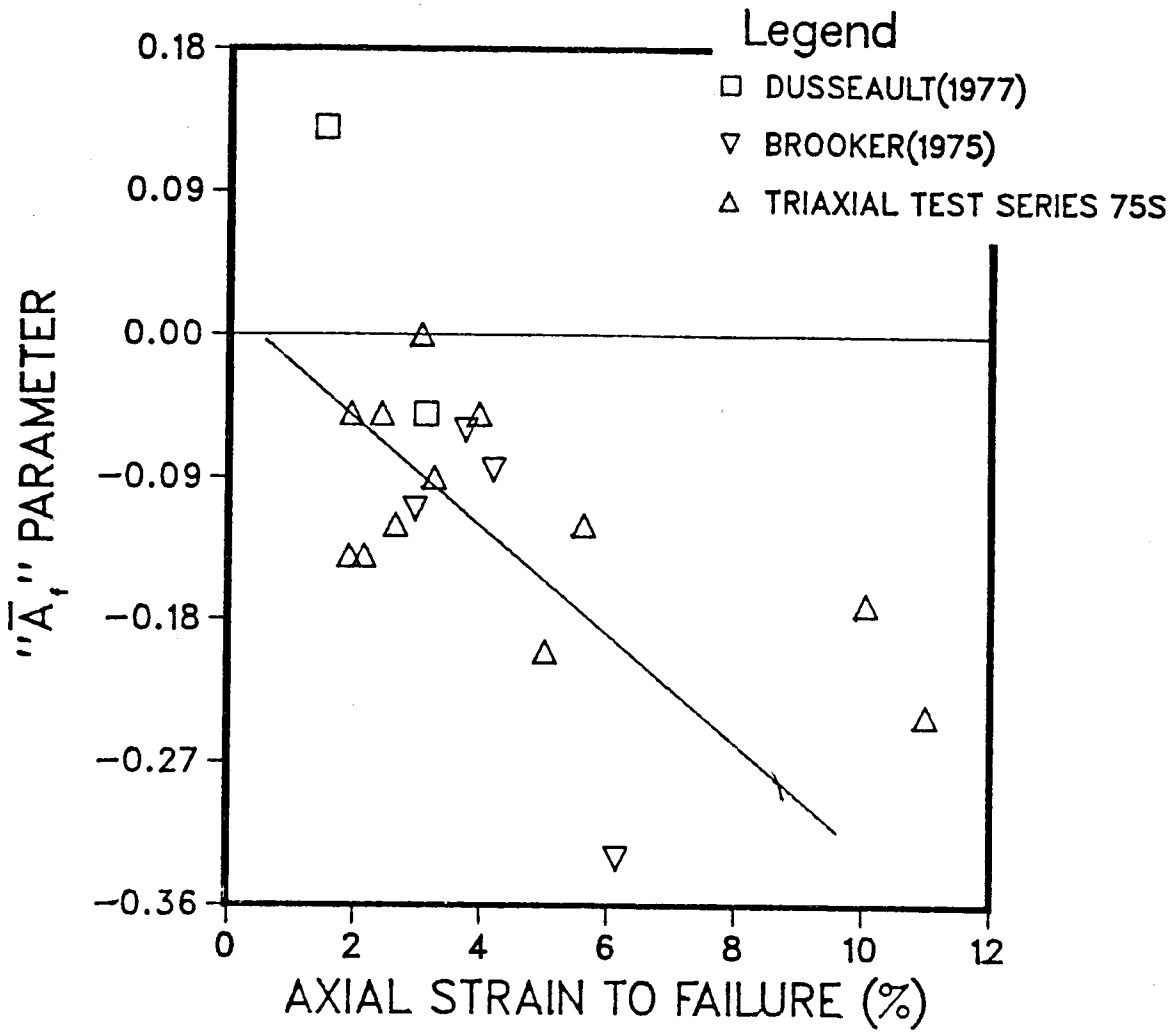

Figure 6.2 VARIATION OF $\bar{A}_f$, THE PORE PRESSURE PARAMETER AT FAILURE WITH THE AXIAL STRAIN AT FAILURE AS MEASURED IN UNDRAINED TRIAXIAL TESTS ON ATHABASCA OIL SANDS

Despite the scattering of the data points in Figure 6.2, extrapolation on the data suggests that the in-situ $\bar{A}$ values are probably between 0 and -0.05. However, it must be cautioned that the stress path generated in the field may be significantly different from the one followed in an undrained triaxial test, and the effect of such discrepancy is not known. Therefore, the values suggested here should be viewed with this point in mind.

Chapter 7

CLAY SHALES ASSOCIATED WITH ATHABASCA OIL SANDS

7.1 Intraformational Clay Shales

The intraformational clay shales refer to the numerous silty and clayey bedding seams within the oil sand of the McMurray Formation. There is a very scanty amount of strength data on the intraformational clay shales. Table 9 briefly summarizes the available strength data.

These data are principally based on direct shear box tests and as shown in Table 9, there is significant variation in strength. The variation is related to the lithology.

7.2 Basal Clay Shales

Dusseault and Scafe(1979) define the Basal McMurray Formation Clay as "a noncalcareous, argillaceous sequence of beds found between the Paleozoic limestone and the major arenaceous transgressive sequence of the McMurray Formation".

The strength of the clay shales had been investigated with direct shear tests. The results are summarized in Table 10. There is considerable variability in the strength properties of the basal clay shale. Brooker and Khan(1980) attributed this to be a result of the complex environment of deposition for the basal clay layer.

TABLE 9. STRENGTH DATA OF INTRAFORMATIONAL CLAY SHALES

AUTHOR	PEAK COHESION c'_p (KPa)	PEAK ANGLE OF FRICTION ϕ'_p	RESIDUAL ANGLE OF FRICTION ϕ'_r
Brooker & Khan (1980)	0 - 45	13° - 29°	8° - 25°
Dusseault & Scafe (1979)	-	-	18°

TABLE 10. STRENGTH PROPERTIES OF BASAL CLAY SHALE

AUTHOR	BULK DENSITY (g/cm^3)	PEAK COHESION c'_p (KPa)	PEAK ANGLE OF FRICTION ϕ'_p	RESIDUAL ANGLE OF FRICTION ϕ'_r
Brooker & Khan (1980)	1.9 - 2.4	$\leq$ 124	$\leq$ 23°	$\geq$ 7°
Dusseault & Scafe (1979)	-	-	-	< 8°

Chapter 8

OBSERVATIONS AND CONCLUSIONS

(a) A typical in-situ bulk density for Athabasca oil sands is in the order of 2.15 g/cm³. High quality undisturbed core samples only have an average bulk density of 2.08 g/cm³. This increase in the porosity of samples results in laboratory tests underestimating shear strength and elastic moduli values and overestimating compressibility.

(b) The Alberta oil sands are highly dilatant and cohesionless. Because of the locked structure of the sandy matrix, the oil sands have unusually high strength, compared to ordinary dense sands, with a $\phi' = 60°$ below a normal stress of 1.3 MPa. The peak shear strength envelope of the oil sands is highly curvilinear at higher normal stresses.

(c) Cycling the confining stress on the sample before shearing appears to increase the shear strength for normal stresses above 3 MPa. This would appear to be caused by the cycling increasing the density of the samples by consolidation and grain crushing.

(d) A comparison of the limited amount of test results on Athabasca oil sands appears to indicate that the triaxial test shows considerably higher strength values than the direct shear test at comparable stress levels. That is perhaps a result of the non-uniform normal

stress and shear stress distributions imposed on a sample in the direct shear test.

(e) Direct shear test results on oil-free sand samples of the Grand Rapids Formation indicate that the oil sands in that formation are perhaps slightly weaker in strength than the Athabasca oil sands. This observation seems to apply to the Clearwater Formation at Cold Lake as well.

(f) As measured in direct shear tests, The residual angle of friction of Athabasca oil sands is in the area of 30° to 33°. On the other hand, triaxial tests estimated the residual friction of Athabasca oil sands to be approximately 40°. The discrepancy is probably because of the difference in the mode of shearing action in the two tests to reach residual strains and the difference in the stress-strain conditions of the triaxial test and the direct shear test.

(g) As the confining pressure increases, the oil sand not only has a lesser tendency to strain-weaken; it tends to be more ductile as well requiring larger strains to reach the residual strength.

(h) Because oil sands are not cemented in general, they have negligible tensile strength. A small tensile strength of 20 kPa may exist due to the interlocked nature of the sand structure.

(i) The modulus of elasticity of the Athabasca oil sands is a function of the confining pressure. Triaxial test

data indicate that the modulus of elasticity increases with the confining pressure but the rate of increase diminishes as the confining pressure becomes higher. Cycling the confining stress on the sample before shearing appears to increase the modulus. The modulus values appear to be more sensitive to sample disturbance than the shear strength values.

(j) Modulus of elasticity values from undrained triaxial tests are considerably smaller than values from drained triaxial tests.

(k) Because of the disturbance to the oil sands prior to testing, the triaxial test may significantly underestimate the in-situ modulus of elasticity. The field sonic method avoids the problem of sample disturbance and yields much higher moduli of elasticity. Unfortunately, there is a poor understanding on the relationship between the dynamic and static moduli of oil sands. As a result, there is still uncertainty associated with the modulus values estimated by the sonic method.

(l) Triaxial test results show that the Poisson's ratio of the Athabasca oil sands is fairly constant around 0.25 over a wide range of confining pressure. Sample disturbance apparently has little effect on the value of Poisson's ratio.

(m) The calculated shear modulus of the Athabasca oil sands, as derived from triaxial test data, increases with the

confining pressure. The variation in shear modulus is similar to the variation in the modulus of elasticity as the Poisson's ratios used in the calculations are fairly constant.

(n) The coefficients of volume compressibility of the McMurray Formation and the Grand Rapids Formation are in the range of 0.3 to 0.7 $x10^{-4}kPa^{-1}$, while that of the Clearwater Formation at Cold Lake is perhaps between 0.4 and 1.0 $x10^{-4}kPa^{-1}$.

(o) Due to the low compressibility of the sand fabric, the pore pressure parameter B of oil sands may be considerably less than unity. Under the field condition, B could perhaps be in the vicinity of 0.4.

(p) The pore pressure parameter $\bar{A}$ decreases with increasing axial strain in an undrained triaxial test on oil sands. The higher is the axial strain at failure, the more negative is the value of $\bar{A}$ at failure. This implies that the better the quality of the sample, the less negative is $\bar{A}$. Extrapolating to the field condition, $\bar{A}$ could be in the range of 0 to -0.05.

(q) The basal clay shales and the intraformational clays in the McMurray Formation at Athabasca have a wide range of strength properties which are related principally to the lithology. Both regimes of clay shales follow the Mohr-Coulomb strength relationship in general. The peak angle of friction can range up to 29° whereas the residual angle can be as low as 7°.

REFERENCES

Agar, J.G., 1983. Personal communication.

Application of Shell Canada Limited and Shell Explorer Limited to the Energy Resources Conservation Board, June, 1973.

Barnes, D.J., 1980. "Micro-Fabric and Strength Studies of Oil Sands". M. Sc. Thesis, University of Alberta, Edmonton, Alberta.

Brooker, E.W., 1975. "Tarsand Mechanics and Slope Evaluation". Proceedings of the 10th Canadian Rock Mechanics Symposium, Queen's University, Kingston, Vol. 1, pp. 409-446.

Brooker, E.W., and Khan, F., 1980. "Design and Performance of Oilsand Surface Mine Slope". Applied Oilsands Geoscience, Edmonton, Alberta.

Byrne, P.M., Smith, L.B., Grigg, R.F., and Stewart, W.P., 1980. "A Computer Model for Stress-Strain and Deformation Analysis of Oilsands". Applied Oilsands Geoscience, Edmonton, Alberta.

Carrigy, M.A., 1967. "The Physical and Chemical Nature of a Typical Tar Sand: Bulk Properties and Behaviour". Proceedings of the 7th World Petroleum Congress, Mexico City, Vol. 3, Tar Sands Section, pp. 573-581.

Carrigy, M.A., and Kramers, J.W., 1973. "Guide to the Athabasca Oil Sands Area". Prepared for the Canadian Society of Petroleum Geologists Oil Sands Symposium, 1973.

Clark, K.A., 1957. "Bulk Densities, Porosities and Liquid Saturations of Good Grade Athabasca Oil Sands". Research Council of Alberta mimeo., Circ. 22, Edmonton, Alberta.

Clark, K.A., 1959. "Permeabilities of the Athabasca Oil Sands". Transactions of the Canadian Institute of Mining and Metallurgy, Vol. 63, pp. 151-156.

Direct Shear Test Series 79G. Unpublished data from Prof. J.D. Scott, Department of Civil Engineering, University of Alberta.

Duncan, J.M., 1980. "Hyperbolic Stress-Strain Relationships". Proceedings of the Workshop on Limit Equilibrium, Plasticity and Generalized

Stress-Strain in Geotechnical Engineering, McGill University, pp. 443-460.

Dusseault, M.B., 1977. "The Geotechnical Characteristics of the Athabasca Oil Sands". Ph. D. Thesis, University of Alberta, Edmonton, Alberta.

Dusseault, M.B., 1980. "The Development of Permeability in Cohesionless Bituminous Sands". Sandia Laboratories Workshop on Permeability Enhancement, Alburquerque, New Mexico.

Dusseault, M.B., 1980. "Sample Disturbance in Athabasca Oil Sand". Journal of Canadian Petroleum Technology, Vol. 19, No. 2, pp. 85-92.

Dusseault, M.B., 1983. Private communication through the assistance of Mr. Hal Soderberg.

Dusseault, M.B., and Scafe, D., 1979. "Mineralogical and Engineering Index Properties of the Basal McMurray Formation Clay Shales". Canadian Geotechnical Journal, Vol. 16, No. 2, pp. 285-294.

Dusseault, M.B., and Simmons, J.V., 1982. "Injection-Induced Stress and Fracture Orientation Changes". Canadian Geotechnical Journal, Vol. 19, No. 4, pp. 483-493.

Hardy, R.M., 1979. "Strength-Deformation Characteristics of Tar Sands". Lecture to Graduate School, University of Alberta, 1979.

Hardy, R.M., and Hemstock, R.A., 1963. "Shearing Strength Characteristics of Athabasca Oil Sands". K.A. Clark Volume, ed. M.A. Carrigy, Research Council of Alberta, Info. series 45, Edmonton, Alberta, pp. 109-122.

Hardy, R.M., and Scott, J.D., 1978. "The 1963 G.C.O.S. Test Shaft". Proceedings of the AOSTRA Seminar on Underground Excavation in Oilsands, Edmonton, Alberta.

Harris, M.C., and Sobkowicz, J.C., 1978. "Engineering Behaviour of Oil Sand". CIM Special Vol. 17, the Canadian Institute of Mining and Metallurgy, pp. 270-281.

Holzhausen, G.R., Wood, M.D., Raisbeck, J.M., and Card, C.C., 1980. "Results of Deformation Monitoring during Steam Stimulation in a Single-Well Test". Applied Oilsands Geoscience, Edmonton, Alberta.

Jaeger, J.C., and Cook, N.G.W., 1979. Fundamentals of Rock Mechanics. John Wiley and Sons, Inc., New York, NY.

Kosar, K.M., 1983. "The Effect of Heated Foundations on Oil Sand". M. Sc. Thesis, University of Alberta, Edmonton, Alberta.

Kolisnyk, Z., and Robinson, J., 1974. "Mildred Lake Utility Plant". Engineering Institute of Canada Western Region Conference on the Athabasca Tar Sands, April, 1975, Edmonton, Alberta.

Lambe, T.W., and Whitman, R.V., 1979. Soil Mechanics, SI Version. John Wiley and Sons, Inc.

Mathews, K.E., 1980. "Potential for the Underground Mining of Oil Sands in Canada". Proceedings of the International Symposium on Subsurface Space for Environmental Protection, Low-Cost Storage and Energy Savings, Stockholm, Sweden, June, 1980.

Physical Properties Set 74S. Unpublished data from Prof. J.D. Scott, Department of Civil Engineering, University of Alberta.

Raisbeck, J.M., and Currie, J.B., 1981. "A Laboratory Investigation of Hydraulic Fracturing in Oil Sands". In Situ, Vol. 5, No. 1, pp. 1-24.

Ren Jen Sun, 1969. "Theoretical Size of Hydraulically Induced Horizontal Fractures and Corresponding Surface Uplift in an Idealized Medium". Journal of Geophysical Research, Vol. 74, pp. 5995-6011.

Round, G.F., 1960. "The Shear Strength of McMurray Oil Sands". Transactions of the Engineering Institute of Canada, Vol. LXIII, pp. 145-150.

Skempton, A.W., 1954. "The Pore-Pressure Coefficients A and B". Geotechnique, Vol. 4, pp. 143-147.

Smith, L.B., Chatterji, P.K., Insley, A.E., and Sharma, L., 1978. "Construction of Saline Creek Tunnel in Athabasca Oil Sand". Proceedings of the AOSTRA Seminar on Underground Excavation in Oil Sand, ed. M.B. Dusseault, Dept. of Civil Eng., University of Alberta, Edmonton, Alberta, Paper no. 7.

Smith, M.B., and Pattillo, P.D., 1980. "Analysis of Casing Deformations due to Formation Flow". Applied Oilsands Geoscience, Edmonton, Alberta.

Sterne, K.B., 1981. "Hollow Cylinder Testing of Oil Sands".

M. Sc. Thesis, University of Alberta, Edmonton, Alberta.

Taylor, D.W., 1939. "A Comparison of Results of Direct Shear and Cylindrical Compression Tests". Proc. ASTM.

Thurber Consultants Ltd., 1977. "Research Observations – Saline Creek Tunnel". Report submitted to and available from AOSTRA, Edmonton, Alberta.

Triaxial Test Series 64G. Unpublished data from Prof. J.D. Scott, Department of Civil Engineering, University of Alberta.

Triaxial Test Series 75S. Unpublished data from Prof. J.D. Scott, Department of Civil Engineering, University of Alberta.

Tustin, T.G., 1949. "The Shear and Consolidation Characteristics of McMurray Tarsands". M. Sc. Thesis, University of Albeta, Edmonton, Alberta.

Zwicky, R.W., and Eade, J.R., 1977. "The Tar Sands Core Analysis versus Log Analysis Controversy – Does It Really Matter?". CIM Special Vol. 17, the Canadian Institute of Mining and Metallurgy, pp. 256-259.

APPENDIX A

TRIAXIAL TESTS PERFORMED FOR THE PRESENT STUDY

A.1 Source of Oil Sand Samples

The samples were obtained at an outcrop on the valley wall of Saline Creek, adjacent to Highway 63, 1 km south of Fort McMurray, Alberta. The samples were oil-rich and were obtained by diamond coring during late winter when the oil sand was frozen to minimize sample disturbance.

During the process of valley formation, the oil sand at this location has undergone gradual stress relief. Hence, it is believed that the gas dissolved in the pore fluid was able to escape without disrupting the structure of the oil sand, and the oil sand retained much of its original in-situ strength.

A.2 Sample Preparation and Testing Procedure

(1) The sample, which had been stored in the cold room at -20°C, was placed in dry ice overnight. The sample was machined the next day in the cold room to two inch diameter and approximately four inches in length. The diameter was then measured at the top, the middle and the bottom of the sample. At least three readings were made on the length of the sample. Immediately afterwards, the sample was weighed.

(2) The base of the triaxial cell, the top cap, and the membrane were brought into the cold room at least two

hours before mounting of the sample onto the triaxial cell. In the cold room, the sample, porous stones and membrane were assembled without side drains in the normal manner on the pedestal by securing an undersized O-ring on the membrane around the pedestal. The top cap was similarly secured on the sample, and the drainage ports were connected.

(3) The base and the sample were immediately transported to the testing laboratory. The triaxial cell was assembled, filled with water, and mounted in the loading frame. A cell pressure of 0.7 MPa (100 psi) was immediately applied on the sample. The purpose of the above procedure was to minimize any possible sample expansion from taking place during thawing of the sample. The entire operation usually took less than half an hour.

(4) A water pressure of 0.35 MPa (50 psi) was used to flush and put into solution most of the air in the porous stones and the pore pressure lines. Afterwards, the cell pressure and the back pore pressure were raised to 2.4 MPa (350 psi) and 2.1 MPa (300 psi) respectively. The sample was allowed to thaw against these pressures overnight. The back pressure of 2.1 MPa was believed to be more than sufficient to fully saturate the sample and the entire drainage system.

(5) A consolidation test was conducted on the sample the next day against a back pressure of 2.1 MPa. A standard

test procedure was used. There were two triaxial tests performed. For the first test, the cell pressure was 4.1 MPa (600 psi) and 5.5 MPa (800 psi) for the second test. In effect, the effective consolidation pressures were 2.1 MPa and 3.4 MPa for the first and second tests respectively. Drainage was allowed at the top and bottom of the sample.

(6) A modified pore pressure parameter (B) test was run for each of the two triaxial tests. Because of the low compressibility of the sand matrix, the oil sand would not yield B = 1 even when it was saturated. For that reason, a modified procedure was adopted. After the consolidation test, the cell pressure was increased by approximately 0.21 MPa (30 psi) and the pore pressure was monitored. If the B value was less than unity, it was brought to unity by increasing the back pressure. These steps were repeated for another cell pressure increment until the cell pressure had increased by approximately 0.7 MPa (100 psi) in total. The accumulative changes of the cell pressure and the pore pressure were plotted. The plot is similar to Figure A-1. If the slope of the plot for one increment is significantly different from those of the other increments, it can be concluded that the sample is not saturated.

(7) The back pressure was reduced to 2.1 MPa (300 psi) and the cell pressure to 4.2 MPa (600 psi). For the second

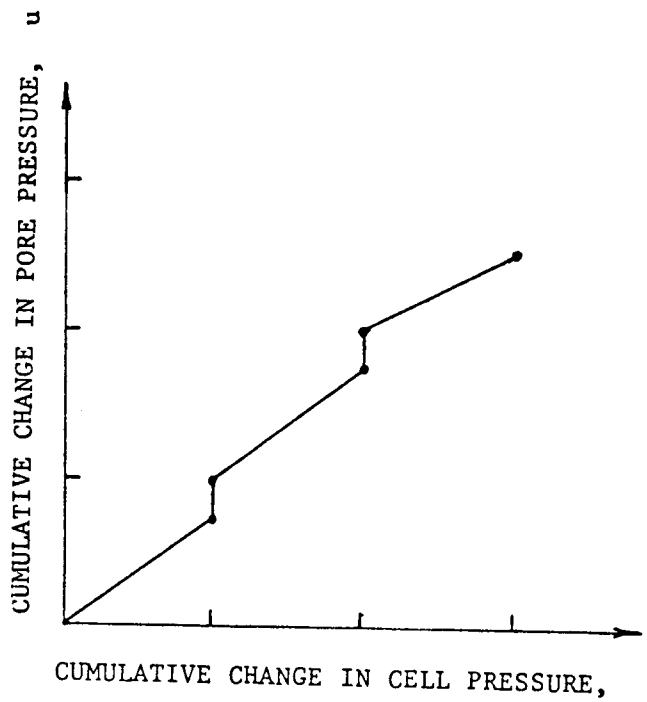

Figure A.1 Pore pressure parameter (B) test

test, the cell pressure was reduced to 5.5 MPa (800 psi). The sample was then sheared in a drained manner at a constant vertical strain rate until after the peak strength was reached. Volume change of the sample was measured by recording the out- and in-flow of water to the sample.

A.3 Results

A.3.1 Stress-Strain Diagrams

The stress-strain data are presented in Figures A-2 and A-3.

A.3.2 Summary of Test Results

The test results are summarized in Table A-1. In Table A-1, the following symbols are used.

ρ = bulk density of oil sand (pre-test)

u = constant back pressure

q = $\left(\frac{\sigma_1 - \sigma_3}{2}\right)_f$
= one half of deviatoric stress at failure

p' = $\left(\frac{\sigma_1' + \sigma_3'}{2}\right)_f$
= mean effective stress at failure

σ_3' = effective confining stress during test

ϵ_f = axial strain at failure

ϕ_f' = secant angle of friction at failure

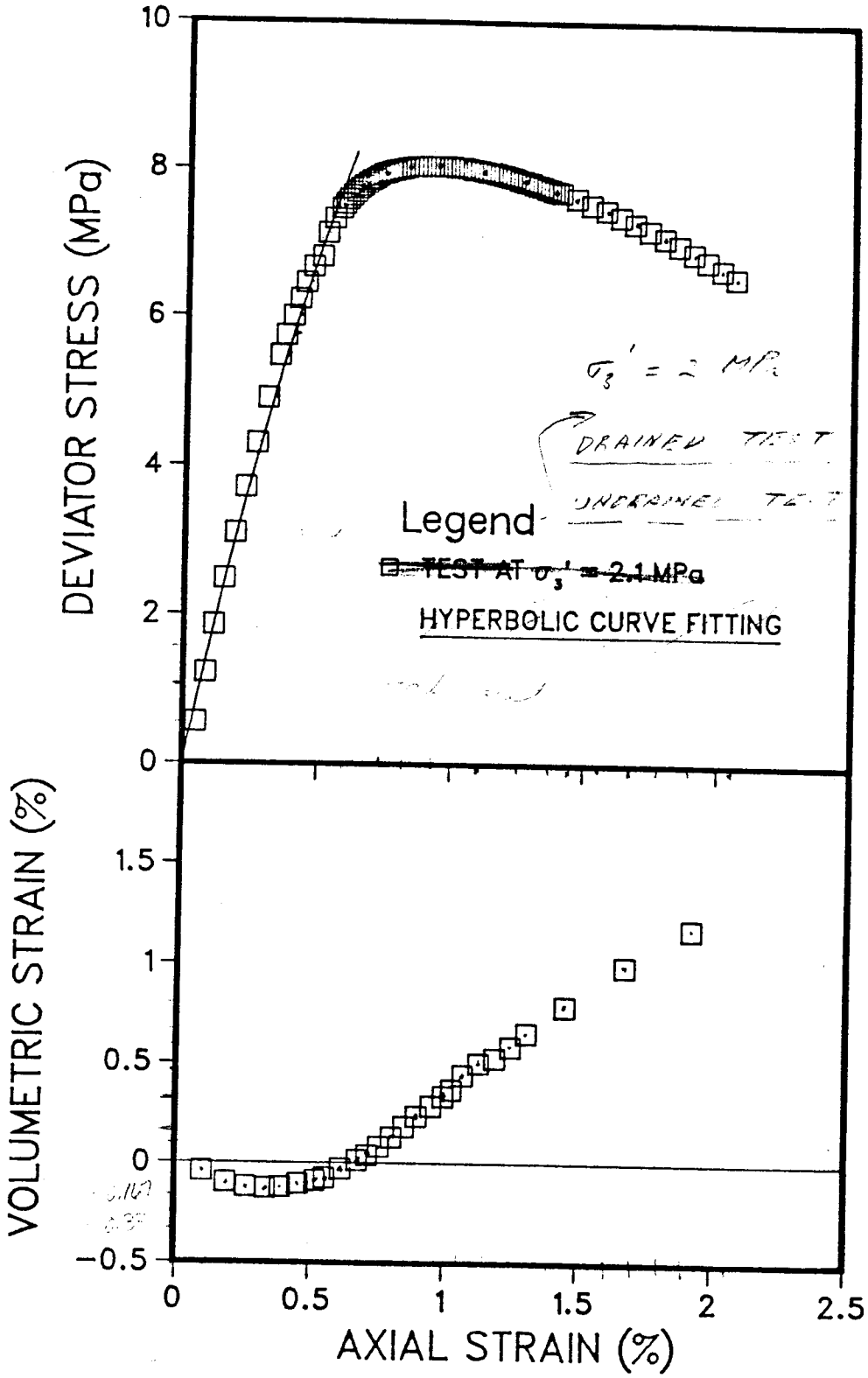

Figure A.2 Stress-strain diagram for Sample 1

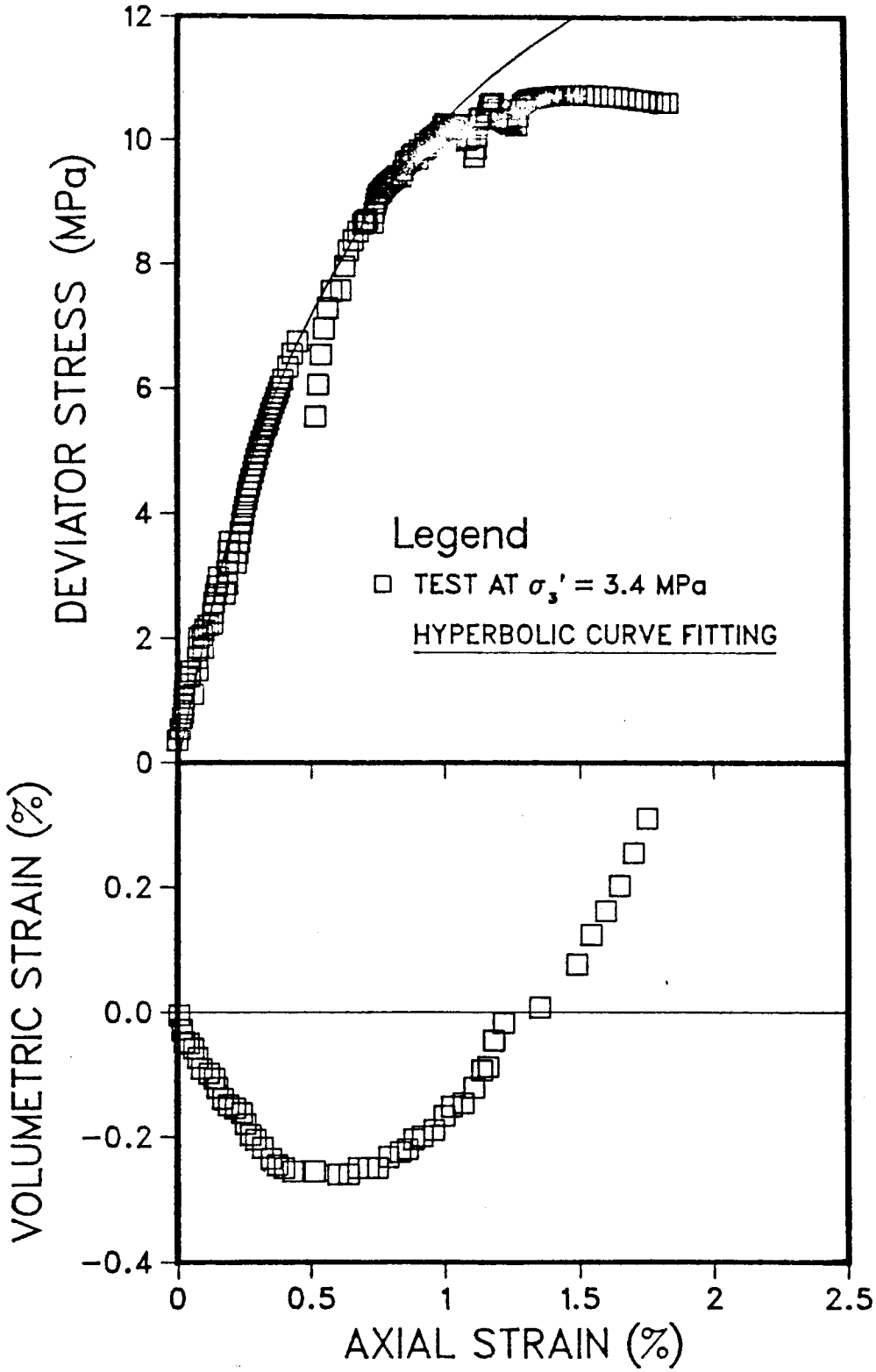

Figure A.3 Stress-strain diagram for Sample 2

TABLE A.1 TRIAXIAL TEST RESULTS OF THE PRESENT STUDY

TEST	ρ (g/cm^3)	u (MPa)	q (MPa)	p' (MPa)	σ_3' (MPa)	ε_f (%)	ϕ'_f	$\left(\frac{\dot{\sigma}_1'}{\sigma_3'}\right)_f$	$\dot{\varepsilon}$ (10^{-6}/sec)
1	2.05	2.1	4.02	6.14	2.1	0.86	41°	4.78	4.2
2	2.03	2.1	5.36	8.80	3.4	1.45	38°	4.12	0.8

(at maximum deviatoric stress)

$\left(\frac{\sigma_1'}{\sigma_3'}\right)_f$ = maximum effective stress ratio

$\dot{\epsilon}$ = strain rate during test

A.3.3 B-Test Results

The B-test results on sample 1 are shown in Table A-2. Unfortunately, for sample 2 there were some procedural errors in the B-test. As a result, the results from that test could not be used.

A.4 Data about the Test Samples

The relevant data on the test samples are tabulated in Table A-3. A sketch of sample 1 after failure is shown in Figure A-4. A thin shear band was found in sample 1. The band was less than 1 mm in thickness and was oriented at about 50° to the horizontal. Sample 2 was also examined after failure. However, no bulging or any apparent shear plane could be found in the sample.

A.5 Corrections for the Test Results

A.5.1 Compliance Tests

The LVDT was so arranged that it measured the relative displacement between the loading piston and the base of the triaxial cell. As a result, the displacement measurements would include the straining of

TABLE A.2 B - TEST RESULTS ON SAMPLE 1 (σ_3' = 2.1 MPa)

$\Delta\sigma_3$ (MPa)	u (MPa)	Cumulative $\Delta\sigma_3$ (MPa)	Cumulative Δ u (MPa)	Incremental $\Delta\sigma_3$ (MPa)	Incremental Δ u (MPa)	B = $\frac{\Delta u}{\Delta\sigma_3}$
4.547	2.648					
		0.441	0.222	0.441	0.222	0.50
4.988	2.870					
		0.425	0.298	-0.016	0.076	-
4.973	2.946					
		0.760	0.474	0.334	0.176	0.53
5.307	3.122					
		0.751	0.609	-0.009	0.135	-
5.298	3.257					
		0.190	0.286	-0.561	-0.323	0.57
4.737	2.934					

TABLE A.3 DATA ON THE TEST SAMPLES

SAMPLE	TIME OF MEASUREMENT	DIAMETER (cm.)			LENGTH (cm.)			MASS (kg)	c_v (cm^2/min)
		TOP	MIDDLE	BOTTOM	1	2	3		
1	Before Test	5.00	5.00	5.00	10.10	10.08	10.08	0.402	1.15
	After Test	5.055	5.05	5.035	9.95	9.97	9.96	0.470	
2	Before Test	5.05	5.06	5.055	10.27	10.26	10.26	0.422	21.8
	After Test	5.055	5.10	5.07	10.495	10.490	10.455	0.426	

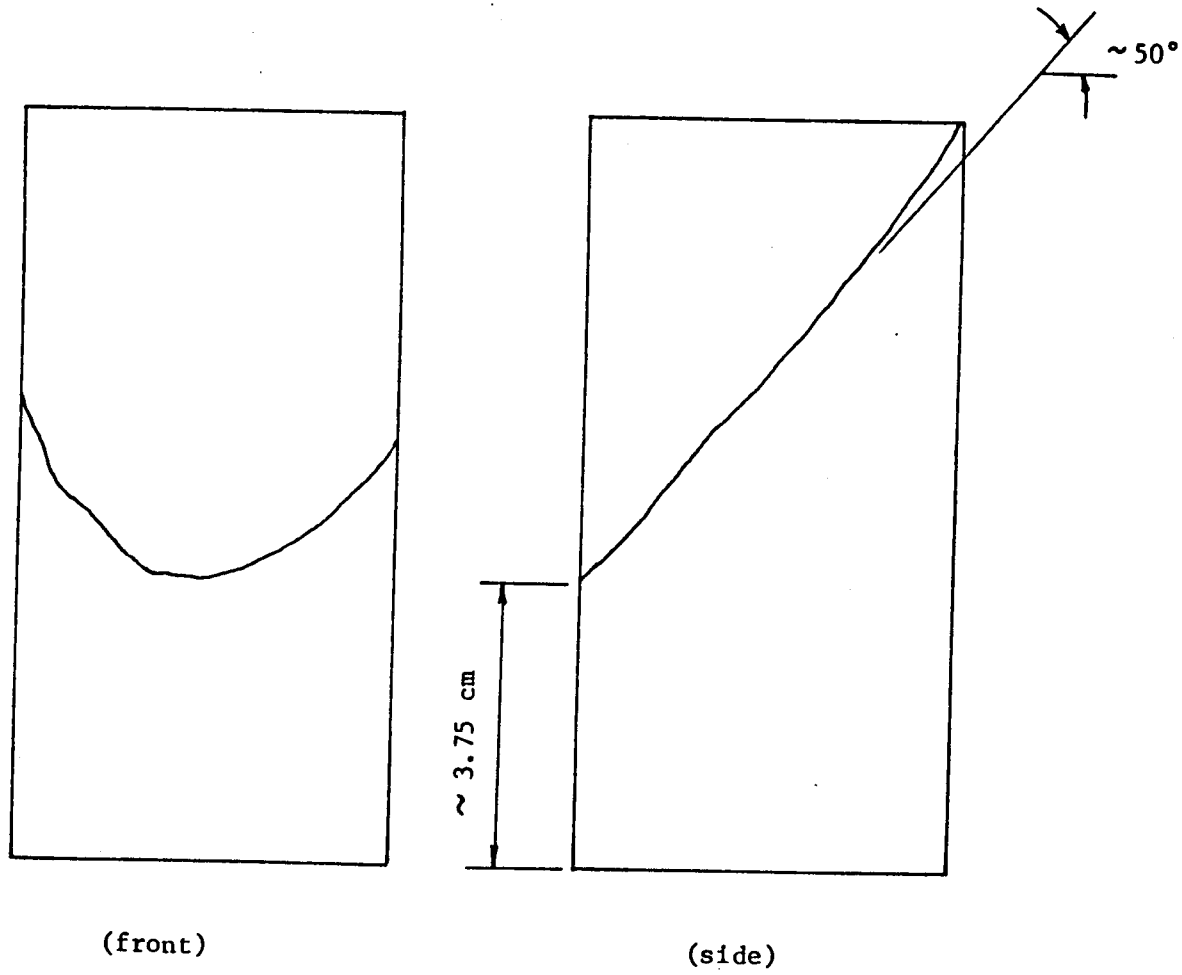

Figure A.4 Sample 1 after shear failure (approximately to scale)

the piston, the porous stones, and the top and bottom caps. To be able to make the necessary corrections, compliance tests at confining pressures of 0, 4.1, and 5.5 MPa were run with an aluminum sample in place of an oil sand sample in the triaxial cell. The results of the compliance tests are plotted in Figure A-5. The correction for a given load level is the difference in displacement between the "aluminum" curve and the "compliance" curve.

A.5.2 Piston Friction

In the triaxial tests of the present study, an external load cell was used to measure the axial load. It was therefore necessary to estimate the piston friction. The approach was to push the piston into the triaxial cell at the testing strain rates against cell pressures of 4.1, 5.5 and 10.3 MPa and monitor the load registered by the load cell. The difference between the force measured by the load cell and the resisting force with which the cell fluid was applying against the advancement of the piston constituted an estimation of the piston friction at that particular cell pressure.

It appeared that there was little increase in the piston friction with the axial load because of the type of seal used for the piston. The piston friction at cell pressures of 4.1 MPa, 5.5 MPa and 10.3 MPa was about 70 N, 100 N, and 250 N respectively. For the two

FIGURE A-5
DISPLACEMENT CORRECTION PLOT

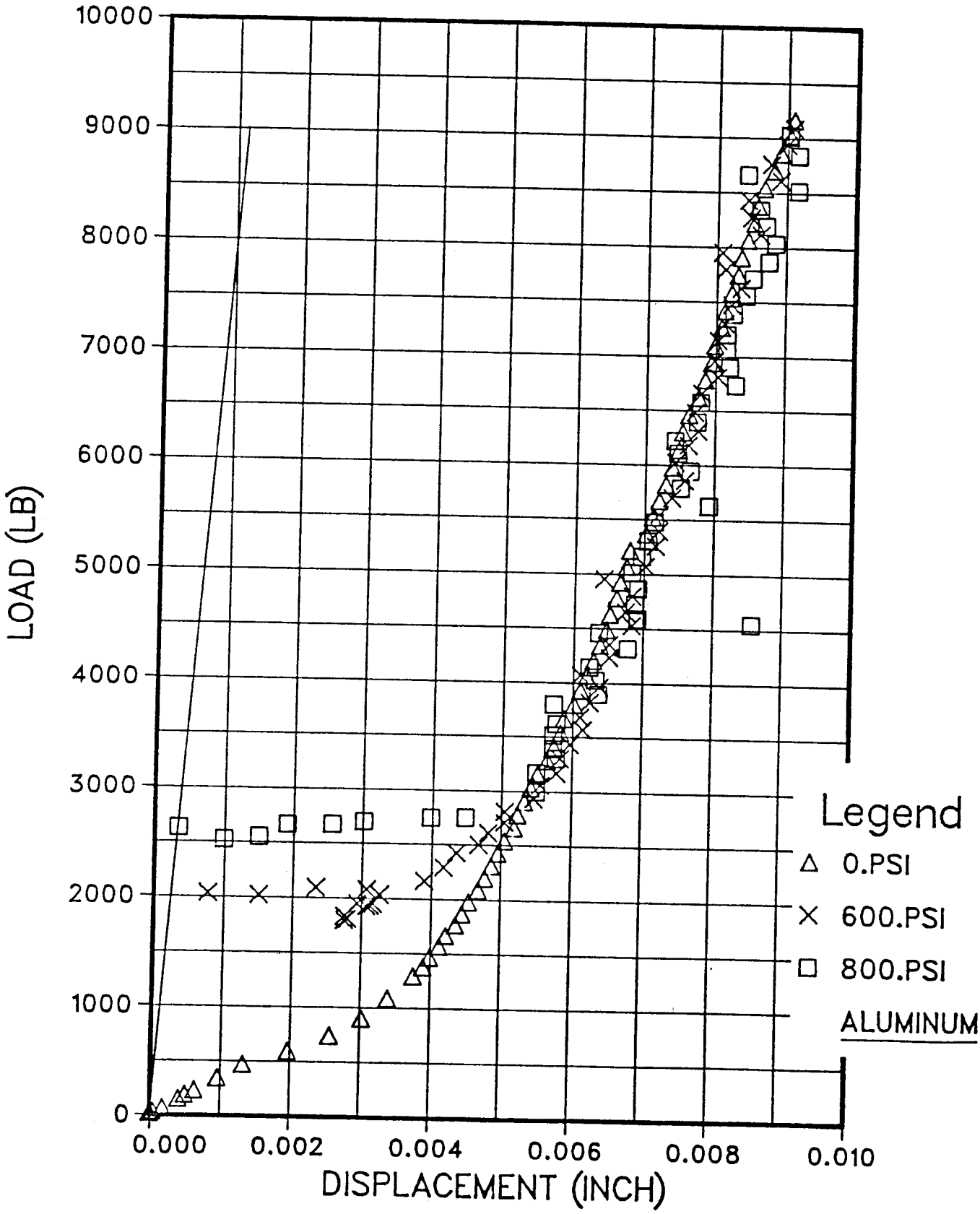

tests which used cell pressures of 4.1 and 5.5 MPa, it was decided to assume a constant piston friction of 100 N for the correction of the axial load. As the piston load at failure was over 25,000N, the magnitude of the friction was not significant.

This method of measuring piston friction does not include the effect of the diameter increase of the piston as the axial load is increased. This diameter increase was calculated for the anticipated maximum piston load and with the type of piston bushing and seal used in this triaxial cell, it was apparent that the piston diameter increase would have little effect on the magnitude of the piston friction.

APPENDIX B

OTHER STRENGTH TESTS

B.1 Standard Penetration Test

The literature review for this study has so far failed to reveal any effort to correlate the shear strength or the friction angle of the oil sands with the blow count in the standard penetration test. For a number of reasons, the standard penetration test is not generally useful for the estimation of the in-situ shear strength of oil sands.

First of all, it is extremely difficult and expensive to obtain truly undisturbed samples for strength testing in the laboratory. Not knowing the true in-situ strength, it is not possible to do any correlation with empirical field measurements such as the STP. Moreover, oil sands are so strong that it is impractical to perform standard penetration tests on oil sands with conventional sampling spoons. If the experience with the usage of the standard penetration tests on ordinary sands is any indication, the correlation of the strength of oil sands with the blow count would have little accuracy.

Figure B.1 shows the results of two standard penetration tests in the upper part of the McMurray Formation (Carrigy, 1967). Although the test results could not measure quantitatively the strength of the oil sand, the high blow counts do indicate that the oil sand is very dense, possibly as strong as soft sandstones. Both tests

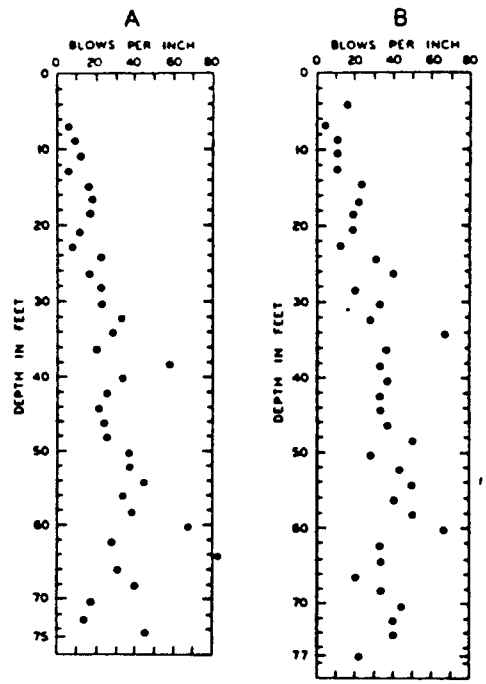

Fig. B-1 Results of standard penetration tests in the upper part of the McMurray Formation (surface to depth of 80 feet) at two locations on Lease 4. (After Carrigy, 1967)

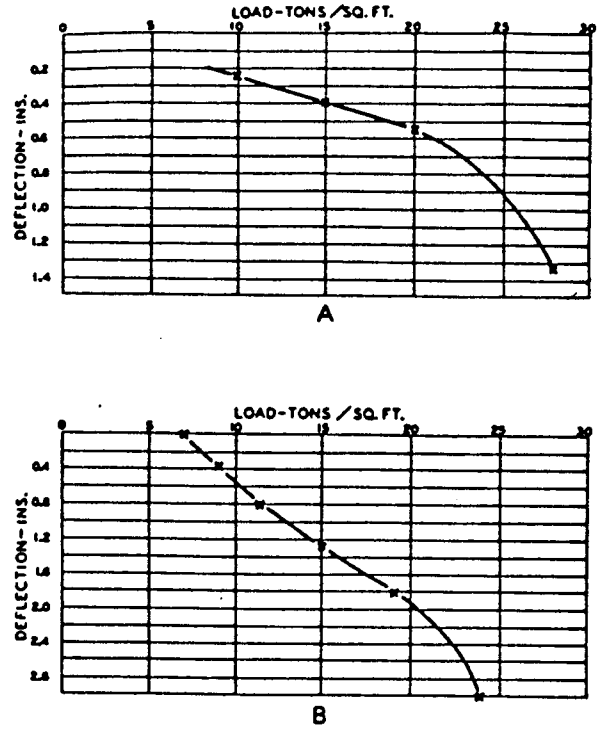

Fig. B-2 Results of plate-bearing tests performed on rich tar sands in test pit on Lease 17. Upper curve A at an elevation of 960 feet, lower curve B at an elevation of 923 feet. (After Carrigy, 1967)
Area of plate 0.25 square feet

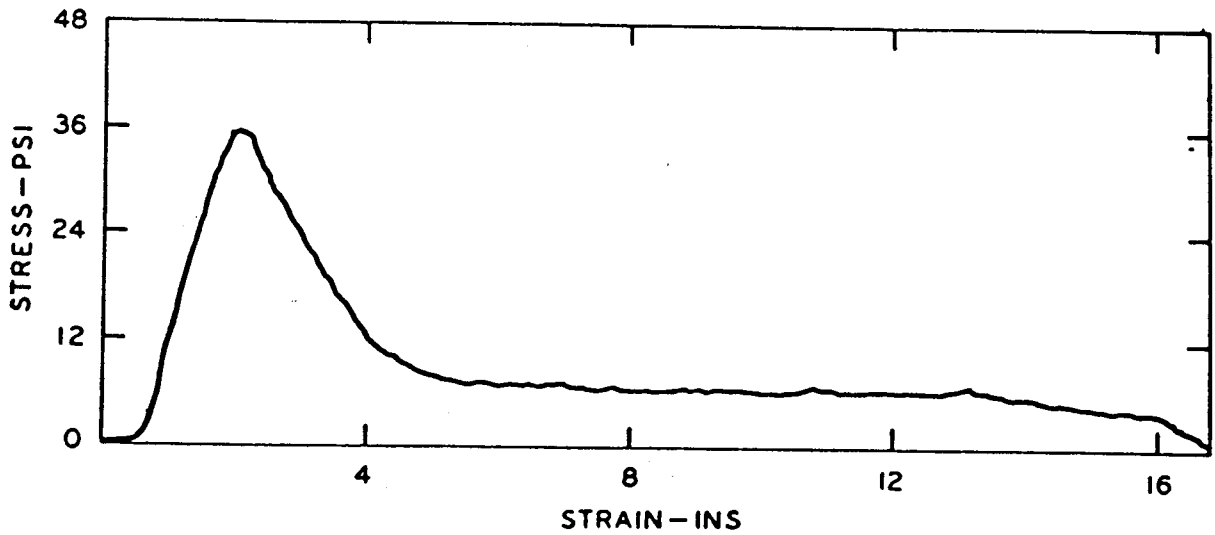

Fig. B-3 Typical result of vane-shearing test on Athabasca Tar Sand (after Carrigy, 1967).
Vane diameter 2 inches.
Rate of shear 2 feet per minute.

suggest that the strength of the oil sand increases with depth when the depth is less than approximately 10m. From 10m on, the strength is fairly constant for the shallow depths shown.

B.2 Plate Bearing Test

Ideally, the plate-bearing tests can be used to predict the in-situ bearing capacity of oil sands in terms of strength and settlement. However, there are a number of problems associated with the use of plate-bearing tests on oil sands.

One major difficulty is the immediate fabric disruption by gas exsolution on stress relief. That means the results of subsequent plate-bearing tests would not reflect the true in-situ behaviour of oil sands.

Secondly, the area of the loading plate is usually small (0.25 square feet or 1 foot in diameter). There is therefore a scale effect associated with the interpretation of the test results. Since up to now the true strength of the oil sands has not been obtained, it is not possible to estimate with any confidence the in-situ properties of the oil sands on the basis of the plate load test. Besides, both the modulus of deformation and the shear strength of the oil sands are functions of the confining stress. Clearly, the nature of the plate-bearing test limits the testing to very low confining stresses. That further depreciates the usefulness of the plate load test on oil

sands.

The results of two plate-bearing tests on Athabasca oil sands are shown in Figure B.2. The failure loads for both tests are above 20 tons/sq.ft. (1.9 MPa). Obviously, oil sands are competent foundation materials. The modulus of elasticity may be derived from the results of plate-bearing tests (Jaeger and Cook, 1979):

$$E = m (1 - \nu)^2 \sqrt{A} \frac{\partial p}{\partial W} \qquad (B.1)$$

where $m = 0.95$ for a square plate

ν = Poisson's ratio

A = area of the plate

p = pressure on the plate

W = average deflection of the plate

Equation (B.1) is used on the results of the two plate-bearing tests shown in Figure B.2. With

$m = 0.95$

$A = 0.25$ sq.ft.

$\nu = 0.25$

the modulus of elasticity is calculated and listed in Table B.1. This method suffers the same problem as the triaxial test: the oil sand on which the test is performed would inevitably be disturbed to a certain degree prior to the test and the measured values would be lower than the true in-situ undisturbed values.

TABLE B.1. THE MODULUS OF ELASTICITY OF ATHABASCA OIL SANDS CALCULATED FROM PLATE-BEARING TEST RESULTS.

TEST	$\frac{\partial p}{\partial w}$ (MPa/cm)	E (MPa)
A	1.262	17.1
B	0.247	3.4

B.3 Vane-Shearing Test

The vane test requires insertion of the vane into the ground. That would seriously disturb the locked structure of the oil sands. For that reason alone, the vane test could not be a viable method of obtaining the true strength of the oil sands. Nevertheless, the test had been attempted on oil sands and a typical result is shown in Figure B.3.

APPENDIX C

SUMMARIZING NOTES ON SELECTED REFERENCES

The following notes are concerned mainly with the strength deformation data contained in the references.

Barnes, D.J. (1980): "Micro-Fabric and Strength Studies of Oil Sands".

Oil-free samples of the McMurray Formation and the Grand Rapids Formation were used for drained direct shear testing. Testing was done at normal stresses up to 5 MPa. Both peak and residual strength properties had been investigated. Oedometer tests were also performed to measure the compressibility of the samples.

Brooker, E.W. (1975): "Tarsand Mechanics and Slope Evaluation".

Information on the engineering geology including the K_o value and joint set orientations of Athabasca oil sands was given. The results of four undrained triaxial tests were reported. Extrapolation to the in-situ strength of the oil sand as a function of void ratio which presumably reflects the quality of the samples was attempted. The bulk density values quoted for the samples were final wet densities.

Brooker, E.W., and Khan, F. (1980): "Design and Performance of Oilsand Surface Mine Slope".

Three separate sets of undrained triaxial test and direct shear test results on Athabasca oil sands were presented. The strength properties of the basal clay shales and the intraformational sity and clayey beddings were discussed.

Direct Shear Test Series 79S

Drained direct shear tests were performed on rich oil sand and oil sand interbedded with clayey silt. Two oedometer tests were carried out for each of the two set of samples. Judging from the bulk density values, the samples were significantly disturbed.

Dusseault, M.B. (1977): "The Geotechnical Characteristics of the Athabasca Oil Sands".

Comprehensive direct shear test data on Athabasca oil sands and intraformational clay were reported. A number of triaxial tests were performed on Athabasca oil sands. For the purpose of comparison, strength testing was done on other materials including sandstones, Ottawa sand, and oil sand tailings.

Bulk density, porosity and saturation of the Athabasca oil sands were discussed in terms of sample disturbance and geophysical measurements.

Dusseault, M.B. (1983).

A series of drained triaxial tests and compressibility tests were performed on Athabasca oil sands for a wide range of effective confining pressures.

Dusseault, M.B. (1980): "The Development of Permeability in Cohesionless Bituminous Sands".

Discussing the mechanics and behaviour of hydraulic fractures in oil sands, some representative properties of the McMurray Formation at Athabasca and the Clearwater Formation at Cold Lake were suggested.

Dusseault, M.B., and Simmon, J.V. (1982): "Injection-Induced Stress and Fracture Orientation Changes".

In the course of simulating the behaviour of hydraulic fractures in oil sands, values of the dynamic and static Young's moduli of the geologic formations at Cold Lake were estimated.

Dusseault, M.B., and Scafe, D. (1979): "Mineralogical and Engineering Index Properties of the Basal McMurray Formation Clay Shales".

In discussing the mineralogical composition and Engineering Indices of the basal clay shales, the residual shear angles of the basal clay shales and the intraformational McMurray Formation clayey silts were briefly reported.

Hardy, R.M., and Hemstock, R.A. (1963): "Shearing Strength Characteristics of Athabasca Oil Sands".

Considerable amount of test results on the unconfined compressive strength of Athabasca oil sands were reported. No bulk density or porosity values were given, but the samples are suspected to be disturbed quite badly.

Physical Properties Set 74S.

The results of the analyses on the water and oil contents, Atterberg limits, bulk densities, and grain size distribution of core samples were presented. The samples were obtained from the McMurray Formation at Athabasca.

Raisbeck, J.M., and Currie, J.B. (1981): "A Laboratory Investigation of Hydraulic Fracturing in Oil Sands".

The stress-strain characteristics, the time-dependent behaviour and the hydraulic fracturing phenomenon were investigated through the use of triaxial tests. Notably, the compressibility, Young's modulus and Poisson's ratio of the samples at various stage of the test were reported. No information on the bulk density was given, but it is suspected to be less than 2.0 g/cm^3 for the test samples.

Round, G.F. (1960): "The Shear Strength of McMurray Oil Sands".

Shear box tests were performed on McMurray oil sands. The samples were clearly badly disturbed. The rate of displacement in the tests ranged from 0.01725 to 0.1869 in/min. It is not sure whether that was sufficient to ensure a drained condition in the tests.

Sterne, K.B. (1981): "Hollow Cylinder Testing of Oil Sands".

Two triaxial hollow cylinder tests were performed on Athabasca oil sands. To investigate the effect of different stress paths, two triaxial compression tests and two constant mean principal stress tests were done. From the test results, the failure envelope, the modulus of deformation and Poisson's ratio were estimated. The compressibility of Athabasca oil sands was measured by isotropic compression and in an oedometer test.

Thurber Consultant Ltd. (1977) : "Research Observation - Saline Creek Tunnel".

Unconfined compression test results were shown in borehole log drawings. Deformation measurements on the tunnel were also reported. Geophysical bulk density logs were included in the report.

Triaxial Test Series 64G

Triaxial compression tests and direct shear tests were performed at room temperatures on Athabasca oil sands obtained from borings. The reference contains no informations on the pore pressure response during testing. It is not sure if the tests were drained or undrained. The result of a compressibility test was

also presented.

Triaxial Test Series 75S:

The reference contains sets of consolidated drained and undrained triaxial test results. The testing also included unconfined compression tests. The testing had been done at various strain rates and confining pressures.

Tustin, T.G. (1949): "The Shear and Consolidation Characteristics of McMurray Tarsands".

Unconsolidated triaxial tests were performed on McMurray oil sands without pore pressure measurements. The loading rate was very quick. The pore pressure probably did not have time to dissipate completely during the tests. Testing had been made on the samples with the beddings perpendicular and horizontal to the loading direction. The testing temperatures were -10°C and room temperature. It is suspected that all the test samples were badly disturbed.